Copyright Warning & Restrictions

The copyright law of the United States (Title 17, United States Code) governs the making of photocopies or other reproductions of copyrighted material.

Under certain conditions specified in the law, libraries and archives are authorized to furnish a photocopy or other reproduction. One of these specified conditions is that the photocopy or reproduction is not to be "used for any purpose other than private study, scholarship, or research." If a, user makes a request for, or later uses, a photocopy or reproduction for purposes in excess of "fair use" that user may be liable for copyright infringement,

This institution reserves the right to refuse to accept a copying order if, in its judgment, fulfillment of the order would involve violation of copyright law.

Please Note: The author retains the copyright while the New Jersey Institute of Technology reserves the right to distribute this thesis or dissertation

Printing note: If you do not wish to print this page, then select "Pages from: first page # to: last page #" on the print dialog screen

Order Number 9107148

Mass transfer of hazardous organic compounds in soil matrices relevant to thermal desorption/incineration

Dong, Jong-In, D.Eng.Sc.

New Jersey Institute of Technology, 1990

U·M·I
300 N. Zeeb Rd.
Ann Arbor, MI 48106

MASS TRANSFER OF HAZARDOUS ORGANIC COMPOUNDS IN SOIL MATRICES RELEVANT TO THERMAL DESORPTION / INCINERATION

By

Jong-In Dong

Dissertation submitted to the Faculty of the Graduate School of the New Jersey Institute of Technology in partial fulfillment of the requirements for the degree of Doctor of Engineering Science

1990

APPROVAL OF DISSERTATION

Title of Dissertation: Mass Transfer of Hazardous Organic Compounds in Soil Matrices Relevant to Thermal Desorption/Incineration

Name of Candidate: Jong-In Dong
Doctor of Engineering Science, 1990

Dissertation and Abstract Approved:

Dr. Joseph W. Bozzelli Professor Department of Chemical Engineering Chemistry and Environmental Science	Date
Dr. Dana E. Knox	Date
Dr. Piero M. Armenante	Date
Dr. Richard S. Magee	Date
Dr. Namunu J. Meegoda	Date

VITA

Name: Jong-In Dong

Degree and Date to be Conferred: Doctor of Engineering Science, 1990

Secondary Education : Masan Senior High School, Masan, Korea ; 2/75

Collegiate Institutions Attended	Date	Degree	Date of Degree
Seoul National Univ.	3/75 - 2/79	BS(ChE)	1979
Korea Adv. Inst. of Sci. and Tech.	3/79 - 2/81	MS(ChE)	1981
New Jersey Institute of Technology	8/87 - 6/90	D.Eng.Sc.(ChE)	1990

Major : Chemical Engineering

Publications : "Mass Transfer Behavior of Organic Contaminants and Equilibria in Heated Soil Matrices", J.I. Dong and J.W. Bozzelli, accepted for AIChE annual meeting, Chicago,Il, Nov.11-16, 1990

"Removal of Hazardous Organic Compounds from Contaminated Soil Matrices Using Thermal Desorption", J.I. Dong and J.W. Bozzelli, ACS national meeting, Boston, MA, Apr.22-27, 1990

"Benzo(a)pyrene Levels in Several Indoor Environments with Kerosene Heaters and Wood-Burning Fireplaces", J.I. Dong and J.W. Bozzelli, Chemosphere, 18, 9/10, pp 1829-1836, 1988

"Total Hydrocarbon Pollutants from a Non-Vented Kerosene Heater", J.I. Dong, K. Banergee and J.W. Bozzelli, Int. J. of Environmental Studies, 32, pp 75-83, 1988

"Organic Vapors and Benzo(a)pyrene in the Indoor Air from Non-Vented Kerosene Heaters and Wood-Burning Fireplaces", J.W. Bozzelli, J.I. Dong, C. Bobenhausen and A. Mishra, Pittsburgh Conference, Atlantic City, NJ, Mar.9-13, 1987

Positions Held :

Aug. 1987 - June 1990	Research Assisstant in N.J.I.T., NJ
Apr. 1981 - July 1987	Senior Researcher in National Institute of Environmental Research, Seoul, Korea

ABSTRACT

Title of Thesis: Mass Transfer of Hazardous Organic Compounds in Soil Matrices Relevant to Thermal Desorption / Incineration

Name: Jong-In Dong

Doctor of Engineering Science, 1990

Thesis Directed by: Dr. Joseph W. Bozzelli

Professor

Soils contaminated with hazardous organic compounds have been known to threaten human health both directly through various contact mechanisms and indirectly through leaching or transfer to the food chain. Thermal desorption of contaminated soil matrices with secondary treatment of the effluent gases (collection, incineration, etc) is one of most feasible and developing technologies for cleaning of contaminated soils. There is, however, little known about the mass transfer principles of organic contaminants through the heated soil matrices. The objectives of this study is, therefore, to learn and understand details of the mass transfer processes of organic compounds in these soil matrices. We have performed several varied types of experiments to determine specific mass transfer parameters and developed a model which accurately describes the process and can be utilized to obtain optimal operation conditions.

Chromatographic response analysis and transient adsorption/

desorption equations of flow through soil columns have been utilized in developing the initial model. We incorporate intra (pore) and interparticle diffusion, equilibria, in addition to normal mass transfer parameters of axial dispersion and film mass transfer around particle surface.

Experiments primarily consist of plug flow deposition of the contaminants on a well characterized soil column and saturation/ desorption of a soil bed, in addition to equilibrium tests. The plug flow deposition experiments connected with chromatographic analysis successfully yielded equilibrium constants, heats of adsorption and mass transfer parameters. In addition we identified a minimum allowable temperature (MAT), below which the organic compounds are not completely desorbed from the soil within a 1 hour operating time. Resulting equilibrium constants were strongly dependent on temperature and were revealed to follow the van't Hoff equation above the MAT's. Analysis of heats of adsorption showed that the organic - soil system can be considered as a moderately weak physical adsorption system.

Analysis results utilizing an experimental equilibrium test apparatus demonstrated that adsorption isotherms show good linearity at lower concentration and that linear zone tends to extend to higher concentrations with increasing temperature. The slopes of linear adsorption isotherms tend to decrease with increasing temperature, indicating less adsorption. As a result of desorption experiments using the equilibrium apparatus, data showed hysteresis phenomena at lower temperatures probably due to irreversibility of adsorption processes. The observed hysteresis tended to become weaker i.e. the

data for desorption closely followed the adsorption isotherm as temperature increases.

An analytical solution and a numerical approach using orthogonal collocation have been utilized for the purpose of predicting the transient mass transfer behavior of organics in a soil column. The two methods result in satisfactory coincidence.

The comparison of numerical analysis results utilizing estimated mass transfer parameters (axial dispersion coefficients, intraparticle diffusion coefficients and equilibrium constants from chromatographic analysis, and film mass transfer coefficient from the calculation of molecular diffusivity) with experimental results of soil column contamination / desorption experiments showed that the experimental data and model results are reasonably well coincident.

Sensitivity analysis involving the variation of mass transfer parameters showed that dimensionless groups related with axial dispersion, intraparticle diffusion and equilibrium have the most significant effects on the concentration profiles in the system.

ACKNOWLEDGEMENT

To complete this dissertation I owe a debt to Dr. Joseph Bozzelli. I am heartily grateful to him for his support, guidance and strong encouragement to pursue scientific research. I am also very proud to have worked with him.

I would like to thank my dissertation committee members Dr. Dana Knox, Dr. Piero Armenante, Dr. Richard Magee and Dr. Namunu Meegoda for their careful review and comments.

A special thank you is to my wife OckMi and wonderful children YuJung and HeeJung for their love, understanding and patience. I am also so thankful to both my and my wife's families for their continuous support.

I would also like to acknowledge my fellow graduate students at NJIT. I have learned a great deal from members of this group and my beloved friends and association with them has made this school year much more enjoyable and fruitful.

Finally, all of our environments belong to God. I hope that our efforts can help recover our damaged environments to blessed land. Thank God for allowing me to do this work and for your eternal love.

TABLE OF CONTENTS

LIST OF TABLES

LIST OF FIGURES

Chapter 1. INTRODUCTION

A. General Background

It is only several decades ago that people realized that there exists a significant threat to human health and environment from the soils contaminated with hazardous toxic substances in various pathways: evaporation of organic compounds from sites, contamination of surface water and goundwater impacting drinking water and aquatic organisms. Efforts have, therefore, been made to effect to this problem, both legally and technologically.

The Superfund law (the Comprehensive Environmental Response, Compensation, and Liability Act, or CERCLA) of 1980 began a national program to clean up chemically contaminated sites across United States. Legal actions to accelerate the implementation of the rules concerning hazardous waste management in addition to continuation of the above was taken in the name of Superfund Amendments and Reauthorization Act (SARA) in 1986. The more general hazardous waste management program was initialized earlier under the Resource Conservation and Recovery Act (RCRA) in 1976.

To comply with these statutes and regulations, a number of technologies have been developed and tried in the treatment of wastes including contaminated soils, hazardous industrial wastes, sludges, process residues, ashes and sediments. Varied treatment technologies for the decontamination of soils have been tried including

incineration of the entire soil mass, thermal desorption with secondary collection or treatment, biological treatment, photo-degradation, solidification, in addition to in-situ washing or air stripping. Among these, the thermal desorption/treatment technology has been considered as one of the most feasible technologies because of the high degree of effectiveness for volatile organics, combined with reasonable energy and equipment costs and relatively rapid process time.

B. Objective

In spite of wide acceptance and application of thermal desorption / treatment technologies for soil decontamination and reclamation, there is little known about the mass transfer principles of organic contaminants through the heated soil matrices and more importantly exactly what limitations the process has, with respect to operating parameters and mass transfer properties of target organic compounds. The main objective of this study is to elucidate mass transfer mechanisms and equilibrium behavior of volatile organic substances in soil matrices through a combined experimental and model development program.

This includes:

experimental study of

- chromatographic response analysis through plug flow deposition on a soil column
- soil contamination/desorption experiments

- vapor/soil equilibrium measurements

and development of model for

- chromatographic response analysis for plug flow deposition on a soil column
- prediction of effluent concentration and intraparticle concentration profile in a packed soil column

Chapter 2. LITERATURE REVIEW AND THEORETICAL BACKGROUND

A. Significance of Soil Contamination by Hazardous Compounds

The introduction of hazardous chemicals into the soil environment may occur as a result of process effluents, landfill and/or dumping, spills, transportation, or release from storage facilities (1). It is quite recent, early eighties, that people started to recognize either a direct public health concern or indirect impact to environment including groundwater contamination, from the contaminated surface soils (2-4).

It is true that the land has been considered as a final solution for either municipal solid waste (MSW) or hazardous waste. One survey indicates that in 1989, the United States generated about 270 million tons of MSW of which 83.5 to 83.9 percent was sent to landfills, 7.8 to 7.9 percent was processed through incinerators and 8.3 to 8.6 percent was recycled (5). Hence, it can be said that approximately 225 million tons of MSW is still introduced to soil environment annually. On the other hand, the U.S. EPA estimated that 247 million metric tons of hazardous waste subject to regulation under RCRA are generated annually (6). Most of it is treated on site by large companies, but commercial facilities handling hazardous waste generated by others, disposed of 7 million metric tons in 1985. These numbers, however, show only the current status; a significant number of sites had been contaminated without any safety precautions

or protection of the environment before legal actions controlling these substances were initiated in the early eighties.

Besides landfill/dumping, the soil environment has been exposed to many different pollutant sources such as spills (7,8), accidents (9), leakage from facilities including underground storage tanks (USTs) (10), waste disposal pits (11), and long-term deposition on the surface from process emissions (12).

To protect soils and groundwater from contamination by hazardous substances, significant efforts have been made including double-lined landfill requirements, strict regulations on USTs (13) and even land bans which have arrived to the final third stage using hard hammer in 1990. Legal actions, on the other hand, were responsible for initializing clean-ups of Superfund sites under CERCLA of 1980 and the following SARA of 1986.

Along with its legal actions, the U.S. Environmental Protection Agency (EPA) has defined a National Priorities List (NPL) for identifying candidate Superfund sites (14). As of July 1989, 30,844 sites had been identified as candidates for potential hazardous waste classification and 9,902 site investigations have been completed (15). Those sites posing the greatest potential hazard and requiring significant long-term action under Superfund have been assessed for placement on the NPL. By July 1989, there were 1,173 sites on the EPA's priority list of hazardous waste sites, among which 890 were final sites. Thomas Grumbly of Clean Sites, Inc., a non-profit organization estimated $ 30 billion to accomplish the clean-up (16). Because the Superfund sites represent only part of the problem, the total expense for potentially hazardous sites will be a tremendous

amount.

While NPL remedial activities are undertaken, Superfund enforcement actions require Responsible Parties (RPs) to pay for, or undertake remediation activities at the sites. Part of expenses have, on the other hand, been compensated by cost recovery of the recovered material from contaminated sites. In 1989, Superfund was operated under a $ 1.5 billion budget for the year.

B. Treatment Technologies for Contaminated Soils

SARA authorized a comprehensive federal research program to improve the scientific and technical basis of the EPA's risk-management decisions at Superfund sites (14), and by December 1986, the Superfund Innovative Technology Evaluation (SITE) was formally established. Under this program, technologies were classified into four categories (17):

- alternative technology which includes any waste treatment and disposal technology other than land disposal and provides a permanent cleanup solution
- available technology which is an existing alternative technology whose safety, cost, and performance characteristics have already been proven in full-scale use
- innovative technology which is a fully-developed alternative technology for which cost and/or performance data are incomplete or unavailable, thereby hindering its direct use at hazardous waste sites

- emerging technology which is an alternative technology that is not yet fully developed and requires further research and development at the laboratory or pilot-scale levels

Although the SITE program was designed to accelerate the development of technology at every level, its primary focus was the demonstration program for fully-developed, innovative technologies. Technologies already tested in the field include: incineration/thermal treatment, solidification and stabilization, solvent extraction and biodegradation (14). Technologies accepted as innovative technologies in 1988 under SITE program included:

- microfiltration for removal of heavy metal and suspended solids in aqueous waste
- organic destruction using ultraviolet radiation and ozone
- in-situ steam or air stripping of volatile contaminants from soil
- soil washing for selected organics
- freeze crystallization to separate organics and inorganics from aqueous liquids or waste
- fixed-film biological treatment of aqueous waste with low organic concentration
- stabilization of metals or organics in soil and sludges
- other biological treatment

Technologies sponsored as emerging technologies under SITE program include (18):

- ultrafiltration with chemical treatment

- in-situ electroacoustic soil decontamination
- metal decontamination with algal sorbents
- constructed-wetlands treatment of degraded water for toxic metal removal
- laser stimulated photochemical oxidation of dissolved organics
- contained recovery of oily waste.

In fiscal year of 1988, EPA issued 111 Records of Decision (RODs) requiring control of site contamination sources. Among 74 technological treatments, 22 cases used incineration/thermal destruction while 18 cases utilized solidification/stabilization/ neutralization and 10 cases vacuum extraction, 7 cases volatilization/ soil aeration and so on (13). In incineration/thermal destruction, rotary kiln systems dominate its applications occupying ca. 80 % of remedial actions (2). Actual applications of incineration/thermal destruction in the sites can be found in many different cases as shown in references (3,7,9,19-21).

Most frequently identified substances at 546 Superfund sites are (22):

- trichloroethylene
- toluene
- polychlorinated biphenyls (PCBs)
- tetrachloroethylene
- arsenic
- chromium
- lead
- benzene
- chloroform
- phenol
- cadmium
- 1,1,1-trichloroethane

The demonstration sites under SITE program have been selected to match waste types to the technologies (17) and similarly, the technologies utilized in actual remediation of contaminated soils are generally chosen by the kinds of hazardous substances and situations of the sites.

C. Theoretical Background

Characteristics of Soils and Related Research

Soil is composite material comprised of minerals, air, water and various kinds of organic matters (23-25). Its main elements include Si, Al, O, Fe and their compounds, relative concentrations of salts, oxides and hydroxides constitute the soil. Their structures have consistent form and primarily include combination of tetrahedral silica units (Silica) and octahedral aluminum hydroxyl units (Gibbsite) according to the types of soil.

In the soil environment, its components exhibit various kinds of physical and chemical phenomena: gaseous diffusion, dissolution, adsorption/desorption, chemical reactions and biological deformation (26,27). Aluminosilicate layers of clays have also been known to catalyze reactions in numerous ways (28).

Recently, there have been a number of research efforts to understand the behavior of chemical substances in soil environment. Mass transport and detailed adsorption/desorption mechanism research was originally aimed at studying the transient behavior of chemicals

including pesticides, herbicides (29-32) and materials for agricultural purposes (33). They were also done to understand their fate and environmental impacts as well as the efficiencies for their own purposes.

Due to the variety of soil components that can influence adsorption, the organic carbon content has been recognized as an important factor governing the adsorption of organic chemicals in addition to distribution coefficients (34). In order to apply these concepts to understanding the behavior of organic substances in complex soil environment, a number of efforts have been made experimentally (35-44) and theoretically (45,46).

In spite of research on the mechanism of transport and equilibria of chemical substances in soil under environmental conditions, little effort has been made to the study of their behavior in soil matrices at elevated temperature important in the process of decontamination using incineration and other thermal treatment technologies.

The group of Pershing and Lighty has done some related research in this field. They utilized thin bed with depth of 1.3 cm (particle characterization reactor) to experimentally observe adsorption/ desorption behavior for p-xylene as a representative compound of gasoline (47). They initialized the observation of desorption for several adsorbent material such as glass beads, sand and clay at an ambient temperature to compare the desorption rates, indicating that more porous material such as clay showed slow decline curves in the desorption of p-xylene. They also varied temperature of the soil bed to observe the temperature effect on desorption rate of p-xylene. They pointed out that temperature is an important factor in desorbing

contaminated soils. From the adsorption data, they roughly compared isotherm models, observing that the trends more likely follow Freundlich isotherm rather than Langmuir isotherm. In the consecutive experiments (48), they utilized a soil bed with depth of 7.6 cm equipped with mass balance under it to measure mass change during experiment (bed characterization reactor). In this reactor, nitrogen gas was allowed to flow over the soil bed to desorb the contaminants from the bed and to observe the mass transfer and heat effect. Utilizing this soil bed, they observed experimentally the temperature effect on the evolution rate of p-xylene from the soil. They also varied the depth of bed to observe its effect on desorption rate, resulting in lower desorption rate for the deeper soil bed.

They also utilized batch-type bench-scale rotary kiln simulator to compare its desorption rate with those of reactors mentioned above. They observed that the desorption rate of their batch-type rotary kiln simulator is between those of the above reactors, however, closer to that of the particle characterization reactor due to the similarity between this system and kiln system.

Previous researchers in our group have done some preliminary studies performing pseudo chromatographic analysis for short columns and depletion decay curve from contaminated packed columns, where they tried to relate physical properties to the experimental results (49-51).

Chromatographic Analysis

Analytical solutions for the mass transfer behavior in a fixed

bed filled with small porous particles can be obtained by solving the mass balance equations by Laplace transformation (74). Although the solution of the model equation for a packed column in the Laplace domain is reasonably straightforward, inversion of the transform is usually difficult. Solutions for the moment of the response of a square pulse input can, however, be derived more easily from the solution in Laplace form.

Chromatographic response analysis in a fixed column involving diffusion terms inside particles was first performed by Kubin and Kucera (52-54). This was further extended to the case with chemical reaction of first order (55). This approach could be done by moment analysis incorporating van der Laan's theorem (56), in which average retention time and variance of the response for the pulse input can be estimated by differentiating the solution in Laplace form and taking limits to zero. Through this kind of approach combined with chromatographic data, values of mass transfer parameters including equilibrium constants can be estimated.

The fundamental chromatographic theory has been widely adopted, modified and/or further developed for specific purposes. Smith and Suzuki et al. utilized this method to determine adsorption rate constants from experimental data. They performed estimation of mass transfer rate constants of ethane, propane and n-butane in silica gel (57), and also did kinetic studies involving first order reaction on the surface of solid phase (58), axial dispersion studies for small particles (59), adsorption of gases on molecular sieving carbons (60), adsorption of carbon dioxide on carbon particles (61), tortuosity factor study in catalyst pellets (62), and intraparticle diffusion

coefficient measurements (63).

Another approach to study the diffusion inside particles was initiated by Haynes et al.(64-67). They introduced a bidisperse structured adsorbent or catalyst concept which can be applied to catalysts manufactured by making finely powdered microporous catalyst material into a pellet (64). This approach was tested by applying numerical values (65), and experiments were performed to verify this concept through measurements of diffusion of hydrocarbons in zeolite (66,67).

Heat effects in the pulse gas chromatography was also studied along with experimental data (68). In this paper, the effect of heats of adsorption on the nonisothermality of the chromatographic system was discussed, indicating that very minor effect was observed and the isothermality assumption is evidently quite good. Ruthven et al. also tried chromatographic analysis method to study the diffusion of hydrocarbons in zeolites (69,70).

Effluent Concentration Prediction

Prediction of concentrations at the effluent fluid stream from a fixed column has traditionally been an ongoing and valuable research area. A straightforward chromatographic theory describing the basic mass transfer in a packed column was first tried by deVault, incorporating disturbance propagation through the column (71) and it was further extended to multiple adsorption (72). Analytical solutions for the breakthrough curve in a fixed bed for linear and isothermal systems were developed later for more complicated cases and

these are well summarized in reference (73).

Solutions for the transient behavior of adsorbates in an adsorption column incorporating intraparticle diffusion terms were activated by extensive mathematical studies of Rosen (74,75). This approach was further developed by Rasmuson et al. incorporating dispersed plug flow (76,77) and chemical reaction of first order on the particle surface was also considered in the adsorption system (78,79).

Bi-disperse or macropore-micropore diffusion inside particles with external film resistance was involved in the modeling work by Kawazoe and Takeuchi (80) and dispersed plug flow was added to this system by Rasmuson (81). This method was utilized by Ruthven et al. (82-85) in the prediction of breakthrough curve for molecular sieve adsorption columns. An analytical solution of impulse response curve for adsorption column has also been tried analytically in time domain (86).

In spite of the complexity of the real systems and their solutions where multi-stage diffusion and various kinds of mass transfer resistance are considered, less sophisticated models are sometimes believed to yield good approximations to effluent concentrations in specific cases such as linear equilibrium systems (73).

A numerical approach has also been tried to study adsorption columns, as computers are being developed at an unexpectedly rapid pace. The orthogonal collocation method was applied to the simulation of transient behavior of catalytic tubular reactors (87,88) utilizing the methods developed largely by Villadson (89) and

Finlayson (90). Liapis et al. utilized general empirical equations for the adsorption isotherms whose constants were obtained from a finite bath with agitation to mix particles well in a liquid and used same numerical method to solve the appropriate partial differential equations (91-93).

An additional numerical simulation for the adsorption column system with linear equilibrium between outer surface of particles and fluid phase was tried by Raghavan and Ruthven, using the same method as above and they applied this to studying a pressure swing adsorption processes (94,95).

Recently, a faster numerical simulation method, so called Fast Fourier Transform algorithm, was applied to the adsorption column system (96), resulting in much faster prediction of linear adsorption processes than conventional methods.

The development of powerful computers and their wide usage with easily accessible software is expected to accelerate the application of more complicated adsorption system models.

Chapter 3. EXPERIMENTAL METHODS

A. Plug Flow Deposition Experiment

System Description

A gas chromatograph and data acquisition apparatus have been utilized for the chromatographic response analysis experiments. This system is outlined in Figure 3-1. The gas chromatograph used here is Shimadzu model GC8A. Signals generated by the flame ionization detector (FID) from a plug of 0.5 μl injected onto the soil column were integrated using a Hewlett Packard integrator model HP3396A and the converted digital data were manipulated using an installed HP basic program. A series of raw signal data were stored as bunched signal data in internal memory of the integrator in order to save memory space and to expand running time. A data display program and a data manipulating program to obtain average retention time and variance from chromatograms were developed and are listed in Appendix 1.

A data storage unit (a personal computer with a serial port) to store data on diskettes for further analysis was connected to the integrator through a RS-232-C cable. A software program provided by Hewlett Packard was installed in the personal computer to communicate with the integrator for data sending and retrieval.

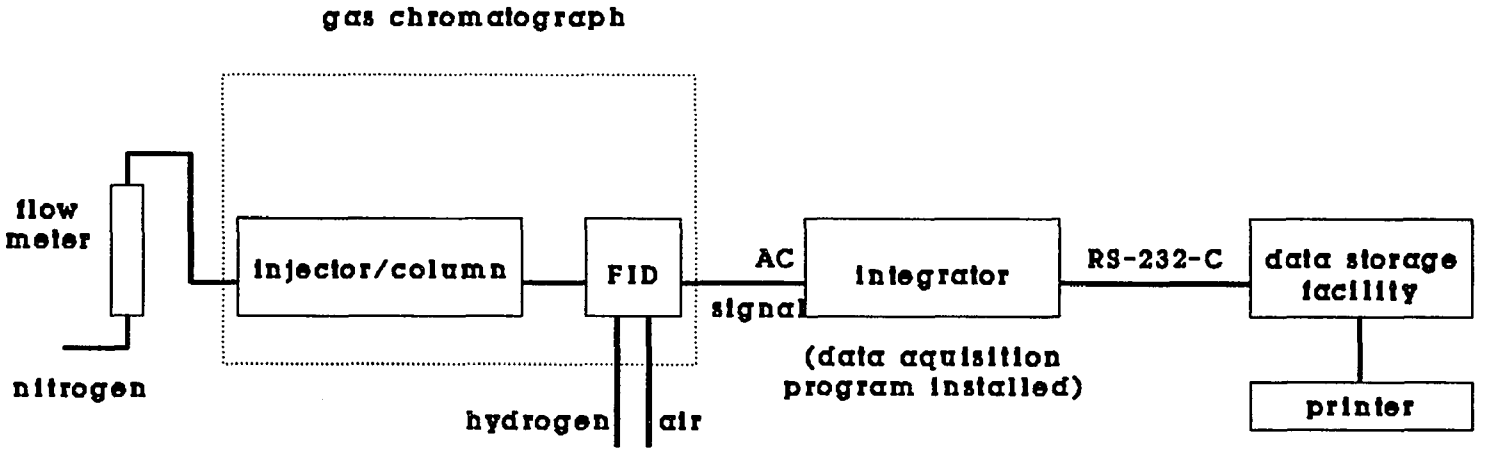

Figure 3-1 System Outline of Equipment for Plug Flow Deposition Experiments

Soil Column Preparation

Soil columns used here were prepared using surface soil stock prepared by Chemburkar and Horsby (49,50). They have taken ground top soil from locations around the New Jersey Institute of Technology and treated it to obtain clean stock soil. Detailed treatment procedure appears in their theses.

Particle size distribution of stock soil is as shown in Table 5-2. Narrow range of soil size was selected using sieve plate numbers 35 and 40 (U.S. Standard Testing Sieve, ASTM-11, Soil Test, Lake Bluff, Il). A stainless steel tube with 5.0 mm I.D. and 6.4 mm O.D. was used as column tubing (GC column). The column was packed with previously prepared soil by applying several gentle taps on it and sealed at both ends of the column with glass wool. The amount of soil packed was determined from the weight difference. The soil column was then cleaned in an oven at a temperature up to 350°C at least 4 hours while pure nitrogen gas was allowed to flow through the column.

Before the experiments, readings of flow meters (rotameters) were calibrated at operating temperature ranges using a bubble flow meter at the end of the column.

Experimental Procedure - Plug Flow Deposition

A series of chromatographic response experiments were performed by varying soil bed temperature and purge gas flow rate. A plug of 0.5 μl volume of the target compound was injected onto the soil (chromatography) column. Chemical compounds used here are chloroform,

methylene chloride, carbon tetrachloride, 1,1,1-trichloroethane, benzene, toluene, chlorobenzene and 1,2,4-trichlorobenzene. Their boiling points range from 40°C to 213°C and detailed values of boiling points are listed in Table 5-3. The purity of organics used was HPLC level or higher in most cases. Along with usual chromatogram analysis in the integrator, generated bunched data were manipulated using the developed HP basic program to estimate average retention time and variance for the chromatogram, and stored in the personal computer using data communication program software.

Operating temperature was changed in 20°C increments. Remaining fraction after one hour of operation at a specific temperature and carrier gas flow rate was checked by increasing the temperature (ca. 100°C higher than the operating temperature) and comparing the fractions eluted. Nitrogen gas flow rate was also changed to estimate mass transfer coefficients at a temperature of mostly ca. 20°C higher than the Minimum Allowable Temperature (MAT), a temperature we have defined in this work. Carrier gas flow rate ranged approximately 4 to 20 cc/min. To take into account the effect of dead volume in front of and after the soil column, the dimensions of each connector were measured and experiments without the column were performed. The results provided experimental information on the dead volume and were considered in the data manipulation stage of each run.

B. Soil Column Contamination/Desorption Experiment

System Description

This experiment apparatus is composed of a gas bubbler, a soil column and a data acquisition unit. Outline of this system is described in Figure 3-2. A gas bubbler containing glass beads was utilized to supply constant concentration of the target organic pollutant in the gas stream to the soil column. The depth of organics in the tube saturator was maintained at approximately 5 cm during the process. A six-way valve was used to change the flow to the inlet of the column bypassing the saturator, thus determining the stage of adsorption or desorption. A flow diagram of the six-way valve is shown in Figure 3-3.

Remaining components of the apparatus are similar to those of plug flow deposition experiments except the data manipulating software programs.

Experimental Procedure - Soil Column Contamination/Desorption

Continuous flow of vapor in carrier gas was utilized for the contamination of the soil column until saturation was reached while pure nitrogen gas flow was utilized for the column desorption. Soil columns for this experiments were prepared in the similar way to those of plug flow deposition experiments. A moderate flow rate of pure nitrogen gas was allowed to form fine bubbles at sufficient pressure to pass through the soil column. Before the experiments, gas flow

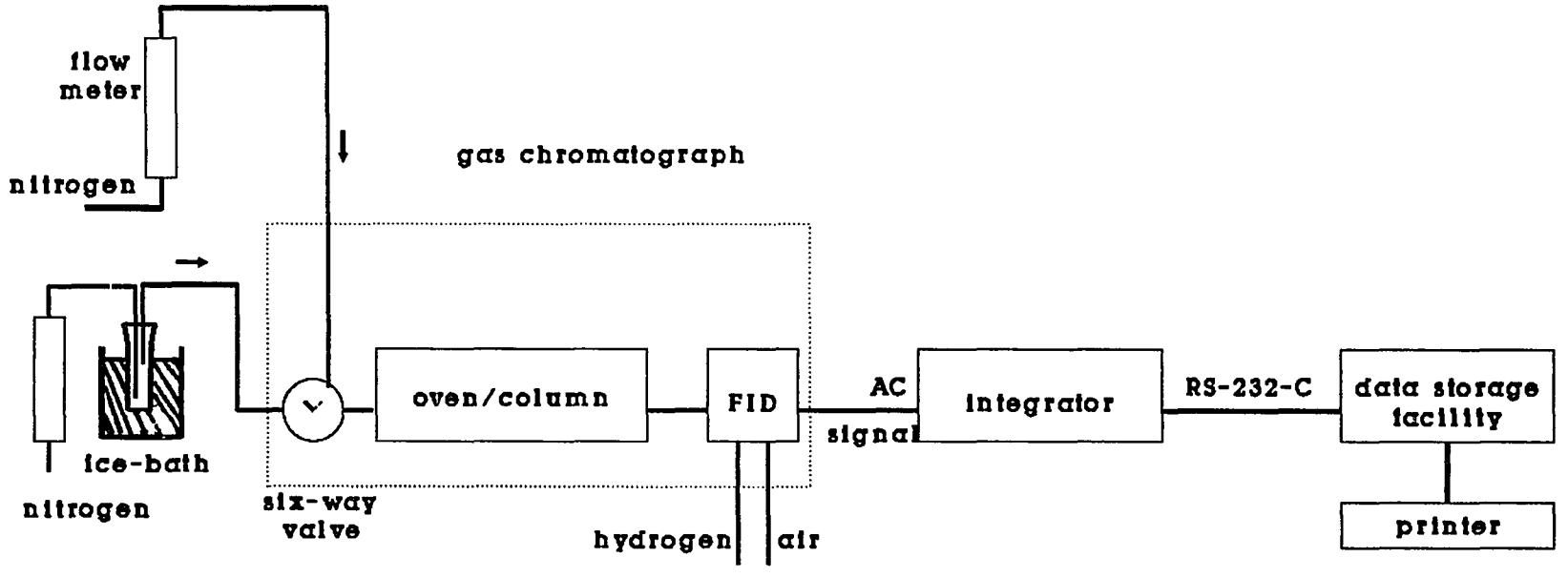

Figure 3-2 System Outline of Equipment for Soil Contamination/Desorption Experiments

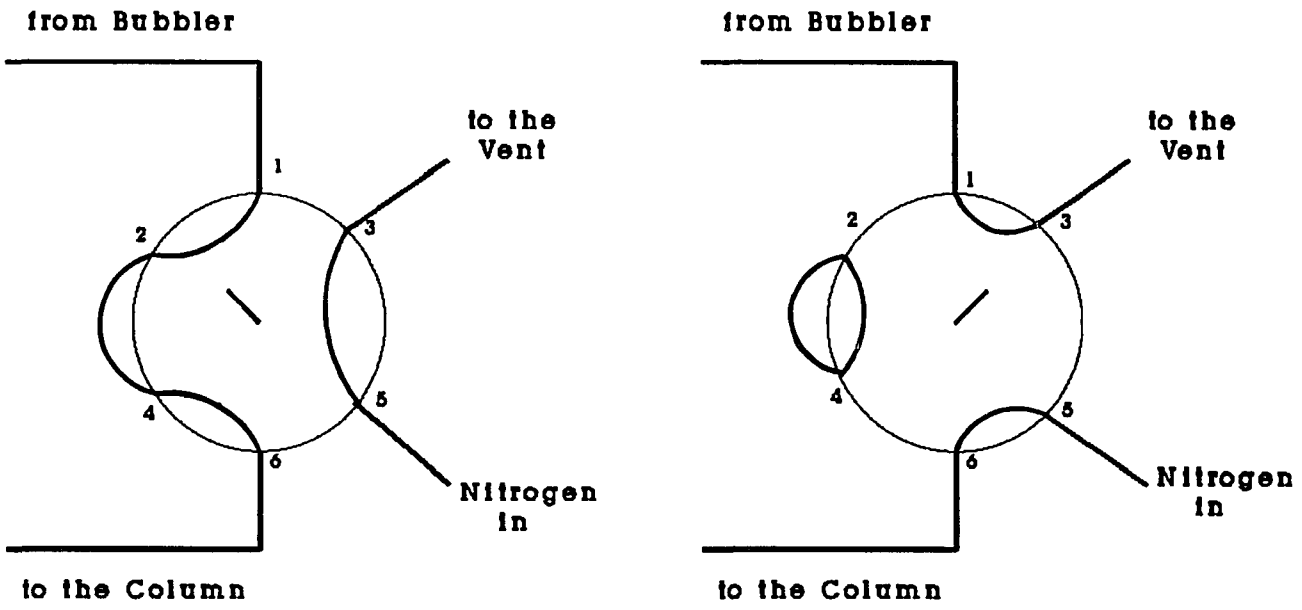

Figure 3-3 Flow Diagram of 6-Way Valve in Soil Contamination/Desorption Experiments

rates were calibrated using a bubble flow meter and rotameters for both of the continuous contamination and desorption stage of the column operation.

For the contamination stage, the valves and switches were turned to the contamination positions after the system was operated with purge of pure nitrogen until a constant oven temperature was reached. Signals from the FID were then recorded and observed until the outlet concentration of the column reached an asymptotic value. Bunched digital data were then saved in a diskette of the data storage facility for further analysis.

Desorption experiments started by changing the six-way valve position to bypass the saturator after the system conditions were stabilized. The same data management procedure as in the contamination process was followed to obtain data files for desorption experiments. Saturation and desorption experiments generally required 10 to 20 minutes to complete, depending on the operational conditions.

C. Soil Equilibrium Test

System Description

Quantitative amount of the target pollutants was added to or removed from a known volume of constant temperature soil bed apparatus and the absolute vapor phase or pollutant concentrations were then determined after equilibrium was achieved at each concentration.

The Soil equilibrium test system consists mainly of a heated injection and sampling unit, a ten-way valve, an equilibrium chamber and a magnetically-coupled micropump. This system is outlined in Figure 3-4. A magnetically-coupled metering gear pump (Cole Parmer, Concord, CA, pump head model 000-361, motor: 0-500 rpm, 0.01 hp, max. flow of 20 ml/min.) and a speed controller (Cole Parmer model 2630) were used to circulate the gas at low flow rates. Speed controller settings were calibrated using rotameters and a bubble flow meter. The injection and sampling port was heated and maintained at a temperature approximately 30 °C higher than boiling point, high enough to vaporize organic chemicals injected.

The temperature was measured through type-K thermocouple/reader (Omega 650, Stamford, CT) and controlled using autotransformer (Variac W5MT3, Concord, MA) supplying voltage (ca. up to 115 volts) to heating tapes. Detailed flow diagram of ten-way valve is shown in Figure 3-5. It contains two loops of length of 115 cm and 4.7 mm I.D. which act as a premixing chamber in phase I (adsorption phase) and as a pure nitrogen gas supplying unit by switching over the valve in phase II (desorption phase).

The equilibrium chamber was made of conical aluminum flanges (flange size of ISO NW 40 to 50), aluminum adapters (stub tapped 1/4″ NPT female, flange size of ISO NW 40), aluminum centering rings (flange size of ISO NW 50 for the connection of the middle part and ISO NW 40 for the connection of the both ends) with viton O-rings and aluminum clamps (wing nut and screw closure, flange size of ISO NW 50 and NW 40) connecting these components (HPS, Corp., Boulder, CO) which are generally used in vacuum devices.

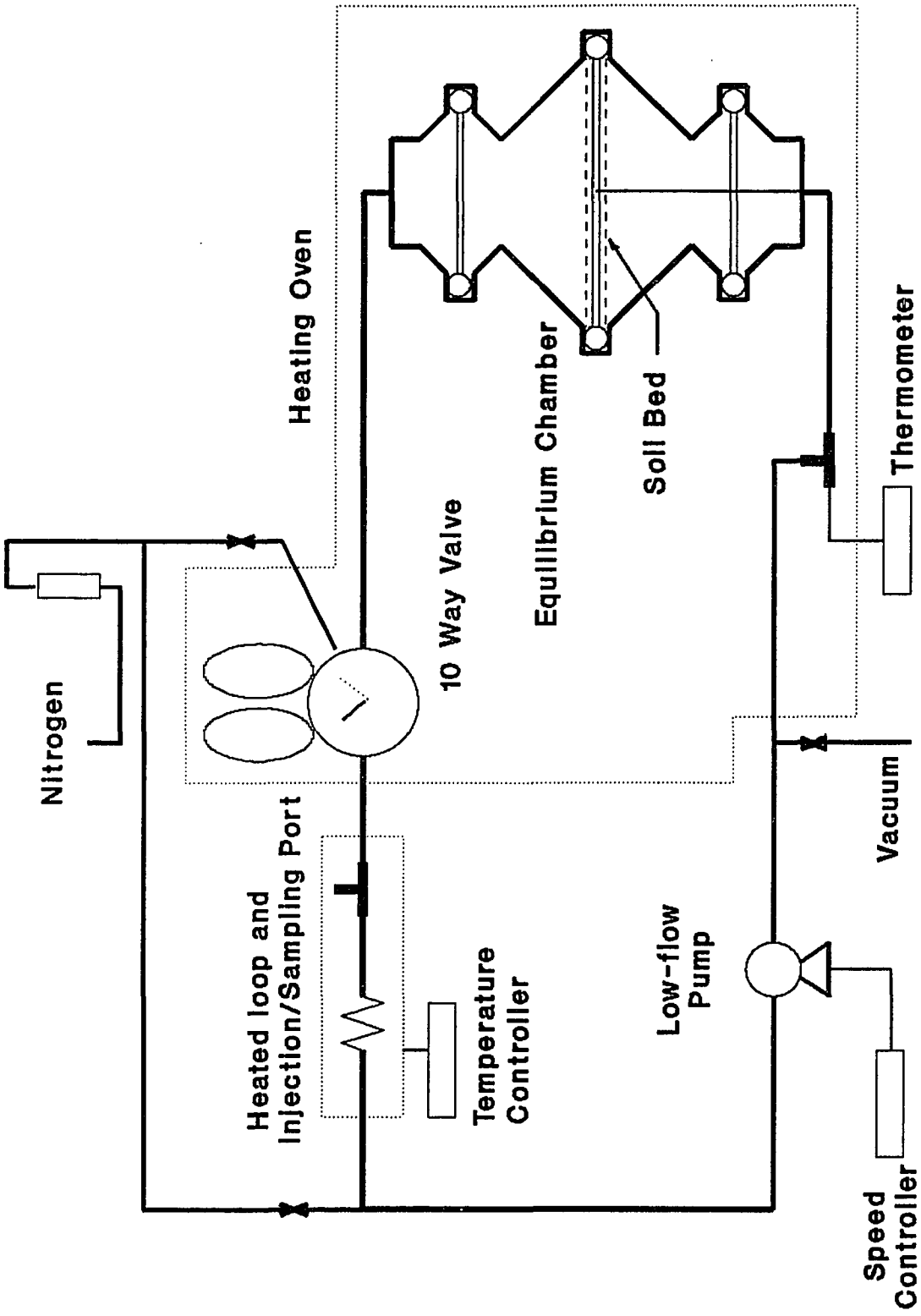

Figure 3-4 Soil Equilibrium Test System

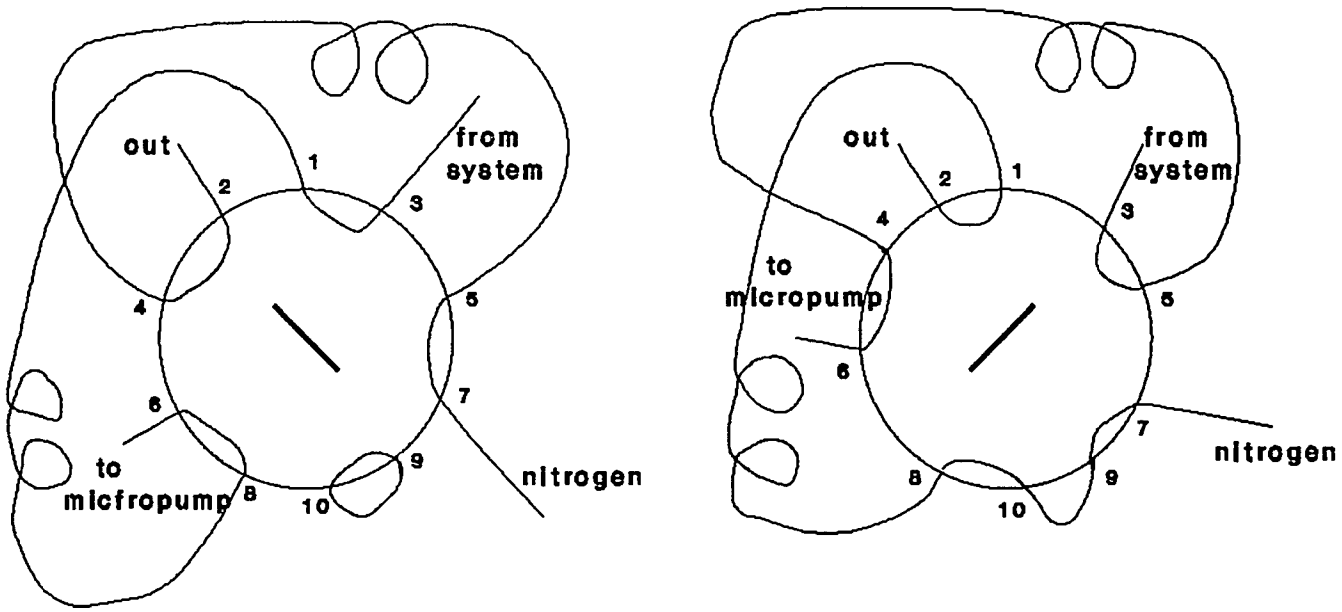

Phase I

Phase II

Figure 3-5 Flow Diagram of 10 Way Valve in Soil Equilibrium Test System

A soil bed was secured by replacing phosphor-bronze 49 mm diameter of mini-sieve inserts (Bel-Art Products, Pequannock, NJ) between the reducer surface and seals. Mesh numbers of sieves were 80/120. Amount of soil loaded was ca. 18 - 20 grams. A K-type thermocouple lead was installed at the center of soil bed with depth of 8 mm to monitor soil bed temperature accurately and connected to a thermocouple/meter (Omega T/C, Stamford, CT).

System components including a ten-way valve with loops and equilibrium chamber were installed in a gas chromatograph oven which is used as a constant temperature heat bath. Vacuum was connected to the system line near the chamber to evacuate any remaining hazardous organic compound after each run.

Sampled gas (sample size = 3.0 cc) taken by a gas syringe during the operation was analyzed and quantified in the Shimadzu gas chromatograph. Organic chemicals selected in this experiment include chloroform, methylene chloride, carbon tetrachloride, benzene, 1,1,1-trichloroethane and trichloroethylene.

Experimental Procedure - Soil Equilibrium Test

Prior to the equilibrium experiments, vacuum was applied to the total system, then flow of pure nitrogen was allowed while circulating it by the micropump until the concentration level of the gas phase inside the system decreased below the detection limit.

System calibration was done by adding certain amount of organic compounds (at least three replicates) through the injection and sampling port and analyzing gas phase concentration after a minimum of

30 minutes circulation at a moderate flow rate (approximately 10.0 cm^3/min.). From the data obtained here, standard calibration curves (chromatograph response vs. gas phase concentration) could be prepared.

For the adsorption experiment, a thermocouple was inserted through the mini-sieve. Weighed soil mass was then carefully loaded and all components were connected tightly and the system was verified not to leak. The soil used was pretreated in a separate oven at temperature of 200°C at least 4 hours. After the soil bed temperature reached the test temperature and the system is allowed to operate in the adsorption phase, the organic compound was injected slowly in 1.0 microliter units using micro syringes into the gas stream through the injection and sampling port. The system was then allowed to reach equilibrium (at least one hour). Gas phase concentration was determined by sampling gas at the sampling port by a gas syringe and analyzing it in the gas chromatograph immediately. Additional amounts of the target organic compound were then applied to the system and analyzed repeatedly until a satisfactory adsorption isotherm could be finally obtained. Soil was changed for every different temperature test.

For the desorption experiment, the soil bed was first contaminated following the procedure described in the adsorption process. The concentrations of both phases were then calculated by the mass balance. After the position of the ten-way valve was changed to replace a known volume of contaminated gas phase with pure nitrogen, the micropump was operated to circulate the gas phase to reach equilibrium and samples were taken from the sampling port using

a gas syringe and analyzed in the GC. This procedure is similar to that of the adsorption experiments except for the steps of depleting target organic compounds from the system, in place of adding compounds to the system.

Chapter 4. MODEL DEVELOPMENT

A. Chromatographic Response of a Soil-Packed Column

1. Chromatographic Response of a Porous Soil Matrix Column

Since the 1960's when the chromatographic response analysis technique was developed by Kubín and Kučera (52,54), a significant number of varied applications have been applied both experimentally and theoretically to explain different specific systems. Many authors have used different definitions of terms and different mass transfer mechanisms for their own analysis. One should, therefore, be careful in utilizing expressions of others' to be sure that they are appropriate to the experiment or model. A derivation is outlined here for the chromatographic response of a packed soil column. In developing the chromatographic response equation, basic mass transfer steps involved are as follows:

(a) Axial dispersion of components along the column axis.
(b) Diffusion from the main fluid phase to the particle surface or external film diffusion.
(c) Diffusion through the pore space inside individual particles or intraparticle diffusion.
(d) Adsorption/desorption of components between gas phase of the the intraparticle pore space and particle surface. Direct equilibrium was assumed because the adsorption process is rapid

and the accuracy of estimated adsorption rate constant is uncertain (57).

Mass balance equations for the adsorbing component can be set up and rearranged as below.

Mass balance for the gas phase in the column gives :

$$D_L \frac{\partial^2 C}{\partial z^2} - v \frac{\partial C}{\partial z} - \frac{3(1-\theta_b)}{\theta_b R_p} N_{Rp} = \frac{\partial C}{\partial t} \qquad (1)$$

$$\text{where } N_{Rp} = D_p \left(\frac{\partial C_i}{\partial r} \right)_{r=Rp} = k_f \left[C - C_i|_{Rp} \right] \qquad (2)$$

and mass balance inside particles gives :

$$D_p \left(\frac{\partial^2 C_i}{\partial r^2} + \frac{2}{r} \frac{\partial C_i}{\partial r} \right) = \theta_p \frac{\partial C_i}{\partial t} + (1-\theta_p) \frac{\partial C_p}{\partial t} \qquad (3)$$

with boundary and initial conditions :

$$\left. \frac{\partial C_i}{\partial r} \right|_{r=0} = 0 \qquad (4)$$

$$C_i |_{t=0} = 0 \qquad (5)$$

$$C\ (0,\ 0 \le t \le \tau) = C_o \quad (= 0, \text{ otherwise}) \qquad (6)$$

$$C\ (\infty, t) = 0 \qquad (7)$$

$$C\ (z, 0) = 0 \qquad (8)$$

Here, C = concentration of adsorbing component in the interparticle space in the column, g/cm^3

C_i = concentration of adsorbing component in the intraparticle pore space, g/cm^3

C_o = concentration of adsorbing component in the square input, g/cm^3

r = distance from the center of a particle in the radial direction, cm

z = distance from the inlet of the column, cm

v = linear velocity of the carrier gas in the interparticle space, cm/sec.

t = time, sec.

R_p = radius of a particle, cm

D_L = axial dispersion coefficient, $cm^2/sec.$

D_p = intraparticle diffusion coefficient, $cm^2/sec.$

k_f = mass transfer coefficient in the external film of particle, cm/sec.

C_p = concentration of adsorbing component in the solid phase, g/cm^3

θ_b = interparticle void fraction in the column

θ_p = intraparticle void fraction inside particles

τ = time for the input square pulse

The Laplace transform can be taken on these equations in order to obtain expressions for concentrations at the column outlet in the Laplace domain. Moment analysis technique can, in addition, be utilized so as to have solutions for the absolute and central moments. A more thorough and detailed derivation is presented in Appendix 2.

As a result of this derivation, the first absolute moment can

be obtained as follows:

$$\mu_1 = \frac{\tau}{2} + \frac{L}{v}\left[\,1 + \left(\frac{1-\theta_b}{\theta_b}\right)\theta_p\,(1+K_a)\,\right] \tag{9}$$

where μ_1 = the first absolute moment (physically average retention time or center of mass)

L = length of the adsorption column

K_a = adsorption equilibrium constant defined by

$$K_a = (1-\theta_p)\,C_p \,/\, \theta_p\,C_i \tag{10}$$

while the second central moment could be expressed as follows:

$$\mu_2' = \frac{\tau^2}{12} + \frac{2LD_z}{v^3}\left[\,1 + \frac{1-\theta_b}{\theta_b}\,\theta_p\,(1+K_a)\,\right]^2 + \frac{2}{15}\frac{L}{v}\frac{R_p^2}{D_p}\frac{1-\theta_b}{\theta_b}\,\theta_p^2\,(1+K_a)^2 + \frac{2}{3}\frac{L}{v}\frac{R_p}{k_f}\frac{1-\theta_b}{\theta_b}\,\theta_p^2\,(1+K_a)^2 \tag{11}$$

where μ_2' = the second central moment (physically variance of the chromatographic response)

The above first absolute and second central moment describe the center of mass or average retention time and the variance of the response for the impulse input to the column respectively in the chromatographic response experiment.

These results are consistent with other published expressions (57,58) when different definitions of equilibrium constants are used and the effect of adsorption rate term is considered with the

assumption of no chemical reaction on the particle surface.

2. Chromatographic Response for a Non-Porous Soil Matrix Column

Chromatographic response for non-porous material like sand shows different behavior due to its structural difference. Although mass transfer mechanism is same in the interparticle region, there is no intraparticle diffusion effect and adsorption equilibrium takes place on the surface of particles, instead. Mass transfer governing an adsorption column can be expressed in one differential equation as follows:

$$D_L \frac{\partial^2 C}{\partial z^2} - v \frac{\partial C}{\partial z} - \frac{(1-\theta_b)}{\theta_b} \frac{3}{R_p} N_R = \frac{\partial C}{\partial t} \tag{12}$$

$$\text{where } N_R = k_f [\, C/K_b - (C_i)_{Rp}] = - \frac{\partial C_a}{\partial t} \tag{13}$$

K_b = equilibrium constant (cm), defined by

$$K_b = C_a/C' \tag{14}$$

C' = concentration of adsorbing component in the gas near the particle surface, g/cm^3

C_a = concentration of adsorbing component on the surface of particles, g/cm^2

The procedures for the Laplace transform and the moment analysis to get the first absolute and second central moment are almost the same as the previous case. A more detailed derivation appears in

Appendix 3. The resulting expressions for this case are as follows:

$$\mu_1 = \frac{\tau}{2} + \frac{L}{v}\left(1 + \frac{1-\theta_b}{\theta_b}\frac{3}{R_p}K_b\right) \tag{15}$$

$$\mu_2' = \frac{\tau^2}{12} + \frac{2LD_L}{v^3}\left(1 + \frac{1-\theta_b}{\theta_b}\frac{3}{R_p}K_b\right)^2 + \frac{L}{v}\frac{1-\theta_b}{\theta_b}\frac{6}{R_p}\frac{K_b^2}{k_f} \tag{16}$$

3. Estimation of Equilibrium Constants, Heats of Adsorption and Mass Transfer Parameters

For physical adsorption where there is only sufficiently low concentration of molecules where adsorbed molecules are isolated from their neighboring ones, the equilibrium relationship between fluid and adsorbed phase will be linear (73). This linearity can be expressed by Henry's law, in terms of concentration or pressure as follows:

$$q = K\,c \qquad \text{or} \qquad q = K'\,p \tag{17}$$

where q and c are concentrations of a component in the adsorbed and fluid phase and p denotes partial pressure of a component. From the ideal gas law, Henry's law constants have a relationship each other as follows:

$$K = K' R T \tag{18}$$

The temperature dependency of the Henry's constants obeys the van't Hoff equation:

$$\frac{d\ ln K'}{dT} = \frac{\Delta H_o}{RT^2} \tag{19}$$

where ΔH_o represents enthalpy difference between adsorbed and gaseous phase, or heat of adsorption and R is gas-law constant.

This can be integrated to give

$$K' = K'_o \exp\left[- \frac{\Delta H_o}{RT} \right] \tag{20}$$

Utilizing equation (18), this can be expressed in terms of K :

$$\frac{K}{T} = \left[\frac{K}{T} \right]_o \exp\left[- \frac{\Delta H_o}{RT} \right] \tag{21}$$

Plots of *ln* (K/T) vs. 1/T can, then, be used to obtain heats of adsorption from the slopes.

On the other hand, equilibrium constants can be estimated from the first moment, or average retention time by equations (9) or (15). Mass transfer parameters can also be estimated by utilizing the first absolute moment and the second central moment as shown below.

For the adsorption column system with intraparticle diffusion,

equations (9) and (11) can be combined and simplified with the notation change of μ_2' to σ^2 and μ_1 to μ for convenience to give:

$$\frac{\sigma^2}{2\mu^2}\frac{L}{v} = \frac{D_L}{v^2} + \frac{\theta_b}{1-\theta_b}\left(\frac{R_p^2}{15D_p} + \frac{R_p}{3k_f}\right)\left[1 + \frac{\theta_b}{(1-\theta_b)\theta_p(1+K_a)}\right]^{-2} \quad (22)$$

From the slopes of plots of $\frac{\sigma^2 L}{2\mu^2}\frac{L}{v}$ vs. $\frac{1}{v^2}$, axial dispersion coefficient D_L can be estimated. From the intercepts of the plots, one can calculate values of intraparticle diffusion coefficient, D_p by using empirical equations for the values of film mass transfer coefficient k_f.

The same approach can be utilized for the case of an adsorption column system with no intraparticle diffusion. Equations (15) and (16) can be also combined and simplified to give :

$$\frac{\sigma^2}{2\mu^2}\frac{L}{v} = \frac{D_L}{v^2} + \frac{R_p}{3k_f}\frac{\theta_b}{1-\theta_b}\left[1 + \frac{R_p}{3}\frac{\theta_b}{(1-\theta_b)K_b}\right]^{-2} \quad (23)$$

Values of axial dispersion coefficients and film mass transfer coefficients can be obtained in the same manner as the previous case.

B. Analytical and Numerical Solution for the Effluent Concentration of a Packed Soil Column

1. Analytical Solution

Analytical solutions for the adsorption column system with intraparticle diffusion, longitudinal dispersion and film mass transfer resistance on outer surface of particles were tried and shown to be appropriate in early 80's by Rasmuson et al.(76,77). A simplified form of their result is used here with some modification of the terms and with the assumption of fast adsorption rate. Final solutions are as follows :

$$u(z,y) = \frac{1}{2} + \frac{2}{\pi}\int_0^{\infty} \exp\left[\frac{1}{2}Pe - \sqrt{\left(\sqrt{(z^2x')^2+(z^2y')^2} + z^2x'\right)/2}\right]$$

$$\sin\left[y\lambda^2 - \sqrt{\left(\sqrt{(z^2x')^2+(z^2y')^2} - z^2x'\right)/2}\right]\frac{d\lambda}{\lambda} \qquad (24)$$

where $z^2x' = Pe\,(\,1/4\,Pe + \delta\,H_1\,)$ (25)

$$z^2y' = \delta\,Pe\,(\,2/3\,\frac{\lambda^2}{R_1} + H_2\,) \qquad (26)$$

$$y = 2\,D_P\,t\,/\,K\,R_P^2$$

$$H_1 = \frac{H_{D1} + \upsilon\,(H_{D1}^2 + H_{D2}^2)}{(1+\upsilon H_{D1})^2 + (\upsilon H_{D2})^2} \qquad (27)$$

$$H_2 = \frac{H_{D2}}{(1+\upsilon H_{D1})^2 + (\upsilon H_{D2})^2} \tag{28}$$

$$H_{D1} = \lambda \left(\frac{\sinh 2\lambda + \sin 2\lambda}{\cosh 2\lambda - \cos 2\lambda}\right) - 1 \tag{29}$$

$$H_{D2} = \lambda \left(\frac{\sinh 2\lambda - \sin 2\lambda}{\cosh 2\lambda - \cos 2\lambda}\right) \tag{30}$$

with parameters of

$$Pe = \frac{Lv}{D_L}, \text{ Peclet Number} \qquad \delta = \frac{\gamma L}{mv}$$

$$\upsilon = \gamma R_F \qquad R_1 = \frac{K}{m}$$

$$R_F = \frac{R_p}{3k_f} \qquad K = \theta_p + (1-\theta_p)K_a$$

$$\gamma = \frac{3D_p}{R_p^2} \qquad \lambda = \text{variable of integration}$$

$$m = \frac{\theta_b}{1-\theta_b}$$

In order to estimate the infinite integral term in equation (24), a numerical method was utilized. For this integration in semi-infinite interval, one of IMSL software (QDAGI) was utilized, which uses Gauss-Kronrod rule to estimate the integral and the error (97). A detailed program listing is presented in Appendix 4.

2. Numerical Solution

Solution of boundary value problems by the orthogonal collocation method was initiated by Villadson and Finlayson in the late sixties and has been applied to the explanation of the mass transfer phenomena in adsorption columns. Some of basic principles are shown in reference (90).

From mass balance equations for the contaminants in the interparticle fluid phase :

$$\frac{\partial c}{\partial t} = D_L \frac{\partial^2 c}{\partial z^2} - v\frac{\partial c}{\partial z} - \frac{1-\theta_b}{\theta_b}\frac{3k_f}{R_p}\left(c - c_i|_{r=R} \right) \tag{31}$$

with boundary conditions,

$$D_L \frac{\partial c}{\partial z}\Big|_{z=0} = - v \left(c|_{z=0} - c|_{z=0+} \right) \tag{32}$$

$$\frac{\partial c}{\partial z}\Big|_{z=L} = 0 \tag{33}$$

and an initial condition,

$$c\,(z,0) = c_o \tag{34}$$

Equations (32) and (33) are the correct boundary conditions for a dispersed plug flow system as discussed by Wehner et al. (98).

From mass balance equations for the contaminants inside the particles :

$$\theta p \frac{\partial c_i}{\partial t} + (1-\theta_p)\frac{\partial c_p}{\partial t} = D_p\left(\frac{\partial^2 c_i}{\partial r^2} + \frac{2}{r}\frac{\partial c_i}{\partial r} \right) \qquad (35)$$

with boundary conditions:

$$\left.\frac{\partial c_i}{\partial r}\right|_{r=0} = 0 \qquad (36)$$

$$D_p \left.\frac{\partial c_i}{\partial r}\right|_{r=R} = k_f \left(c - c_i|_{r=R} \right) \qquad (37)$$

and an initial condition,

$$c_i\,(r,0) = c_{i_o} \qquad (38)$$

These equations could be expressed in dimensionless form and the orthogonal collocation method was then utilized to solve these partial differential equations combined with their boundary conditions. Boundary conditions for the column in equations (32), (33) and (37) were utilized to reduce the number of equations for collocation points following the expressions discussed by Finlayson (90). Derivation of this numerical approach is summarized in Appendix 5.

Final expressions are as following :

$$\frac{dQ_k^{(j)}}{d\tau} = \gamma \sum_{i=1}^{N} [\ B_{k,i} - \psi B_{k,N+1} A_{N+1,i}]\ Q_i(j) + P_o B_{k,N+1} C(j) \qquad (39)$$

$$j = 2,3,.....,M+1$$

$$k = 1,2,.....,N$$

$$\frac{dC(j)}{d\tau} = \sum_{i=2}^{M+1} \phi\ [\ (\frac{1}{Pe} B'_{j,i} - A'_{j,i}) + (\frac{1}{Pe} B'_{j,1} - A'_{j,1}) \times (\frac{A'_{1,M+2}}{\alpha} A'_{M+2,i} - \frac{A'_{M+2,M+2}}{\alpha} A'_{1,i}) + (\frac{B'_{j,M+2}}{Pe} - A'_{j,M+2}) \times (\frac{A'_{M+2,1}}{\alpha} A'_{1,i} - \frac{A'_{1,1} - Pe}{\alpha} A'_{M+2,i})\ ]\ C(i)$$

$$- Pe\ C|_{x=0-}\ \phi\ [\ \frac{A'_{M+2,M+2}}{\alpha} (\frac{1}{Pe} B'_{j,1} - A'_{j,1}) - \frac{A'_{M+2,1}}{\alpha} (\frac{1}{Pe} B'_{j,M+2} - A'_{j,M+2})\ ]$$

$$- \frac{3(\eta\phi\xi) \sum_{i=1}^{N} A_{N+1,i} Q_i(j)}{K\phi\xi + A_{N+1,N+1}} - 3(\eta\phi\xi) \frac{A_{N+1,N+1}}{K\phi\xi + A_{N+1,N+1}} C(J) \qquad (40)$$

$$j = 2,3,.....M+1$$

where M =the number of collocation points in the longitudinal direction

N =the number of collocation points in the radial direction in the particles

Other parameters and dimensionless variables are defined in the Appendix 5.

Coefficients of matrices in these equations are those generated from the values of collocation points in the longitudinal and intraparticle radial coordinates. The Gauss-Jordan method was utilized to obtain inverse matrices which are necessary in developing square matrices for the derivatives at collocation points (99). Detailed Fortran program lists of the developed program are shown in Appendix 6.

The above equations (39) and (40) are combined ordinary differential equations (ODE's) with initial conditions which are to be solved simultaneously to obtain the solutions. This has been done using an IMSL software called IVPAG which utilizes Adams-Moulton or Gear method (97). This program was run in VAX/VMS system in NJIT, by linking mentioned IMSL software and output from matrix manipulation program. A detailed Fortran program list for the solution of the ODE's is shown in Appendix 7.

Chapter 5. EXPERIMENTAL RESULTS

A. Chromatographic Response Analysis Results

Soil Bed Characterization and Properties of Chemical Compounds

As described in Chapter 3, an experimental apparatus has been designed to characterize the chromatographic response in a soil matrix column. The specification of this soil column is shown in Table 5-1. These data were obtained by direct measurement and from Wu et al (100,101).

Stock soil used in this system was analyzed by Labtech Corp., Fairfield, NJ, using emission spectroscopy and X-ray diffraction. This analysis provided a nearly complete mineral elemental characterization (49,50). Its major elements include Si, Al, X, Fe, K, Mg, and Mn by emission spectroscopic analysis and its detailed results are listed in Table 5-2. The major compounds detected by X-ray diffraction analysis after grinding the sample into a mesh size of less than 270, include silicon dioxide and feldspar (albite, andesine, anorthite, anorthodase or laboradorite). The last compound can be sodium silicate or calcium aluminum silicates (some of which contain potassium) or mixtures of the two.

Particle size distribution of stock soil has also been determined using sieve and a mechanical shaker (Humbolt Manufacturing Co.) and particle size distribution appears in Table 5-3. Mesh size range utilized in the chromatographic response analysis was 35/40 whose

Table 5-1. Soil Column Specification for Chromatographic Analysis Experiment

Specification		Value	
Column	length	13.1	cm
	diameter	0.50	cm
	cross-sectional area	0.196	cm^2
Soil	mesh size	35/40	
	average diameter	0.46	mm
	intraparticle porosity	0.13	
Soil bed	overall density	1.18	g/cm^3
	interparticle porosity	0.49	

Table 5-2. Emission Spectrographic Analysis Results of Stock Soil

Element	Range of Percent by Mass
Al	> 10 %
B	0.001-0.01 %
Ba	0.01-0.1 %
Ca	1.0-10.0 % (H)
Cr	0.001-0.1 %
Cu	0.001-0.01 %
Fe	1.0-10.0 %
K	1.0-10.0 %
Mg	0.1-1.0 %
Mn	0.1-1.0 % (L)
X	> 10 %
Ni	0.001-0.01 %
Si	> 10 %
Sr	0.001-0.01 %
Ti	0.1-10.0 %
V	0.001-0.01 %
Zn	0.01-0.1 %
Zr	0.001-0.1 %

Note:

1. (H) and (L) indicate high and low end of range.
2. Results are semiquantitative. Accuracy and sensitivity are element and matrix dependent.

Table 5-3. Particle Size Distribution of Stock Soil

Particle diameter (inches)	Mesh size	Mass grams	% of total	% of usable
-	7100	2000	6.9	-
-	100	2910	10.0	-
0.0086	70	480	1.7	4.5
0.0098	60	3200	11.0	29.8
0.0165	40	7060	24.3	65.7
-	<40	13,400	46.1	-
			100 %	100 %

Total mass	29,050 grams
Usable mass	10,740 grams
Bulk density	1.0 grams/cc
Actual density (by water displacement)	0.8 grams/cc

average diameter is 0.46 mm.

Flow rates of the column were calibrated prior to the experiments and dead volumes were also determined experimentally and compensated in the further analysis. An example is shown in Figure 5-1.

Types of organics used in this experiment are listed in Table 5-4 with their physical properties which will be used as basic data for further calculations. The range of boiling points of target organic compounds are 40°C to 213°C.

Vapor pressures of these organic compounds are also shown in Table 5-5. They range from 1.26 mmHg for p-dichlorobenzene to 353.4 mmHg for methylene chloride in vapor pressure at room temperature. In calculating vapor pressures at atmospheric conditions, the Antoine equation was utilized with data of parameters from references (102). As can be seen in Table 5-5, the range in volatilities of the compounds studied is significant and more importantly is relevant for soil decontamination studies.

Analysis Results of Plug Deposition Experiments

The moment analysis technique can be utilized to analyze the chromatographic response in a soil matrix column as discussed in Chapter 4. As a result of the derivation for the impulse deposition to the column (cf. Chapter 4 and Appendix 2 for detail), the first absolute moment for the center of mass can be obtained from equation (9) and can be rewritten as follows:

Figure 5-1. Calibration Curves for Flow Rate and Dead Volume for the Column in Plug Deposition Experiments

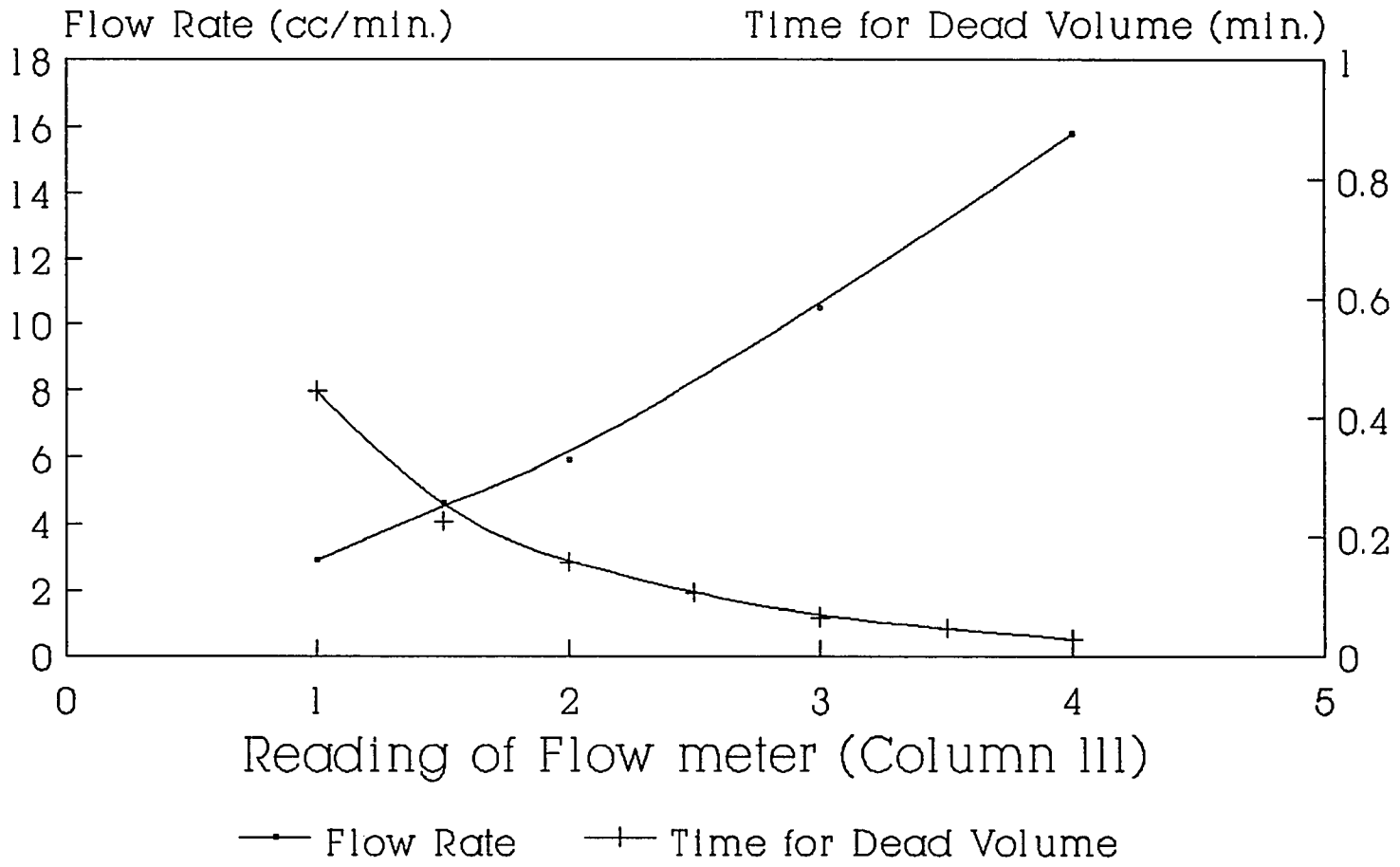

Table 5-4 Physical Constants of Selected Compounds

Compound	Empirical Formula	Formular Weight	Boiling Point °C	Density at 25°C g/cm^3
Methylene chloride	CH_2Cl_2	84.94	40.	1.318
Chloroform	$CHCl_3$	119.38	61.7	1.474
Carbon tetrachloride	CCl_4	153.82	77.	1.594
1,1,1-tri chloroethane	CCl_3CH_3	113.42	74.	1.336
Benzene	C_6H_6	78.11	80.	0.879
Toluene	$C_6H_5CH_3$	92.13	111.	0.866
Chlorobenzene	C_6H_5Cl	112.56	132.	1.107
1,2,4-Tri chlorobenzene	$C_6H_3Cl_3$	181.46	213.	1.463

Table 5-5. Vapor Pressure Calculation of Target Organic Compounds

Antoine vapor-presssure correlation (102)

$$ln\ P_{vp} = A - \frac{B}{T + C}$$

where P_{vp} : mm Hg , T :°K

Compound	T range	Parameter values*** A	B	C	P_{vp} at 273°K	293°K
Methylene chloride	229-332	16.3029	2622.44	-41.70	143.3	353.4
Chloroform	260-370	15.9732	2696.79	-46.16	59.5	155.7
Carbon tetrachloride	253-374	15.8742	2808.19	-45.99	33.2	90.5
1,1,1-Tri chloroethane*	302-428	16.0381	3110.79	-56.16	5.4	18.2
Benzene	280-377	15.9008	2788.51	-52.36	26.1	74.7
Toluene	280-410	16.0137	3096.52	-53.67	6.7	21.7
Chloro-benzene	320-420	16.0676	3295.12	-55.60	2.5	8.9
p-Dichloro benzene**	327-477	16.1135	3626.83	-64.64	0.27	1.26

note * Data of 1,1,2-trichloroethane were utilized.

** This calculation is for the comparison purpose only.

*** Data of parameters were obained from reference (102).

$$\mu_1 = \frac{L}{v} \left[1 + \frac{1-\theta_b}{\theta_b} \theta_p (1+K_a) \right] \qquad (41)$$

Equilibrium constants for the system, therefore, can be estimated from this equation and the computer program described in Appendix 1 to calculate the averaged retention time.

As described in Section A of Chapter 3, chromatographic analysis experiments were performed by varying soil column temperature and gas flow rate and analyzing the response curves.

Temperature for this experiments was changed in 20°C increments to observe the behavior of equilibrium constants according to temperature change. Temperature ranged from low's near the MAT's (minimum allowable temperatures, which will be defined shortly) to temperatures 60 to 80 °C higher than the MAT's. Experimental results were analyzed following the equation of the first absolute moment as described in equation (41). Values of the first absolute moment or the center of the mass (expressed as average retention time in an experimental concept) were obtained by analyzing chromatograms generated and stored as digital data files through an installed program in the HP integrator as mentioned above. Summarized results of this experiment for listed target organic compounds are shown in Table 5-6.

The van't Hoff equation as described in Chapter 4 was utilized to observe the temperature dependency of equilibrium constants and plots of *ln* (K_a/T) vs. 1/T can be found in Figure 5-2. The plots show good linearity and heats of adsorption are obtained with good accuracy as described below.

Table 5-6. Results for Equilibrium Constant Estimation from Chromatographic Analysis

Methylene chloride

Temperature °C	°K	10^3/T(K)	Corrected avg. retention time min.	Equilibrium constant K_a	*ln* (K_a/T)
100	373	2.681	3.806	234.54	- 0.464
120	393	2.545	1.744	109.41	- 1.279
140	413	2.421	0.976	61.31	- 1.908
160	433	2.309	0.612	37.77	- 2.439

Chloroform

Temperature °C	°K	10^3/T(K)	Corrected avg. retention time min.	Equilibrium constant K_a	*ln* (K_a/T)
100	373	2.681	1.846	111.09	- 1.211
120	393	2.545	1.202	73.11	- 1.682
140	413	2.421	0.624	36.53	- 2.425
160	433	2.309	0.444	25.37	- 2.837
180	453	2.208	0.310	15.82	- 3.355

Table 5-6. (continued)

Carbon tetrachloride

Temperature °C	°K	10^3/T(K)	Corrected avg. retention time min.	Equilibrium constant K_a	*ln* (K_a/T)
60	333	3.003	3.305	180.17	- 0.614
80	353	2.832	2.058	116.41	- 1.109
100	373	2.681	1.091	61.96	- 1.795
120	393	2.545	0.657	36.61	- 2.374
140	413	2.421	0.468	25.55	- 2.783

1,1,1-Trichloroethane

Temperature °C	°K	10^3/T(K)	Corrected avg. retention time min.	Equilibrium constant K_a	*ln* (K_a/T)
80	353	2.832	2.364	134.82	- 0.963
100	373	2.681	1.380	80.33	- 1.535
120	393	2.545	0.741	42.24	- 2.231
140	413	2.421	0.526	29.63	- 2.635
160	433	2.309	0.381	20.72	- 3.039

Table 5-6. (continued)

Benzene

Temperature °C	°K	10^3/T(K)	Corrected avg. retention time min.	Equilibrium constant K_a	*ln* (K_a/T)
100	373	2.681	2.240	135.0	- 1.016
120	393	2.545	1.434	88.65	- 1.489
140	413	2.421	0.840	51.73	- 2.077
160	413	2.309	0.532	31.87	- 2.609
180	433	2.208	0.376	20.76	- 3.083

Toluene

Temperature °C	°K	10^3/T(K)	Corrected avg. retention time min.	Equilibrium constant K_a	*ln* (K_a/T)
140	413	2.421	1.517	99.38	- 1.424
160	433	2.309	1.079	72.23	- 1.791
180	453	2.208	0.606	37.98	- 2.479
200	473	2.114	0.418	26.30	- 2.889
220	493	2.028	0.318	19.33	- 3.239

Table 5-6. (continued)

Chlorobenzene

Temperature °C	°K	10^3/T(K)	Corrected avg. retention time min.	Equilibrium constant K_a	*ln* (K_a/T)
140	413	2.421	2.260	151.68	- 1.002
160	433	2.309	1.410	96.66	- 1.500
180	453	2.208	0.905	60.37	- 2.015
200	473	2.114	0.574	38.88	- 2.450
220	493	2.028	0.423	28.15	- 2.863

1,2,4-Trichlorobenzene

Temperature °C	°K	10^3/T(K)	Corrected avg. retention time min.	Equilibrium constant K_a	*ln* (K_a/T)
220	493	2.028	1.294	101.33	- 1.582
240	513	1.949	0.942	74.96	- 1.923
260	533	1.876	0.625	49.38	- 2.379
280	553	1.808	0.451	35.12	- 2.757
300	573	1.745	0.329	24.74	- 3.143

Figure 5-2. Temperature Dependence of Ka

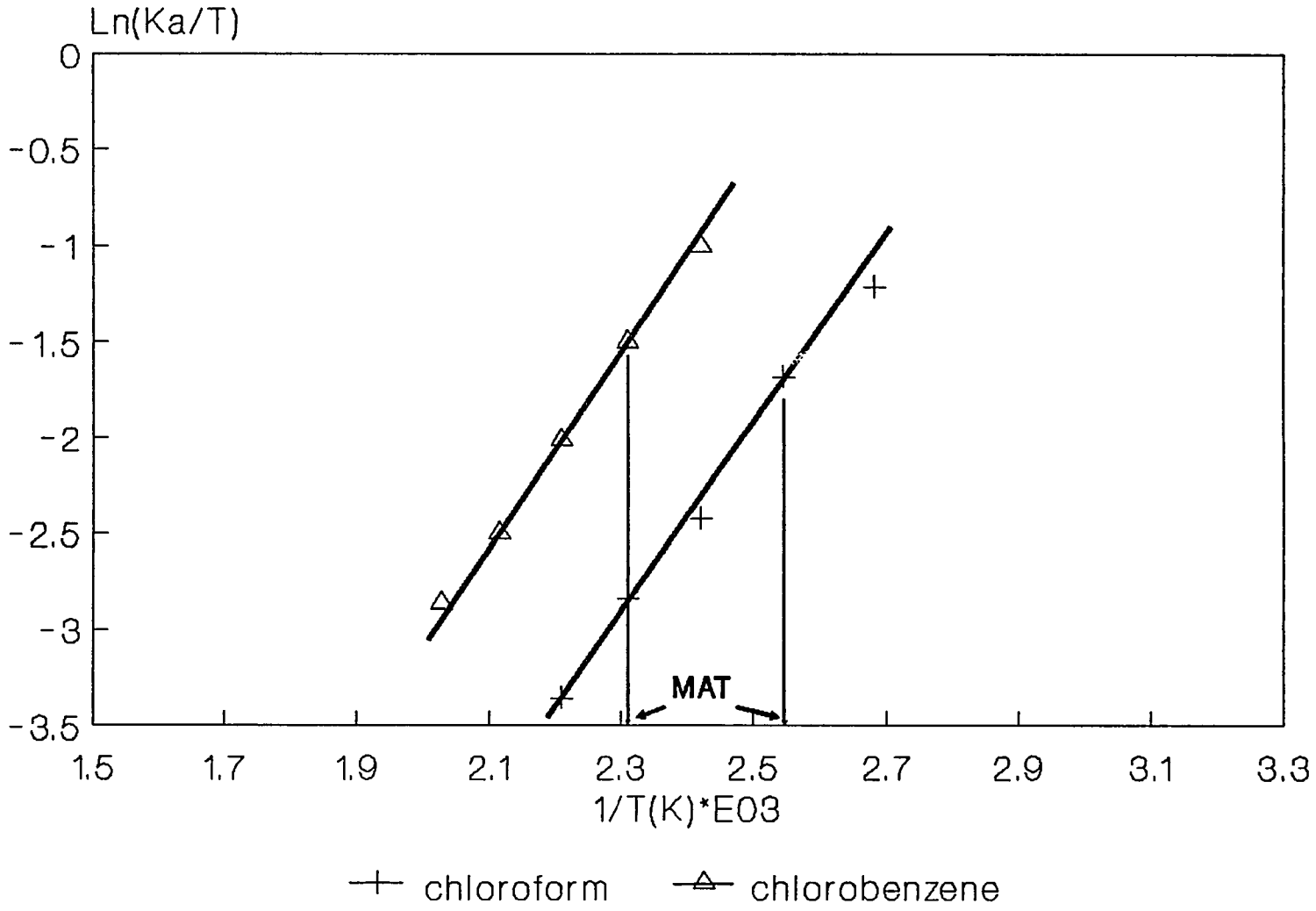

Figure 5-2. (continued)

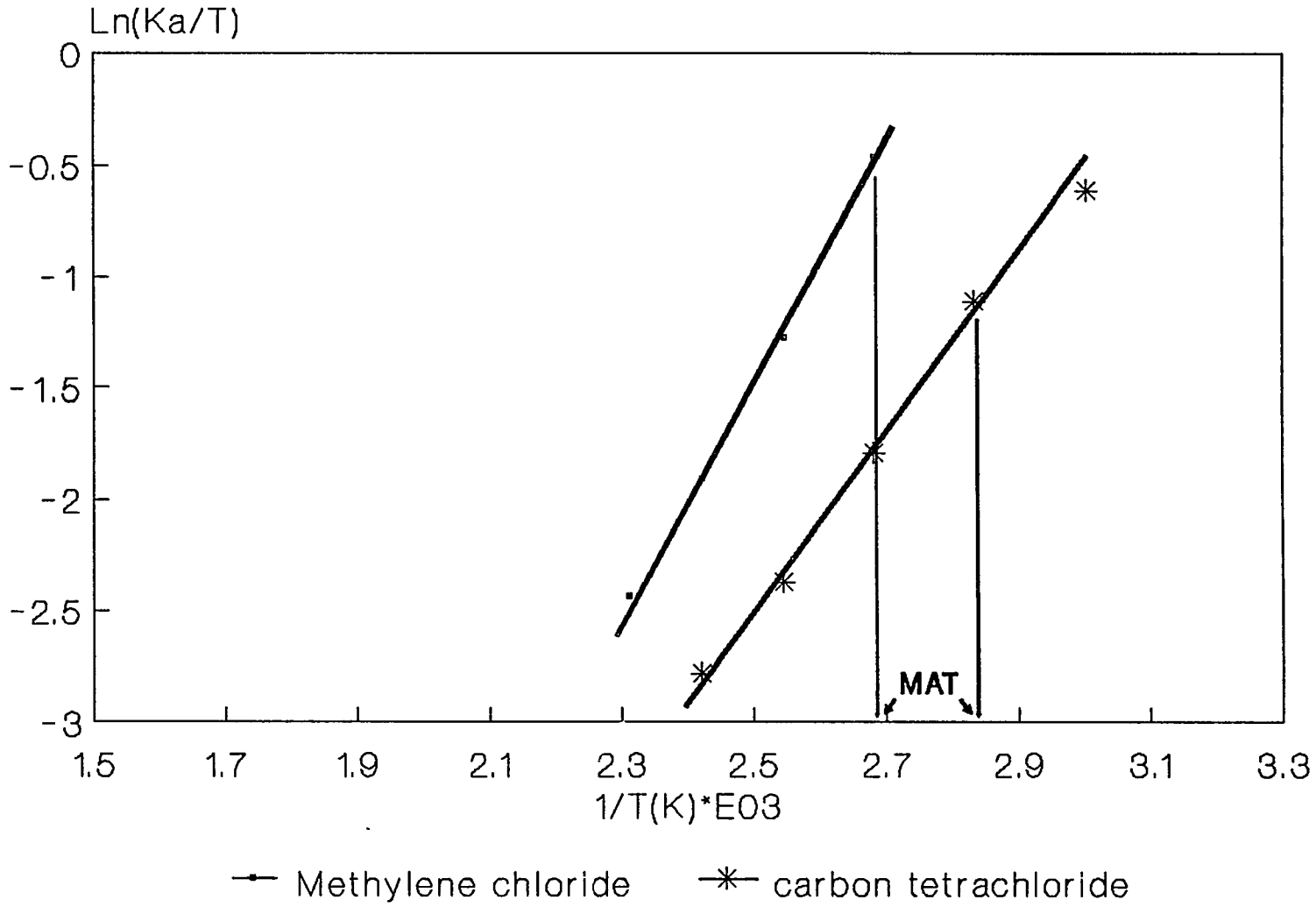

Figure 5-2. (continued)

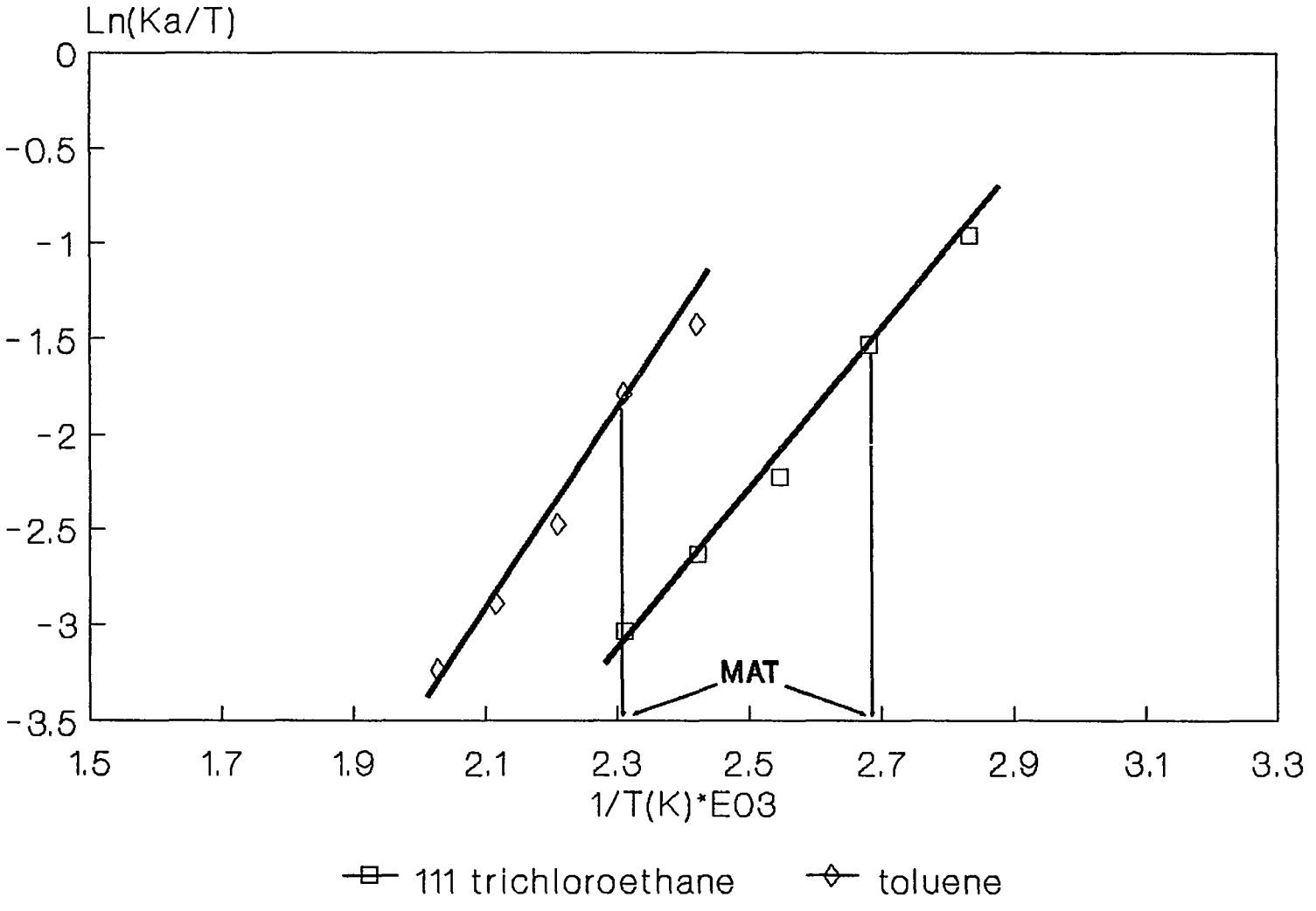

Figure 5-2. (continued)

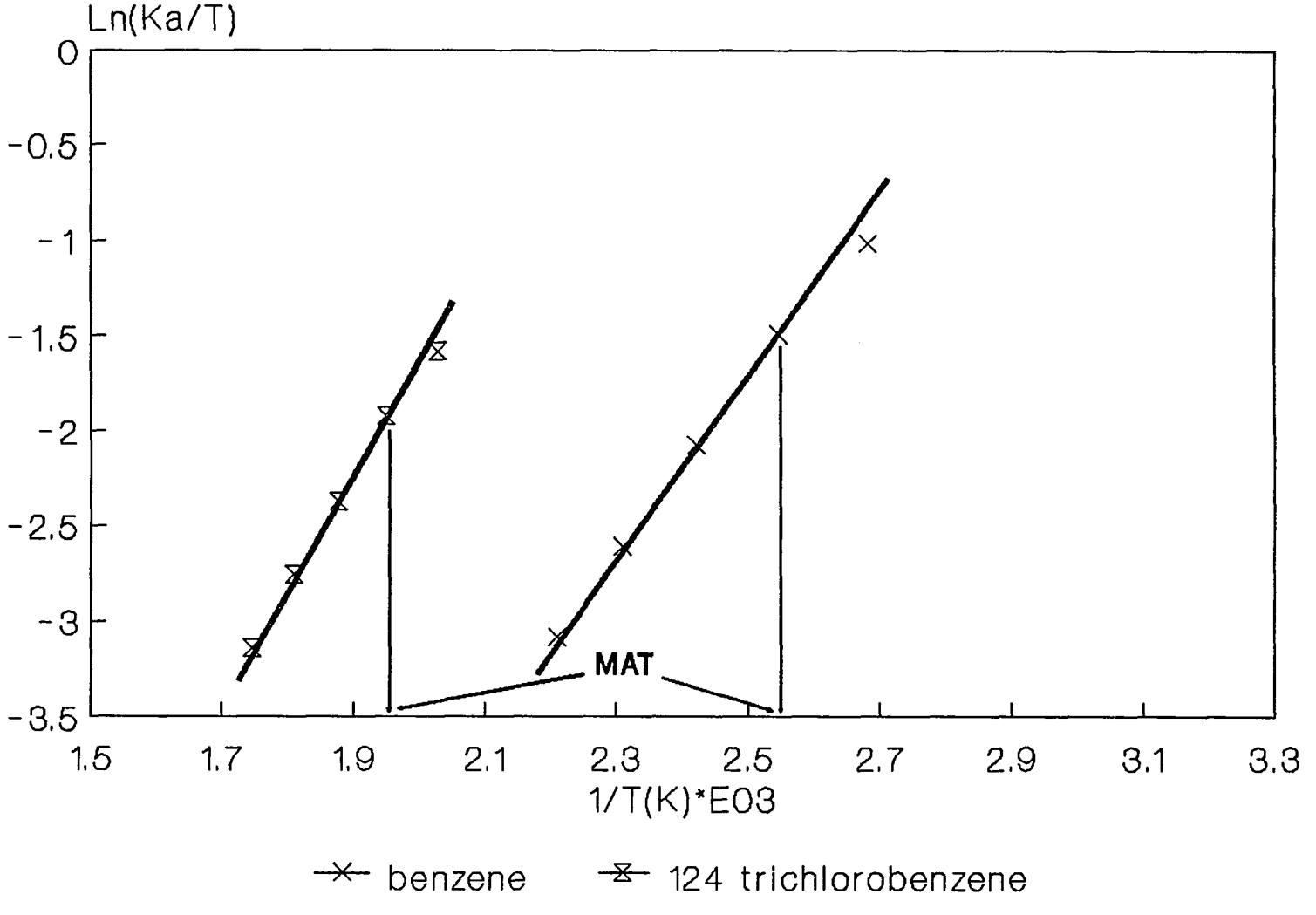

After each chromatographic response experiment before the next 20 °C increment, the temperature was raised approximately 100°C above the operating temperature in order to remove and quantify any remaining fraction of organics. We define, here, Minimum Allowable Temperature (MAT) which indicates the minimum temperature at which more than 95 % of the input plug of organic material is removed from the column after one hour operation at continuous flow. Results of MAT values are shown in Table 5-7 with remaining fractions. The temperature increase of 100 °C is considered reasonably sufficient to desorb remaining fraction of organics because the subsequent increase of temperature did not evolve additional organics from the column. The MAT value is higher than the boiling point of each organic compound, ranging approximately from 30°C to 60°C above boiling points with the exception of carbon tetrachloride.

When the plots in Figure 5-2 are observed in detail, we can also see that there exists a slight deviation from linearity at the temperature region below the MAT's. This non-linearity of the plots is due to the remaining fraction of the organics in the column. Temperatures sufficiently higher than the MAT's should, therefore, be applied to accomplish acceptable removal of the organics from soil matrices in reasonably short-time processes, in actual treatment of contaminated soils. This implies that there exist minimum conditions in addition to optimum conditions above the minimums between temperature and process time for organics decontamination of soil matrices, depending on types of organic substances and thermal treatment facilities.

One also observes good linearity above the MAT's for plots of

Table 5-7. Minimum Allowable Temperatures and the Estimation of $-\Delta H/R$ from the Plots of *ln* (K_a/T) vs. 1/T

Compound	MAT* °C	Remaining** Fraction	Corr.*** Coeff.	$(-\Delta H/R)$*E-03 °K
chloroform	120	.025	.995	4.85
methylene chloride	100	.027	.998	5.30
carbon tetrachloride	80	.009	.997	4.10
1,1,1-tri chloroethane	100	.034	.994	3.98
benzene	120	.013	1.00	4.73
toluene	160	.021	.991	5.10
chloro benzene	160	.021	.999	4.89
1,2,4-tri chlorobenzene	240	.030	.999	5.94

Note] * MAT = minimum allowable temperature ± 20 °C

Flow rate for this experiment is approximately 8.5 cm^3/ sec at room temperature.

** indicates the fraction remaining in the column after one hour operation.

*** applies to data of *ln*(K_a/T) vs. (1/T)*E03 at temperatures higher than MAT's.

$ln(K_a/T)$ vs. 1/T. Heats of adsorption can be obtained from the slopes of these plots as explained by van't Hoff equation.

As a result of this analysis, a list of MAT's and heats of adsorption on soil could be obtained for the target organic compounds with fairly good correlation coefficients as shown in Table 5-7. As shown in this table, the values of $-\Delta H/R$ range from 3.98*E03 to 5.94*E03°K. ΔH can then be calculated as shown in Table 7-1 for the soil described in this study, ranging from -7.91 to -11.8 kcal/g mole.

The second central moment from equation (11) and its combined form with equation (9), or equation (22) can, in addition, be utilized to obtain other mass transfer parameters. As described in Chapter 4, plots of $(\sigma^2 L/2\mu^2 v)$ vs. $1/v^2$ from equation (22) (σ^2 denotes variance or the second central moment μ_2' while μ means average retention time or the first absolute moment μ_1) can be utilized to obtain the axial dispersion coefficient from the slope of this plot and the intraparticle diffusion coefficient from the value of intercept and an estimation of film mass transfer coefficient. Equilibrium constants needed in this calculation can be obtained from the first moment analysis for the respective temperature. Experimental values (values of σ^2 and μ) for this analysis were obtained via the BASIC program installed in the integrator as explained in Chapter 3 and Appendix 1.

Analysis results for the estimation of mass transfer parameters as described above with varied gas phase flow rates are summarized in Table 5-8. Temperatures for this experiments were chosen approximately 20 °C higher than the MAT's in order to ensure complete removal of organic input. Plots for the calculation of mass transfer parameters

Table 5-8. Results for Mass Transfer Parameter Estimation from Chromatographic Analysis

Methylene chloride

Temperature = 120 °C (393 °K)

Flow reading	Inter-particle linear gas vel. v, cm/s	Corrected average retention time μ, min.	Variance σ^2, min^2	$1/v^2$ s^2/cm^2	$\frac{\sigma^2}{2\mu^2}\frac{L}{v}$ sec.
1.5	1.10	2.775	2.547	0.827	1.970
2.0	1.395	2.454	2.084	0.514	1.625
2.5	1.980	1.742	1.402	0.255	1.529
3.5	3.072	0.899	0.477	0.106	1.259
4.0	3.585	0.799	0.407	0.078	1.165

Chloroform

Temperature = 140 °C (413 °K)

Flow reading	Inter-particle linear gas vel. v, cm/s	Corrected average retention time μ, min.	Variance σ^2, min^2	$1/v^2$ s^2/cm^2	$\frac{\sigma^2}{2\mu^2}\frac{L}{v}$ sec.
1.5	1.156	1.049	0.387	0.749	1.993
2.0	1.466	0.829	0.268	0.465	1.743
2.5	2.081	0.684	0.208	0.231	1.400
3.0	2.716	0.505	0.140	0.136	1.324
3.5	3.228	0.400	0.091	0.096	1.154
4.0	3.768	0.349	0.076	0.070	1.085

Table 5-8. (continued)

Carbon tetrachloride

Temperature = 100 °C (373 °K)

Flow reading	Inter-particle linear gas vel. v, cm/s	Corrected average retention time μ, min.	Variance σ^2, min^2	$1/v^2$ s^2/cm^2	$\frac{\sigma^2}{2\mu^2}\frac{L}{v}$ sec.
2.0	1.324	1.358	0.465	0.571	1.247
2.5	1.879	1.091	0.418	0.283	1.224
3.0	2.453	0.746	0.200	0.166	0.960
3.5	2.915	0.515	0.120	0.118	1.017
4.0	3.403	0.500	0.086	0.086	0.662

1,1,1-Tricholoroethane

Temperature = 120 °C (393 °K)

Flow reading	Inter-particle linear gas vel. v, cm/s	Corrected average retention time μ, min.	Variance σ^2, min^2	$1/v^2$ s^2/cm^2	$\frac{\sigma^2}{2\mu^2}\frac{L}{v}$ sec.
1.5	1.100	1.726	0.669	0.827	1.337
2.0	1.395	1.107	0.285	0.514	1.092
3.0	2.585	0.588	0.096	0.150	0.919
3.5	3.072	0.483	0.076	0.106	0.695
4.0	3.585	0.408	0.061	0.078	0.670

Table 5-8. (continued)

Benzene

Temperature = 140 °C (413 °K)

Flow reading	Inter-particle linear gas vel. v, cm/s	Corrected average retention time μ, min.	Variance σ^2, min^2	$1/v^2$ s^2/cm^2	$\frac{\sigma^2}{2\mu^2}\frac{L}{v}$ sec.
1.5	1.156	1.507	0.905	0.749	2.258
2.5	2.081	0.840	0.413	0.231	1.843
3.0	2.716	0.676	0.292	0.136	1.541
3.5	3.228	0.537	0.224	0.096	1.576
4.0	3.768	0.431	0.166	0.070	1.554

Toluene

Temperature = 160 °C (433 °K)

Flow reading	Inter-particle linear gas vel. v, cm/s	Corrected average retention time μ, min.	Variance σ^2, min^2	$1/v^2$ s^2/cm^2	$\frac{\sigma^2}{2\mu^2}\frac{L}{v}$ sec.
1.5	1.212	1.882	1.098	0.681	1.676
2.0	1.537	1.273	0.544	0.423	1.431
2.5	2.181	1.079	0.472	0.210	1.217
3.0	2.848	0.789	0.278	0.123	1.027
3.5	3.384	0.690	0.256	0.087	1.041

Table 5-8. (continued)

Chlorobenzene

Temperature = 180 °C (453 °K)

Flow reading	Inter-particle linear gas vel. v, cm/s	Corrected average retention time μ, min.	Variance σ^2, min.^{2}	$1/v^2$ s^2/cm^2	$\frac{\sigma^2}{2\mu^2}\frac{L}{v}$ sec.
1.5	1.268	1.694	0.844	0.622	1.520
2.0	1.608	1.177	0.482	0.387	1.417
2.5	2.282	0.905	0.367	0.192	1.286
3.0	2.979	0.686	0.233	0.113	1.089
3.5	3.541	0.620	0.183	0.080	0.881

1,2,4-Tricholorobenzene

Temperature = 260 °C (533 °K)

Flow reading	Inter-particle linear gas vel. v, cm/s	Corrected average retention time μ, min.	Variance σ^2, min.^{2}	$1/v^2$ s^2/cm^2	$\frac{\sigma^2}{2\mu^2}\frac{L}{v}$ sec.
1.5	1.492	1.156	0.387	0.449	1.272
2.0	1.892	0.817	0.214	0.279	1.110
2.5	2.685	0.625	0.160	0.139	0.999
3.0	3.505	0.456	0.094	0.081	0.845
3.5	4.166	0.420	0.078	0.058	0.695

are also shown in Figure 5-3 and reasonably good linear plots are observed. From the slopes and intercepts, axial dispersion coefficients and other mass transfer parameters could be estimated as described above.

In order to obtain intraparticle diffusion coefficient, mass transfer coefficient for the mass transfer resistance film on the outer surface of particles should be first estimated using empirical equations (73).

The appropriate dimensionless group characterizing film mass transfer is the Sherwood number which is the analog of the Nusselt number for heat transfer (103). The limiting value of Nusselt number for low Reynolds number flow is 2.0, and this should also, be applicable to Sherwood number in mass transfer. At higher Reynolds number, convective effects become significant and a correlation of Sherwood number with Schmidt number and Reynolds number can be expressed empirically as follows (73):

$$Sh = \frac{2k_f R_p}{D_m} = 2.0 + 0.6\ Sc^{1/3}Re^{1/2} \qquad (42)$$

where Sh = Sherwood number

Sc = Schmidt number, $\mu/\rho D_{AB}$

Re = Reynolds number, $Dv\rho/\mu$

μ = viscosity

ρ = density

D_{AB} = diffusion coefficient

D = particle diameter

v = fluid velocity

Figure 5-3. Plot for Mass Transfer Coefficient Calculation

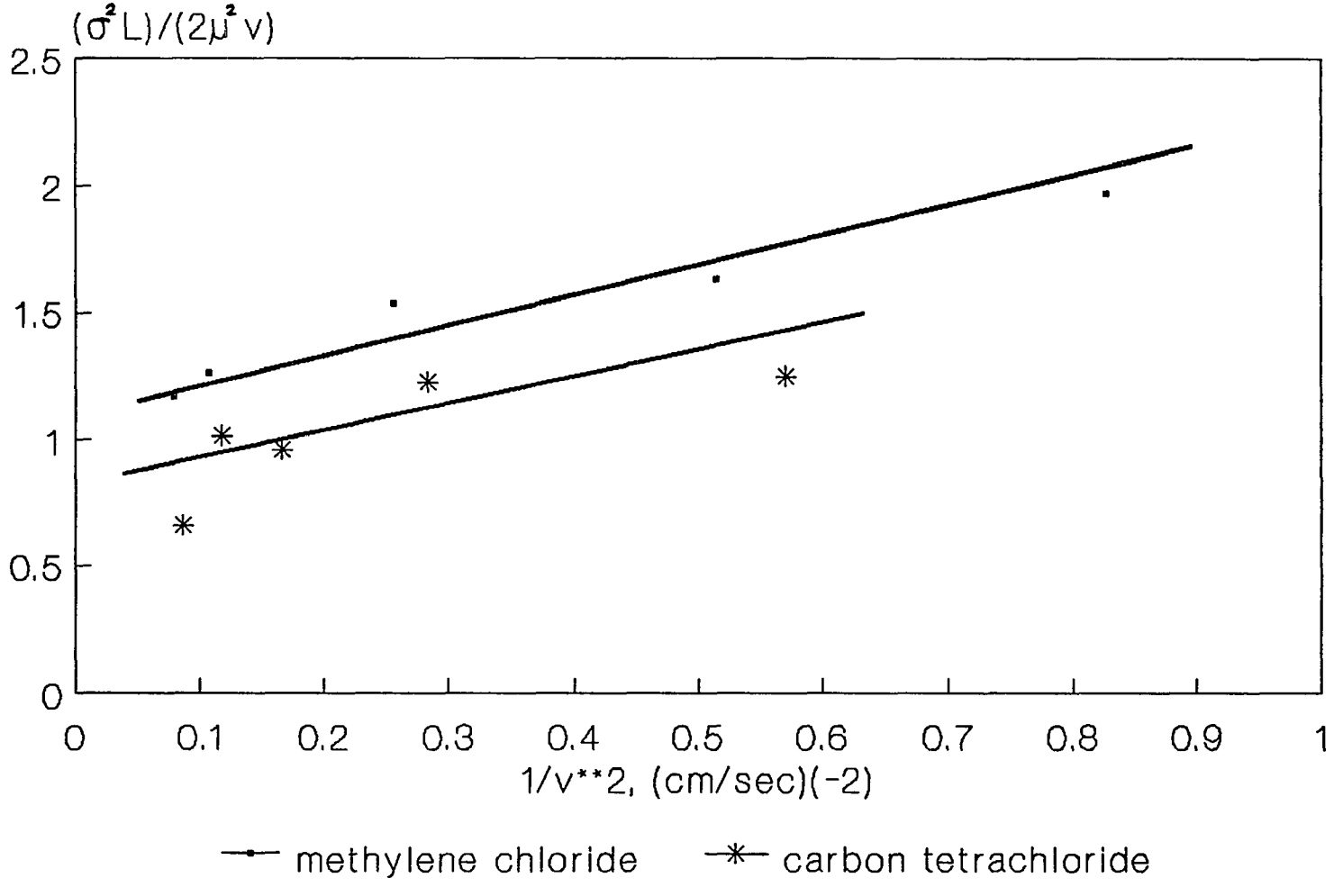

Figure 5-3. (continued)

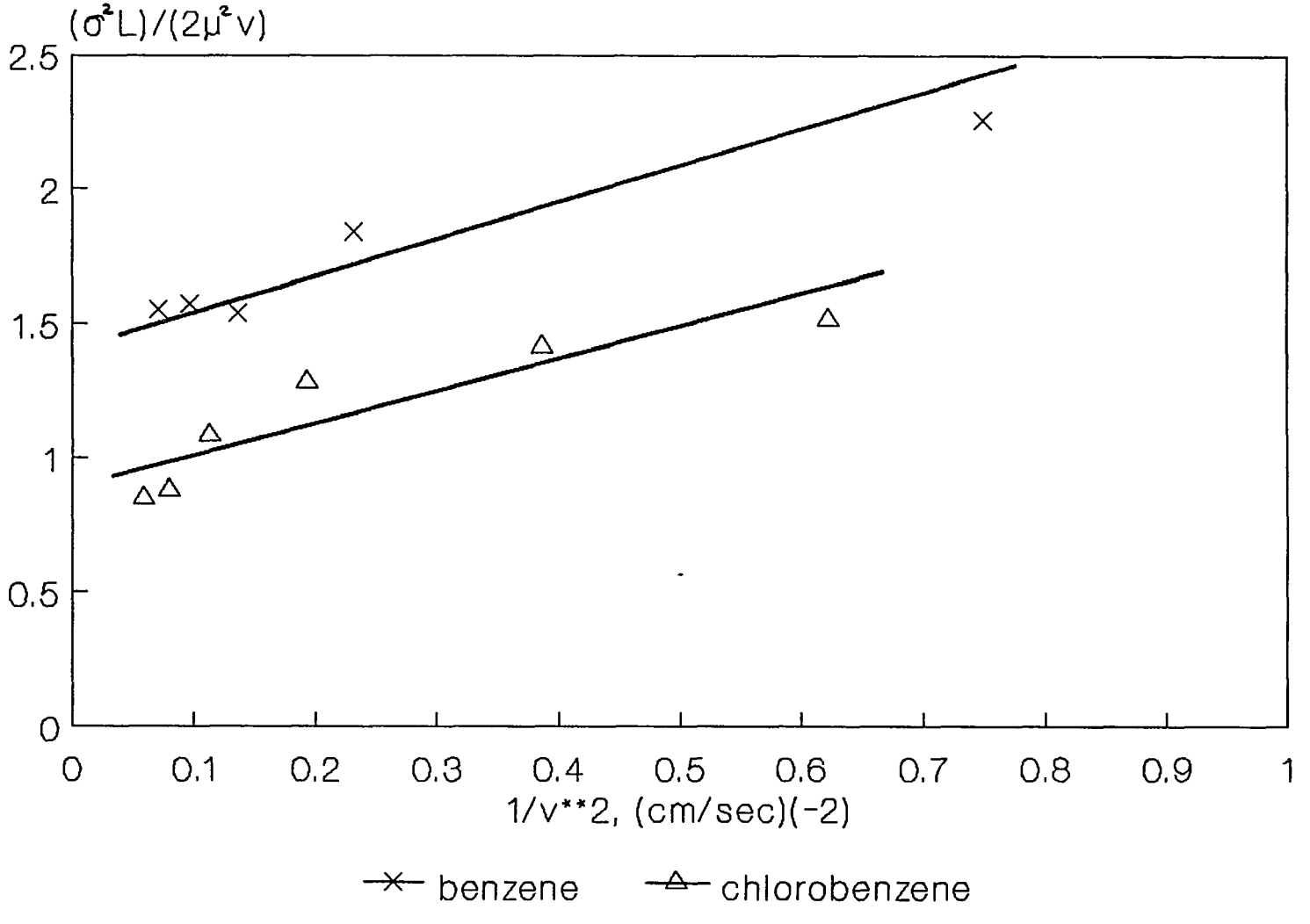

Figure 5-3. (continued)

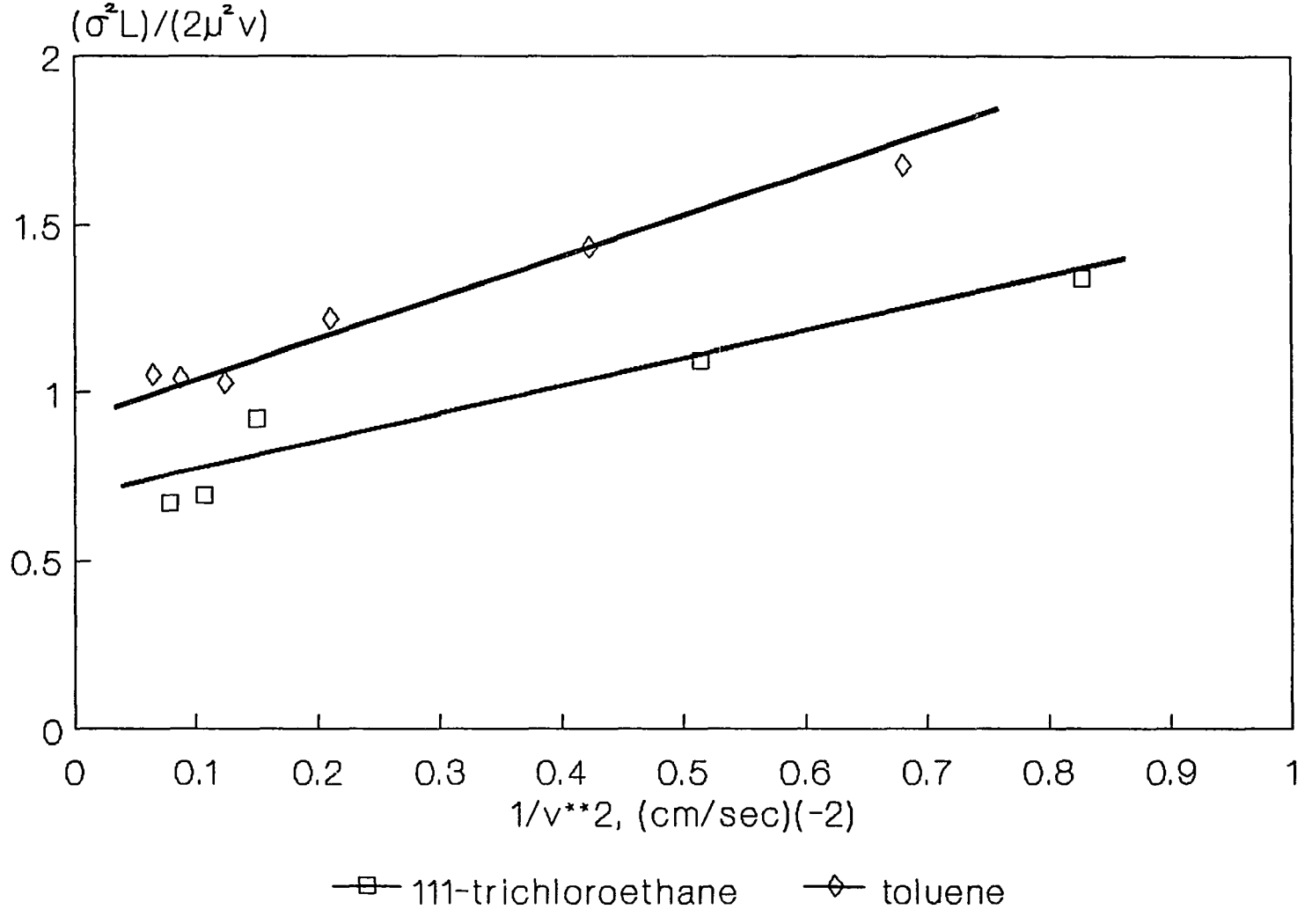

Figure 5-3. (continued)

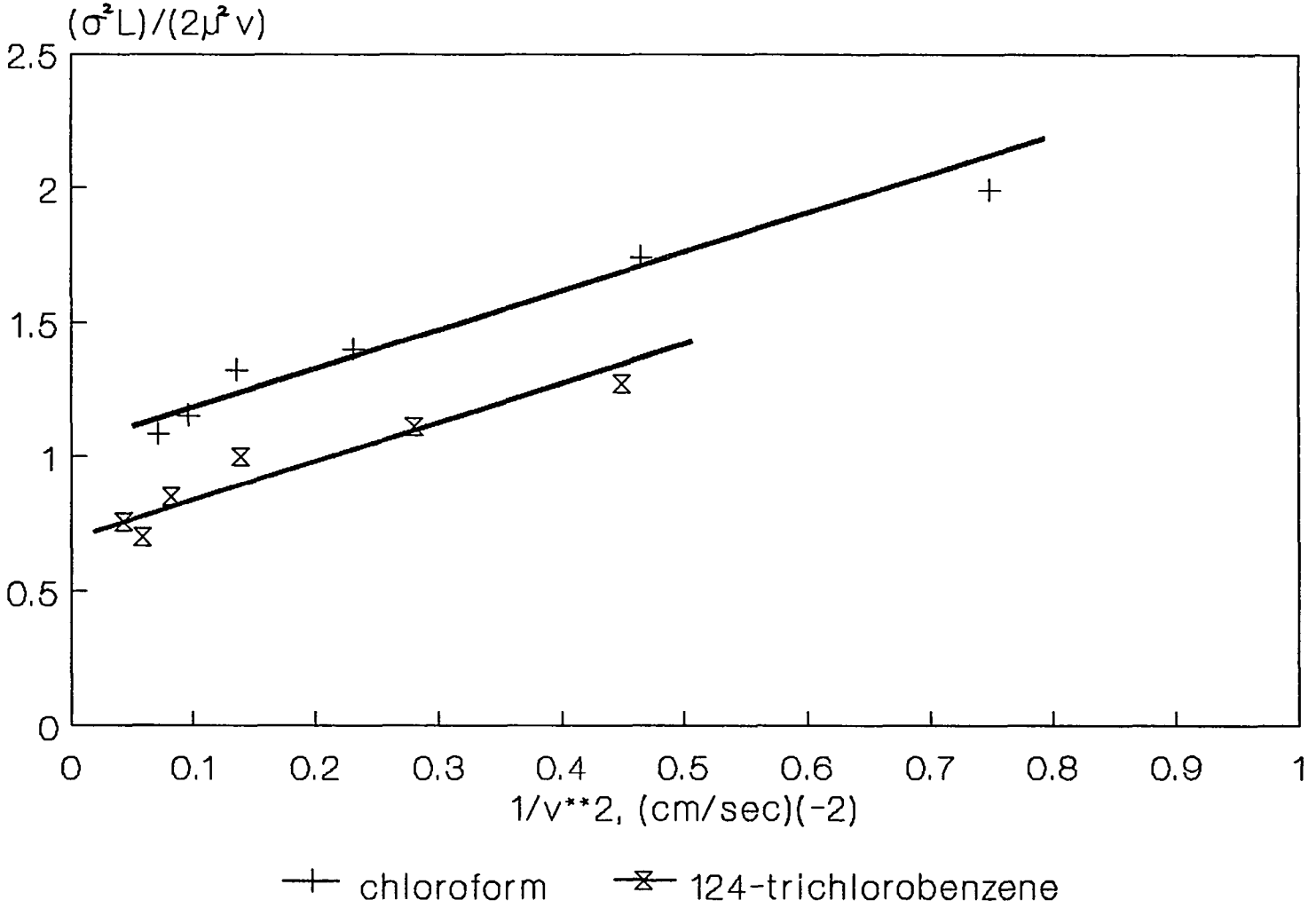

which has been widely applied to packed beds. This equation implies that the Sherwood number approaches a limiting value of 2.0 at low velocities for a single particle, as expected in this experiment.

As depicted in the above equation, data of molecular diffusion coefficients need to be secured to estimate mass transfer coefficients in the mass transfer film on the outer surface of particles.

Chapman-Enskog theory can be utilized for accurate estimation of molecular diffusivity. Using ideal gas law, this can be expressed as follows (103):

$$D_m = \frac{0.001858\ T^{3/2}\ (\ 1/M_A + 1/M_B\ )^{1/2}}{p\ \sigma_{AB}^{\ 2}\ \Omega(\varepsilon/\kappa T)} \qquad (43)$$

where D_{AB} = molecular diffusivity, cm^2/sec

T = temperature, °K

M_A, M_B = molecular weight of the two compounds

p = pressure, atm

$\sigma_{AB} = \frac{1}{2}(\sigma_A + \sigma_B)$, Å

$\varepsilon_{AB} = \sqrt{\varepsilon_A \varepsilon_B}$, erg

σ, ε = Lennard-Jones parameters

κ = Boltzmann's constant, 1.380 E-16 erg/molec/ °K

Ω = dimensionless function of the temperature and the intermolecular potential field of two molecules

Basic data needed for the calculation of molecular diffusivities are listed in Table 5-9 and its calculation results are also shown in Table 5-10.

Intraparticle diffusion coefficient can then be obtained by utilizing the intercept values of the plots of equation (22) and molecular diffusivity data as explained above.

Following this procedure mass transfer parameters needed in this system can be estimated and results are summarized in Table 5-11. More detailed discussion for the estimated mass transfer parameters will be given in Chapter 7.

B. Results of Soil Column Continuous Contamination/Desorption Experiments

Soil columns used in contamination/desorption experiments are similar to those used in the plug flow deposition experiments, with the exception of column length. Column length here is 30 cm in order to more readily observe prominent mass transfer behavior both in contamination and desorption phases.

Plots for the experimental results will be shown in Chapter 7.

Table 5-9. Data Needed for the Calculation of Molecular Diffusivities

Compound	Boiling Point °K	ε/κ °K	V_b cm^3/gmol	σ A	Mol. Weight	ε_{AB}/κ °K
chloroform	334	327	-	5.430	119.4	173.0
methylene chloride	313	406	-	4.759	84.9	192.7
carbon tetrachloride	350	327	-	5.881	153.8	173.0
benzene	353	440	-	5.270	78.1	200.6
nitrogen	-	91.5	-	3.681	28.0	-
1,1,1-tri chloroethane	347	399.1	105.5	5.567	133.4	191.1
chlorobenzene	405	465.8	128.9	5.951	112.6	206.4
toluene	384	441.6	133.2	6.016	92.1	201.0
1,2,4-tri chlorobenzene	487	560.1	164.7	6.457	181.5	226.4

Note 1. Values of ε/κ and σ for the last four compounds were calculated following the expression by Hirschfelder et al. (104).

$$\varepsilon/\kappa = 1.15\ T_b \quad (T_b\text{: boiling point})$$

$$\sigma = 1.18\ V_b^{1/3}$$

2. Values of V_b (molal volume of liquid at normal boiling point) were also obtained from reference (104).

Table 5-10. Calculation Results of Molecular Diffusion Coefficients

Compound	Temp. °K	$\kappa T/\varepsilon_{AB}$	Ω	σ_{AB} (A)	D_m cm^2/sec
chloroform	413	2.387	1.015	4.556	0.155
methylene chloride	393	2.039	1.068	4.220	0.166
carbon tetrachloride	373	2.156	1.048	4.781	0.115
benzene	413	2.059	1.064	4.476	0.161
1,1,1-tri chloroethane	393	2.057	1.064	4.624	0.132
chlorobenzene	453	2.195	1.042	4.816	0.157
toluene	433	2.154	1.048	4.849	0.147
1,2,4-tri chlorobenzene	533	2.354	1.018	5.069	0.178

Table 5-11. Summary of Mass Transfer Parameters Estimation Results

Compound	Temp °C	K_a	Axial Dis. Coefficient cm^2/sec	Film Mass Transfer Coeff. cm/sec	Intrapart. Diff. Coeff. xE05, cm^2/sec
methylene chloride	120	109.4	0.987	7.209	2.573
chloroform	140	36.5	1.300	6.757	2.210
carbon tetrachloride	100	62.0	0.928	4.991	3.419
1,1,1-tri chloroethane	120	42.2	0.826	5.748	3.716
benzene	140	51.7	1.062	7.004	1.760
toluene	160	72.2	1.079	6.374	2.932
chlorobenzene	180	60.4	1.140	6.804	3.009
1,2,4-tri chlorobenzene	260	49.4	1.325	7.717	3.614

C. Soil Equilibrium Test Results

Equilibrium Chamber and System Characterization

As described in Chapter 3, this test system largely consists of an equilibrium chamber, a micropump for gas circulation, a heated injection/sampling unit, heated connecting tubes and valves. This system is characterized in Table 5-12. Before the experiments, preliminary calibration tests were done including flow rates and standard calibrations. Figure 5-4 shows gas flow rate in the system and superficial linear gas velocity across the soil bed, corresponding to the reading of speed controller connected to the magnetically-coupled micropump.

A controller setting of 3.0 (ca. 5.5 cm^3/min.) has been used except during initial experiments and during injection, in order to obtain uniform slow gas flow (0.28 cm/min. or 0.0047 cm/sec.) across the soil bed.

The system was evacuated prior to equilibrium experiments and filled with pure inert nitrogen gas and calibration was performed for gas concentrations without the soil bed by injecting organics through the injection/sampling port and recirculating. An example of responses of the gas chromatograph versus gas phase concentrations is shown in Figure 5-5. Their response curves are quite linear. These results indicate that there is no systematic effect or error throughout the operating temperature and concentrations. Specifically, there is no loss or nonuniformities in the system, for either injection or dilution experiments.

Table 5-12. System Characteristics of Soil Equilibrium Test

Void Volume of System	
Chamber not Including Soil Bed	119.6 cm^3
Loop	21.5
Soil Bed	15.7
Remaining Parts (including injector/sampler, thermocouple ten-way port and connecting parts)	4.8
Total	161.6 cm^3

Soil Bed	
Diameter	5.0 cm
Depth	0.8 cm
Soil Loading	~18.0 gram

Figure 5-4. Gas Flow Rate in Equilibrium Test System and Linear Velocity across Soil Bed

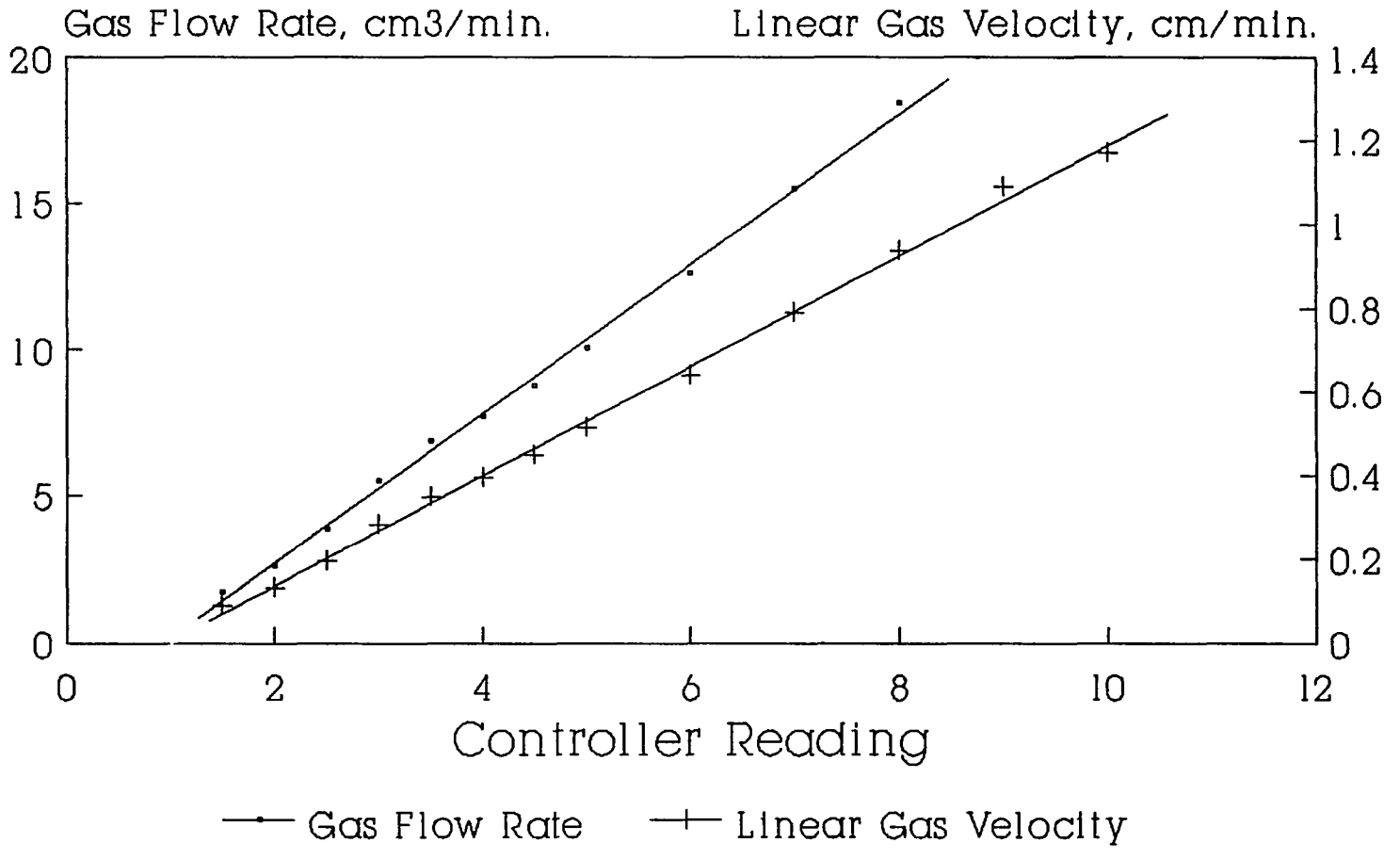

Figure 5-5. Calibration Chart for Equil. Test System

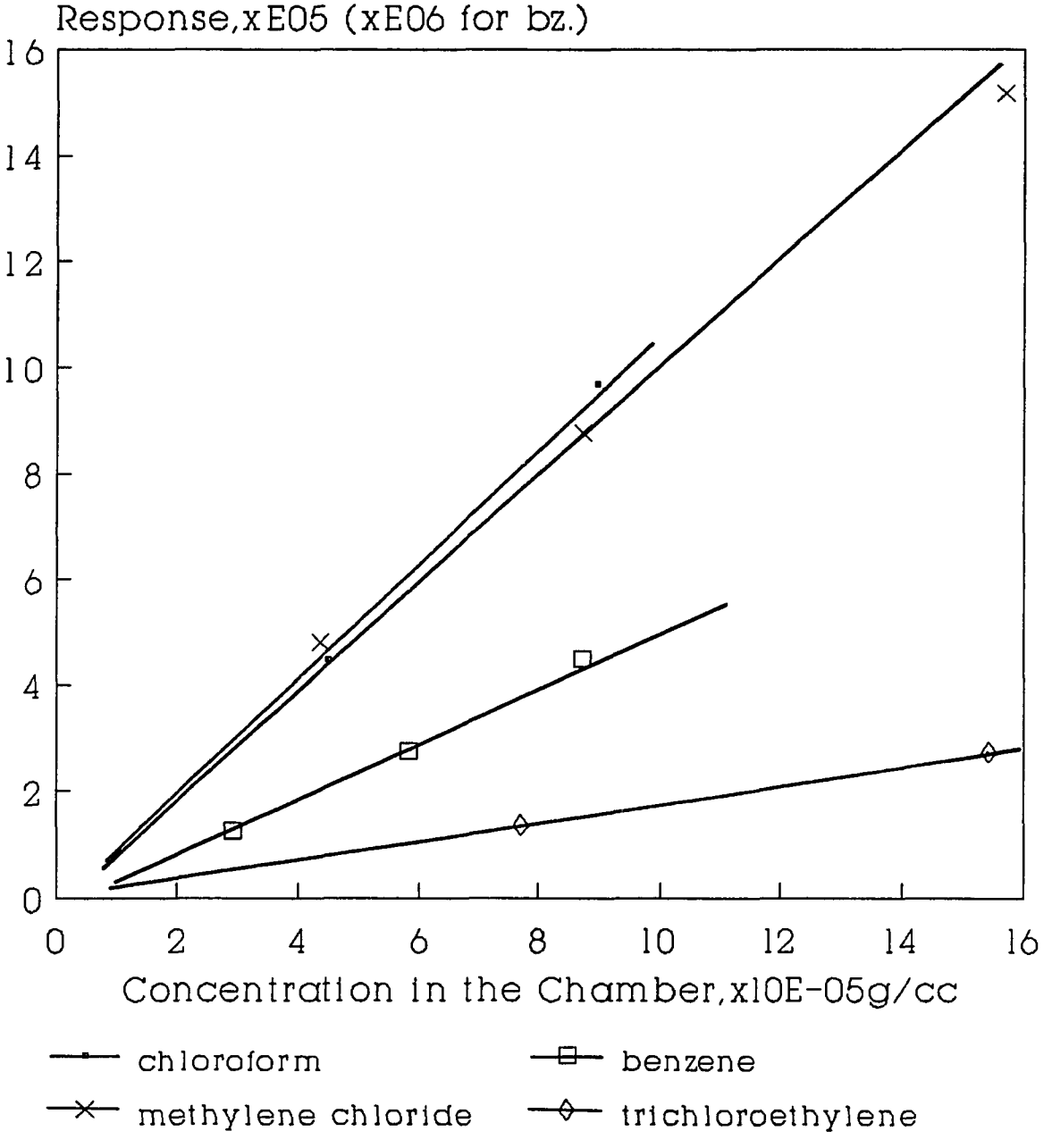

Experimental Results

Soil equilibrium tests have been performed using our devised experimental apparatus as described in the above section for organics including chloroform, 1,1,1-trichloroethane, carbon tetrachloride, benzene, methylene chloride and trichloroethylene. Their results with operational conditions are shown in Figure 5-6.

As shown in this figure, adsorption isotherms showed fairly linear relationship at the lower concentrations and the ratios of solid phase concentration to gas phase concentration tended to decrease as the concentration increases. As temperature increases, the linear zones expanded to higher concentrations. Slopes of linear zone tend to decrease with increasing temperature, indicating that organic molecules favor transfer to the gas phase as expected with higher temperature.

Even though the direct comparison between two data sets of equilibrium test result and the results from plug deposition experiment is not rigorous because of temperature difference and the dissimilarity between two systems, rough comparison shows that they are well within the same order of magnitude. When the values of equilibrium constants estimated from the chromatographic analysis (equilibrium constants resulting from chromatographic analysis will be expressed as K_1 in the following expression) are recalculated following the direct equilibrium equation $C_a = K\ C$ and compared with the equilibrium test results (these will be denoted as K_2), K_1 of carbon tetrachloride at 100°C, for example, is 9.3 and K_2 is 10.9 at 86°C while K_1 of 1,1,1-trichloroethane at 100°C is 12.0 and K_2 is 14.2

Figure 5-6. Soil Equilibrium Test Results
Carbon tetrachloride

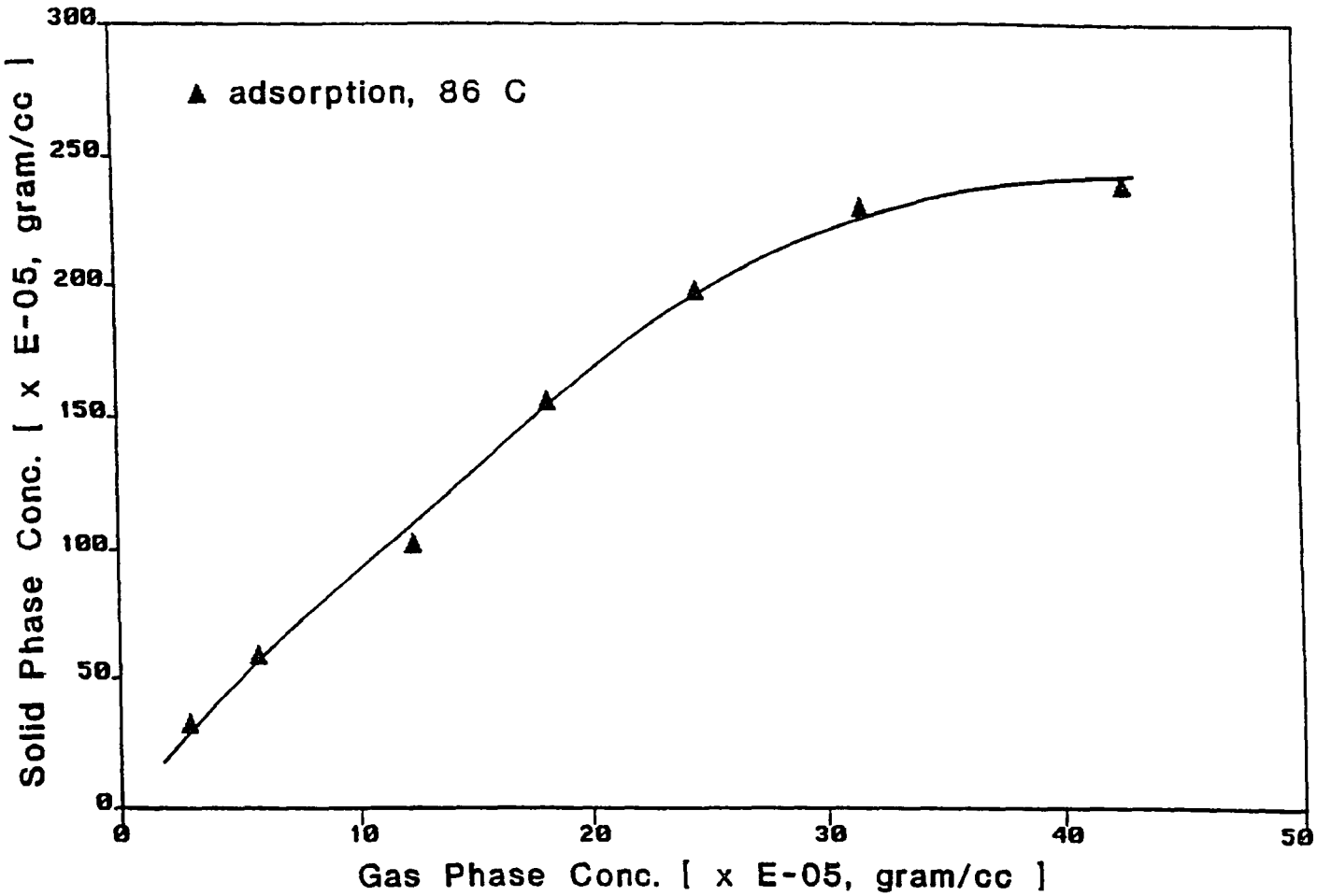

Figure 5-6. (continued)

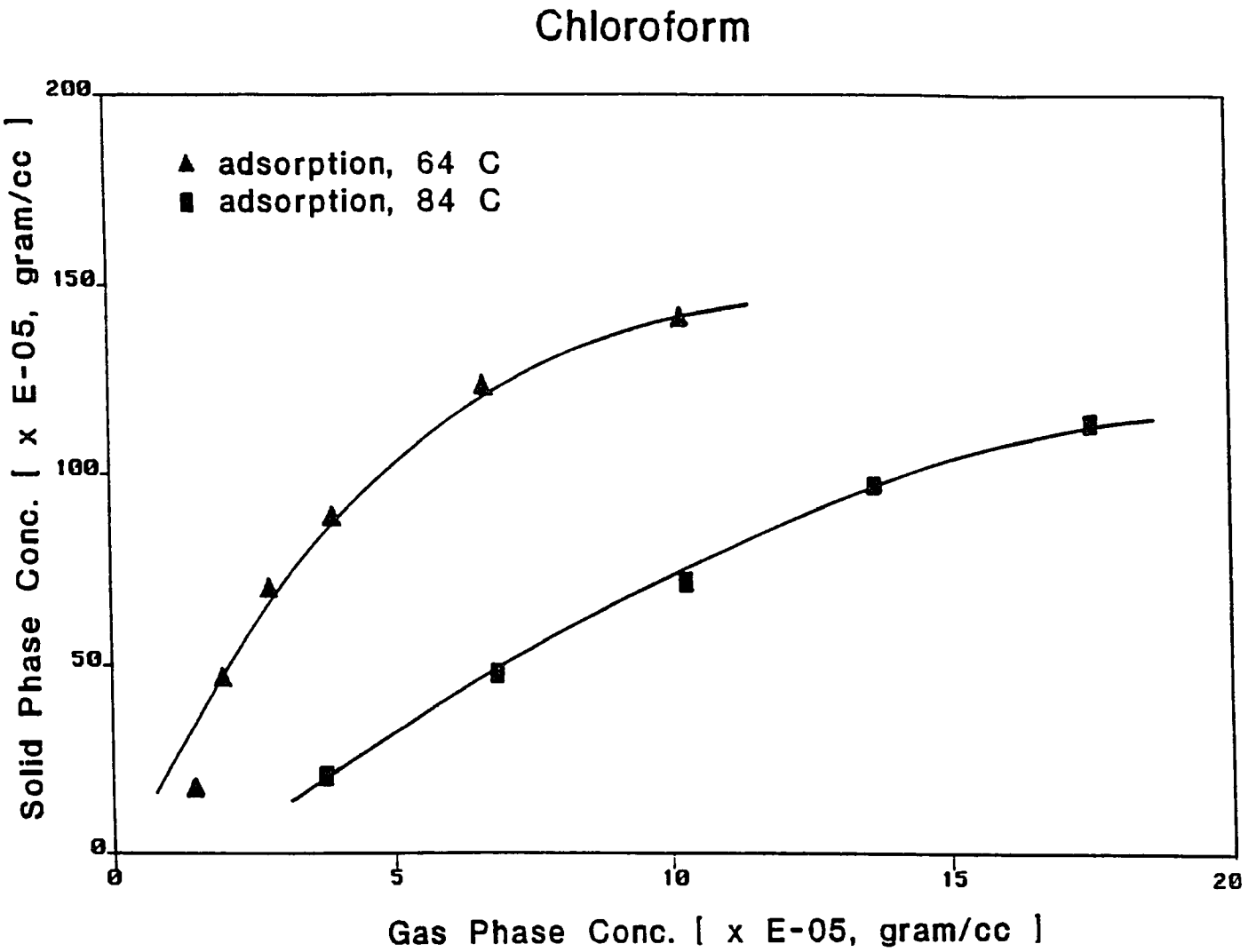

Figure 5-6. (continued)

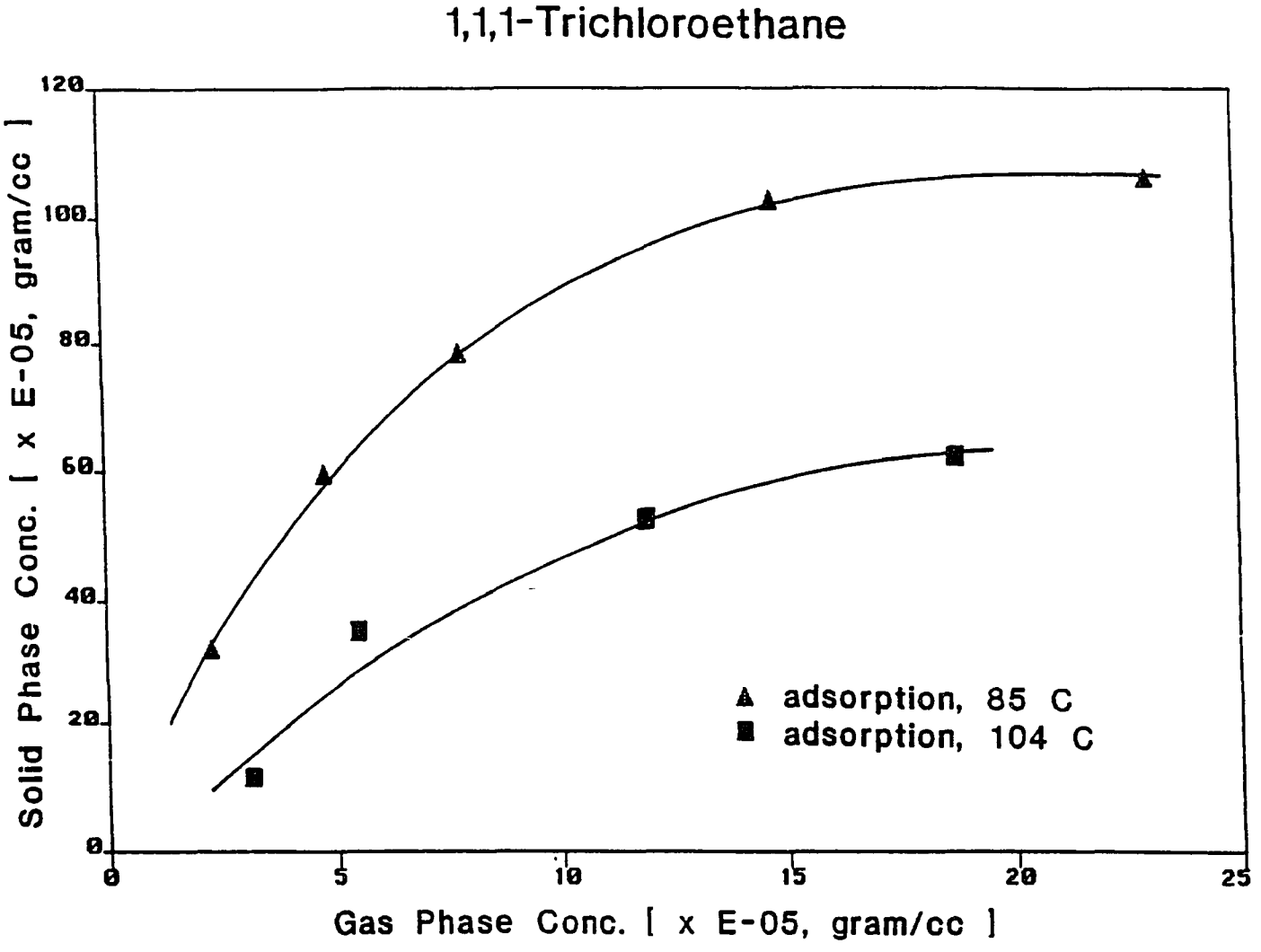

Figure 5-6. (continued)

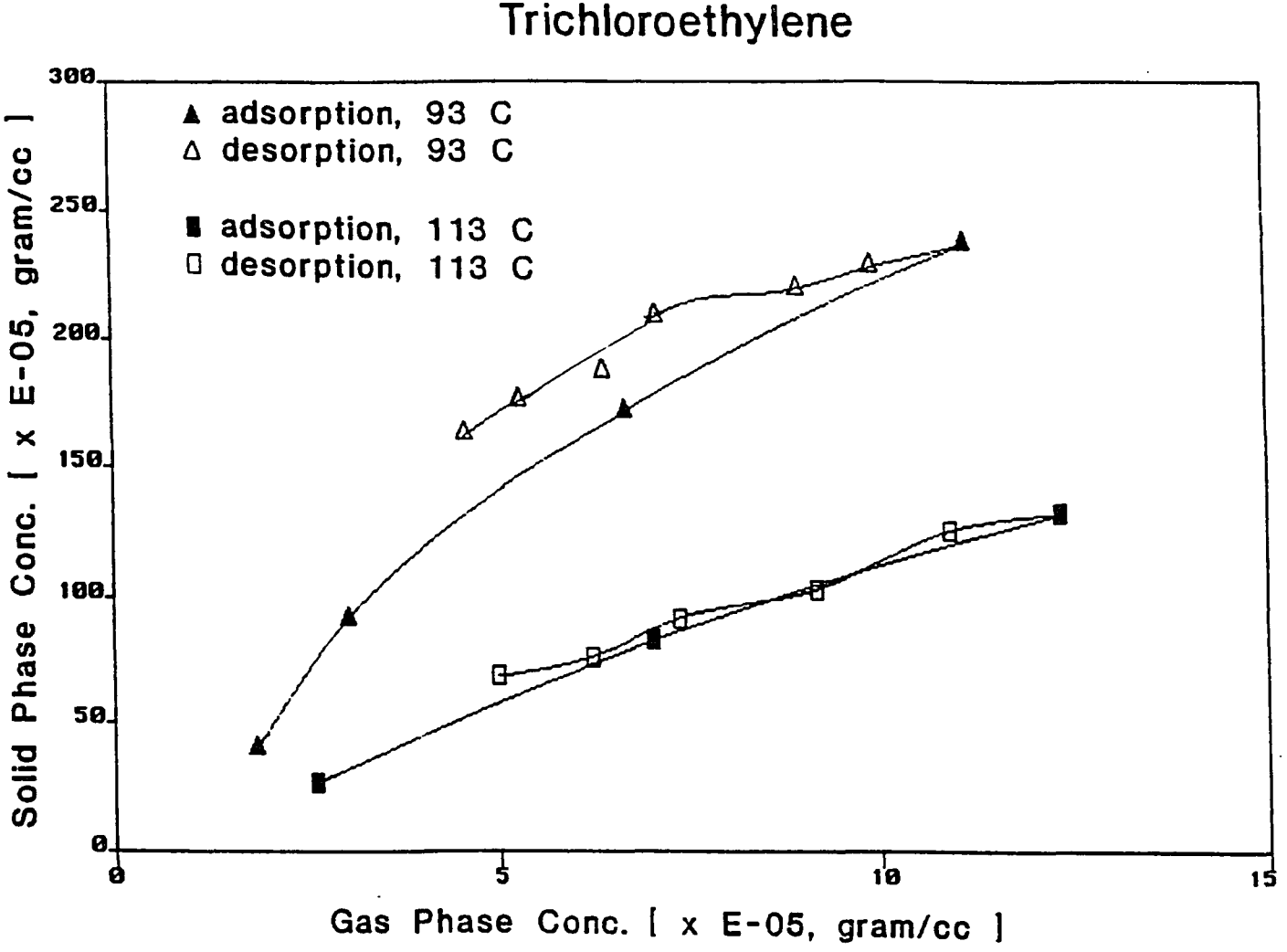

Figure 5-6. (continued)

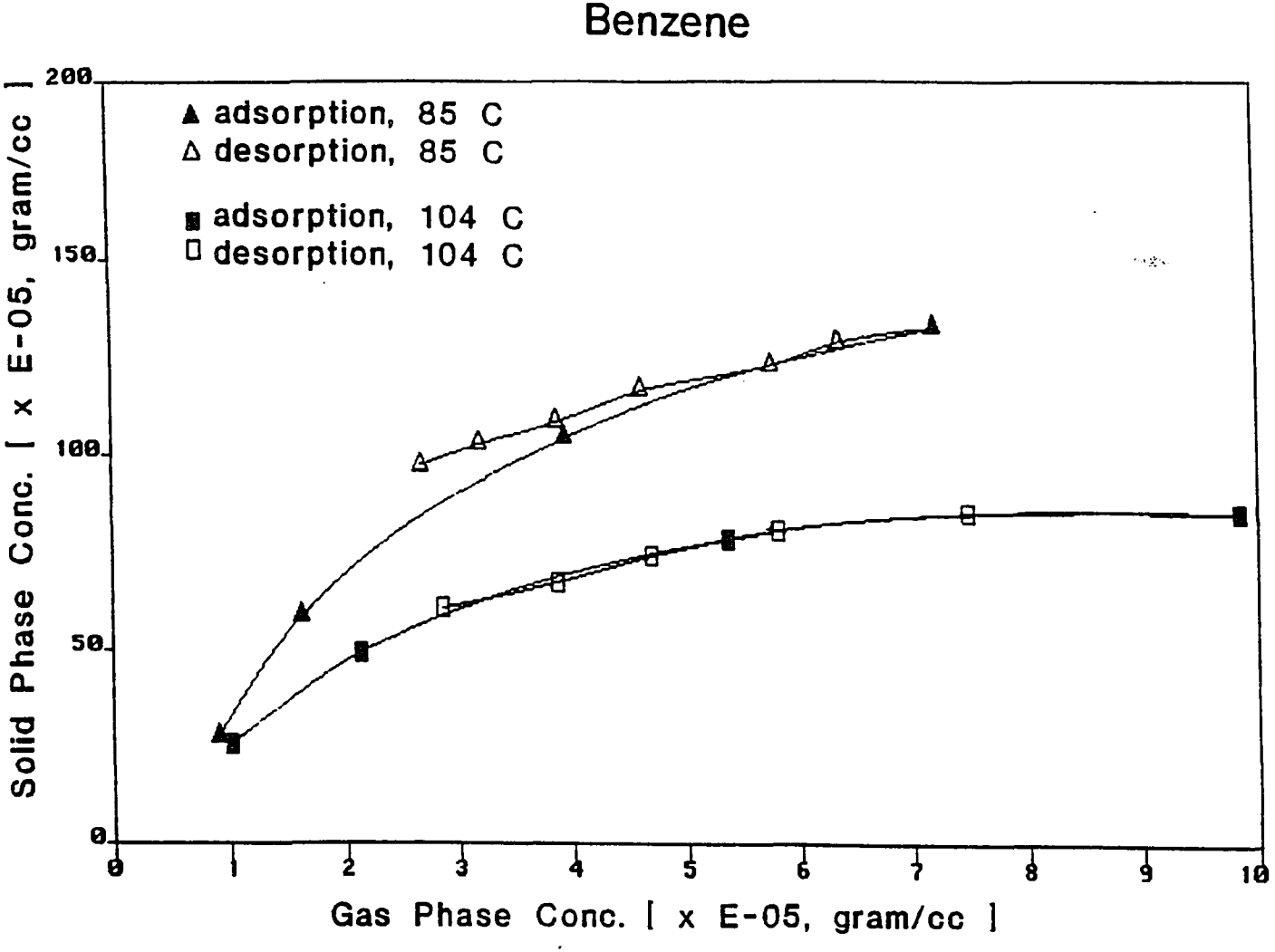

Figure 5-6. (continued)

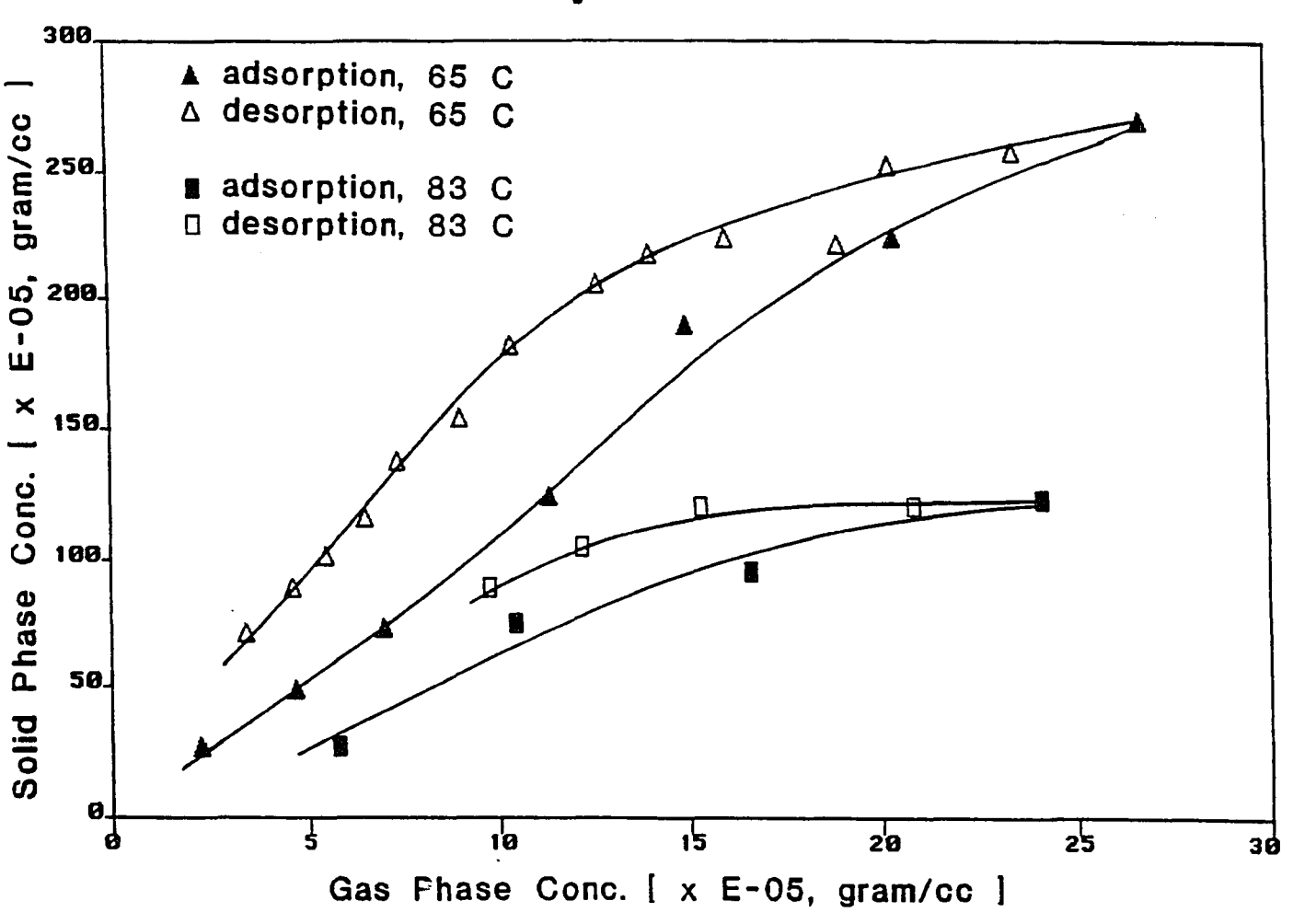

at 85°C.

Experimental data from the equilibrium test system (data collected here) seem to be more important and physically meaningful because one can observe the direct equilibrium data, especially in the mixed material like standard soils and in matrices of different particle sizes.

Figure 5-6 also contains the experimental results of the combined adsorption/desorption for benzene, methylene chloride and trichloroethylene. At relatively low temperatures, it tends to show hysteresis phenomena. There is plenty of evidence that systems of organic chemicals - natural materials including soils, sediments and clay show adsorption-desorption hysteresis or nonsingularities. (105-107). Even though there are different arguments, the main suggestion is that this hysteresis phenomenon is produced by irreversibility of the adsorption processes (105). This phenomenon, however, tends to become weaker at elevated temperatures as observed in the figures.

Chapter 6. PREDICTION RESULTS OF SOIL BED ADSORPTION/ DESORPTION

A. Prediction Results of Breakthrough Curves of a Soil Bed by Analytical Solution

As described in Chapter 4 section B, an analytical solution for the contamination process of a soil column was utilized to observe the behavior of breakthrough curves, enabling the comparison of its results with numerical simulation and experimental results.

Equation (24) in Chapter 4 Section A was utilized for the analytical solution for this system, with accompanied parameters defined in equations (25) through (30).

A Fortran program was developed to calculate the semi-infinite integration term in equation (24). An IMSL package called QDAGI was utilized as a subroutine for this program. This program was run in the NJIT VAX system with reasonably short time (ca. 30 seconds of CPU time).

Data of mass transfer parameters including axial dispersion coefficients, intraparticle diffusion coefficients and equilibrium constants were obtained from the results of chromatographic analysis experiments and plot results while film mass transfer coefficients were obtained from the estimation results of molecular diffusivities. Other system parameters such as column dimension were obtained from direct measurements and operational variables such as gas velocity were obtained from the calibration curves.

The program list for the analytical solution appear in Appendix 4.

Test simulation results for toluene and chloroform are shown in Table 6-1. Their results will be compared with numerical simulation results in Chapter 7.

B. Concentration Profile inside Soil Bed and Effluent Concentration Prediction by Numerical Solution

A numerical method to solve equations (39) and (40) to predict the adsorption and desorption behavior inside an adsorption column by using orthogonal collocation method was described in Chapter 4. This method has been utilized to simulate adsorption and desorption processes of organic substances in a soil column and to compare its results with experimental results.

In this simulation using orthogonal collocation method, two different types of matrix needed to be used together. As described briefly in Chapter 4, these matrices have been developed, verified and modified to be suitable for our purpose. The Gauss-Jordan method was utilized to obtain inverse matrices and the detailed program listings appear in Appendix 6.

In order to verify our matrix generating program for the collocation method and to compare the results with reference data, we calculated the matrices of smaller size utilizing the developed Fortran program mentioned above. Its results are shown in Table 6-2. Finlayson (90) lists matrices A and B (matrices used to describe equation (39)) for the radial coordinate of a particle and

Table 6-1. Test Result of Analytical Solution for Toluene and Chloroform

[Concentration Profile Calculation]

File Name = TOL401
Chemical = Toluene
Temperature = 160. deg. C
Linear Velocity = 1.76 cm/sec
Ka = 72.23
Dp = 0.29E-04 cm2/sec

time(s)	u value *	time(s)	u value	time(s)	u value
10.0	0.00000	20.0	0.00001	30.0	0.00049
40.0	0.00379	50.0	0.01371	60.0	0.03336
70.0	0.06414	80.0	0.10586	90.0	0.15721
100.0	0.21612	110.0	0.28026	120.0	0.34722
160.0	0.60418	200.0	0.79250	240.0	0.90285
280.0	0.95852	320.0	0.98366	360.0	0.99392
400.0	0.99778	440.0	0.99918	480.0	0.99992
520.0	1.00015	560.0	0.99992	600.0	0.99980
680.0	1.00005	760.0	0.99998	840.0	0.99974
920.0	0.99994	1000.0	0.99993	1080.0	1.00019

* u = effluent concentration, dimensionless

[Concentration Profile Calculation]

File Name = TOL402
Chemical = Toluene
Temperature = 160. deg. C
Linear Velocity = 2.63 cm/sec
Ka = 72.23
Dp = 0.29E-04 cm2/sec

time(s)	u value *	time(s)	u value	time(s)	u value
10.0	0.00000	20.0	0.00086	30.0	0.01361
40.0	0.05232	50.0	0.11638	60.0	0.19785
70.0	0.28842	80.0	0.38131	90.0	0.47153
100.0	0.55565	110.0	0.63162	120.0	0.69845
160.0	0.87814	200.0	0.95684	240.0	0.98615
280.0	0.99593	320.0	0.99883	360.0	0.99963
400.0	1.00002	440.0	0.99995	480.0	1.00007
520.0	0.99994	560.0	0.99997	600.0	0.99994
680.0	0.99991	760.0	0.99995	840.0	1.00003
920.0	0.99998	1000.0	1.00010	1080.0	1.00006

* u = effluent concentration, dimensionless

Table 6-1. (continued)

[Concentration Profile Calculation]

File Name = TOL403
Chemical = Toluene
Temperature = 160. deg. C
Linear Velocity = 3.42 cm/sec
Ka = 72.23
Dp = 0.29E-04 cm2/sec

time(s)	u value *	time(s)	u value	time(s)	u value
10.0	0.00001	20.0	0.01011	30.0	0.06850
40.0	0.16748	50.0	0.28194	60.0	0.39650
70.0	0.50325	80.0	0.59829	90.0	0.68011
100.0	0.74869	110.0	0.80492	120.0	0.85018
160.0	0.95230	200.0	0.98639	240.0	0.99642
280.0	0.99906	320.0	0.99976	360.0	1.00000
400.0	0.99996	440.0	0.99997	480.0	1.00007
520.0	1.00000	560.0	0.99992	600.0	1.00002
680.0	1.00005	760.0	1.00005	840.0	0.99993
920.0	0.99999	1000.0	1.00007	1080.0	0.99998

* u = effluent concentration, dimensionless

[Concentration Profile Calculation]

File Name = CLFM401
Chemical = Chloroform
Temperature = 140. deg. C
Linear Velocity = 1.68 cm/sec
Ka = 36.53
Dp = 0.22E-04 cm2/sec

time(s)	u value *	time(s)	u value	time(s)	u value
10.0	0.00000	20.0	0.00108	30.0	0.01600
40.0	0.06180	50.0	0.13935	60.0	0.23909
70.0	0.34929	80.0	0.45971	90.0	0.56294
100.0	0.65450	110.0	0.73241	120.0	0.79650
160.0	0.94120	200.0	0.98585	240.0	0.99700
280.0	0.99941	320.0	0.99989	360.0	0.99998
400.0	1.00000	440.0	1.00002	480.0	0.99999
520.0	1.00001	560.0	1.00003	600.0	0.99990
680.0	1.00008	760.0	1.00008	840.0	1.00006
920.0	1.00006	1000.0	1.00007	1080.0	1.00002

* u = effluent concentration, dimensionless

Table 6-1. (continued)

[Concentration Profile Calculation]

File Name = CLFM402
Chemical = Chloroform
Temperature = 140. deg. C
Linear Velocity = 2.51 cm/sec
Ka = 36.53
Dp = 0.22E-04 cm2/sec

time(s)	u value *	time(s)	u value	time(s)	u value
10.0	0.00004	20.0	0.02215	30.0	0.12576
40.0	0.27748	50.0	0.43387	60.0	0.57394
70.0	0.68965	80.0	0.78000	90.0	0.84761
100.0	0.89653	110.0	0.93094	120.0	0.95458
160.0	0.99263	200.0	0.99879	240.0	0.99988
280.0	0.99998	320.0	1.00000	360.0	0.99997
400.0	1.00012	440.0	0.99991	480.0	0.99995
520.0	1.00003	560.0	0.99980	600.0	1.00000
680.0	0.99993	760.0	0.99997	840.0	0.99858
920.0	0.99999	1000.0	0.99975	1080.0	1.00001

* u = effluent concentration, dimensionless

[Concentration Profile Calculation]

File Name = CLFM403
Chemical = Chloroform
Temperature = 140. deg. C
Linear Velocity = 3.27 cm/sec
Ka = 36.53
Dp = 0.22E-04 cm2/sec

time(s)	u value *	time(s)	u value	time(s)	u value
10.0	0.00110	20.0	0.09925	30.0	0.30058
40.0	0.49063	50.0	0.64346	60.0	0.75822
70.0	0.84024	80.0	0.89675	90.0	0.93446
100.0	0.95908	110.0	0.97480	120.0	0.98467
160.0	0.99808	200.0	0.99968	240.0	0.99999
280.0	0.99994	320.0	1.00003	360.0	1.00005
400.0	0.99999	440.0	0.99999	480.0	0.99983
520.0	1.00004	560.0	0.99978	600.0	0.99998
680.0	1.00006	760.0	0.99997	840.0	1.00005
920.0	1.00001	1000.0	1.00000	1080.0	0.99999

* u = effluent concentration, dimensionless

Table 6-2. Examples of Calculation Results of Matrices Generated for Orthogonal Collocation Simulation

CALCULATION RESULTS OF MATRICES GENERATED FOR
ORTHOGONAL COLLOCATION SIMULATION
(radial direction of particles)

NUMBER OF COLLOCATION POINTS = 2

ROOTS OF POLYNOMIALS

0.4688487947
0.8302239180
1.0000000000

Qji

1.0000	0.2198	0.0483
1.0000	0.6893	0.4751
1.0000	1.0000	1.0000

QINVji

1.8819	-1.5069	0.6250
-4.6122	8.3622	-3.7500
2.7303	-6.8553	4.1250

Aji

-3.1993	5.0152	-1.8158
-1.4087	-1.8067	3.2154
1.6968	-10.6968	9.0000

Bji

-15.6700	20.0349	-4.3649
9.9651	-44.3300	34.3649
26.9328	-86.9328	60.0000

Table 6-2. (continued)

CALCULATION RESULTS OF MATRICES GENERATED FOR
ORTHOGONAL COLLOCATION SIMULATION
(longitudinal direction of the column)

NUMBER OF COLLOCATION POINTS = 2

ROOTS OF POLYNOMIALS

0.0000000000
0.2113248706
0.7886751294
1.0000000000

Qji

1.0000	0.0000	0.0000	0.0000
1.0000	0.2113	0.0447	0.0094
1.0000	0.7887	0.6220	0.4906
1.0000	1.0000	1.0000	1.0000

QINVji

1.0000	0.0000	0.0000	0.0000
-7.0000	8.1962	-2.1962	1.0000
12.0000	-18.5885	12.5885	-6.0000
-6.0000	10.3923	-10.3923	6.0000

Aji

-7.0000	8.1962	-2.1962	1.0000
-2.7320	1.7320	1.7321	-0.7321
0.7321	-1.7320	-1.7320	2.7321
-1.0000	2.1962	-8.1962	7.0000

Bji

24.0000	-37.1769	25.1769	-12.0000
16.3923	-24.0000	12.0000	-4.3923
-4.3923	12.0000	-24.0000	16.3923
-12.0000	25.1770	-37.1769	24.0000

matrices A′ and B′ (matrices used to describe equation (40)) for the axial coordinate of the column, up to two collocation points, and Villadson et al.(89) also lists matrices A and B for the radial coordinate of a particle up to three collocation points.

When the calculated results are compared with data from Finlayson (90), they exactly coincided with the matrices given in Finlayson (90). This program is therefore verified and can be, further, applied for the cases with larger matrices.

Program operation results for higher order matrices up to six collocation points for both the intraparticle radial coordinate and axial coordinate in the column are shown in Appendix 9. Values of collocation points could be found from Villadson et al.(89,90) and more accurate values (double precision accuracy) were obtained from Stroud et al.(108) and utilized here. Resulting matrices were utilized in simulating orthogonal collocation method and each matrix size was compared for its effectiveness in predicting the concentration profiles in the column.

Concentration distributions along the axial direction were obtained using different number of collocation points along this direction and the results are shown in Figure 6-1. The number of collocation points in the radial direction of particles was also varied and these results are shown in Figure 6-2. As will be discussed in Chapter 7, a matrix of 8x8 in the axial direction and that of 7x7 in the radial direction of particles are determined to be sufficient in this numerical solution.

Using these matrices and numerical simulation program combined with software (IVPAG) in the NJIT VAX system, mathematical

Figure 6-1. Concentration Distribution along the Axial Direction of Soil Column with Varied Number of Collocation Points

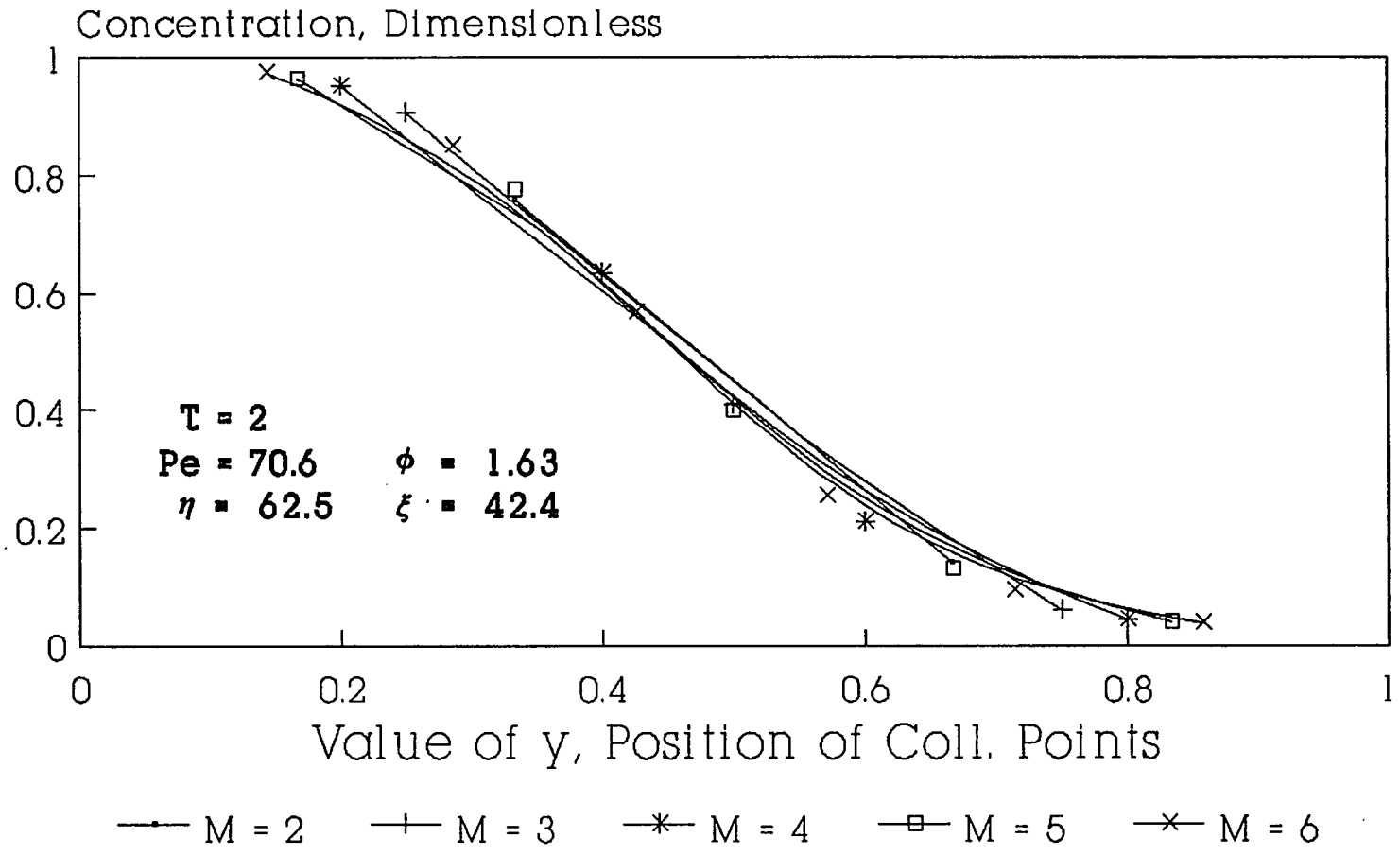

Figure 6-1. (continued)

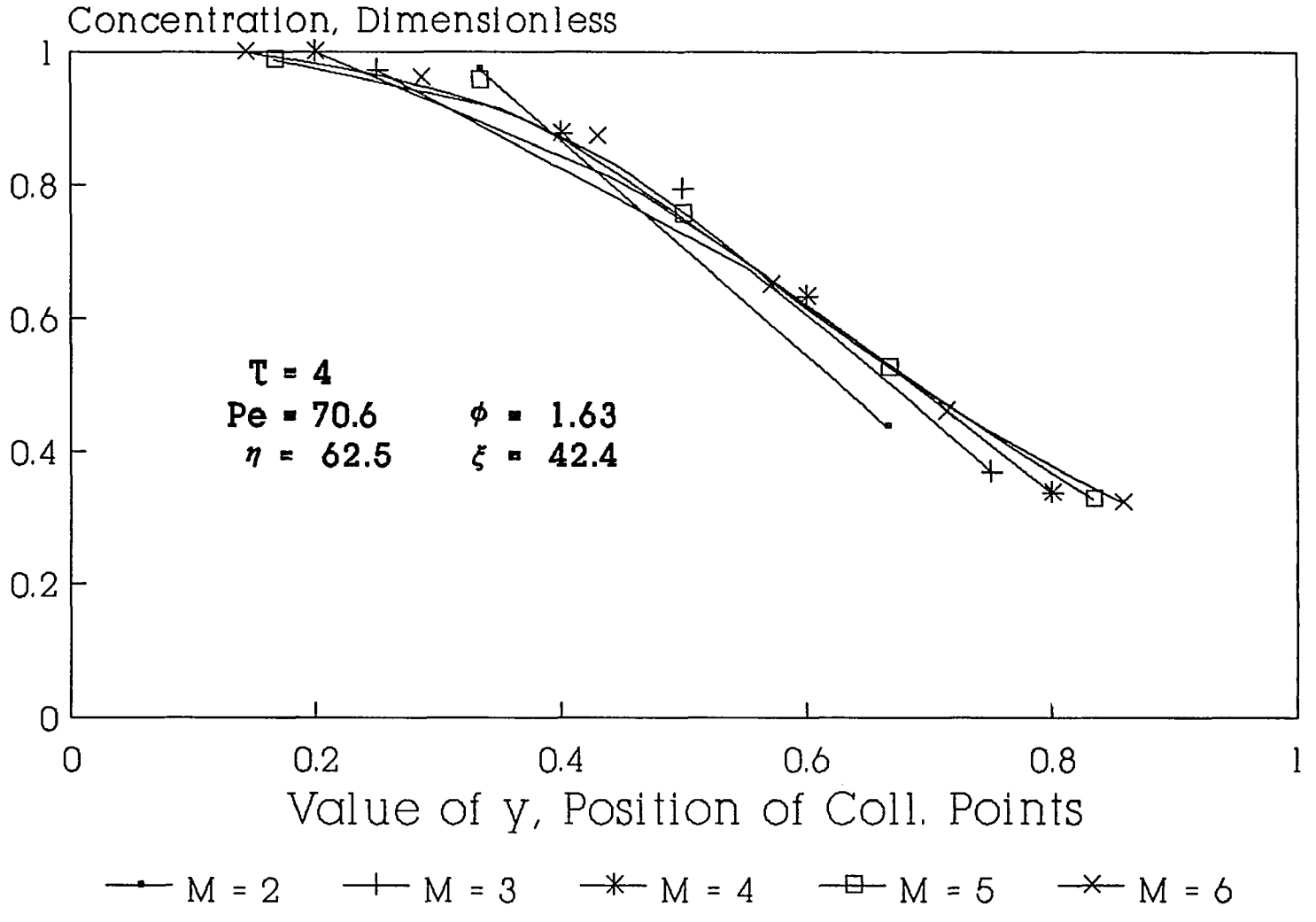

Figure 6-2. Concentration Distribution along the Radial Direction of Soil Part. with Varied Number of Collocation Points

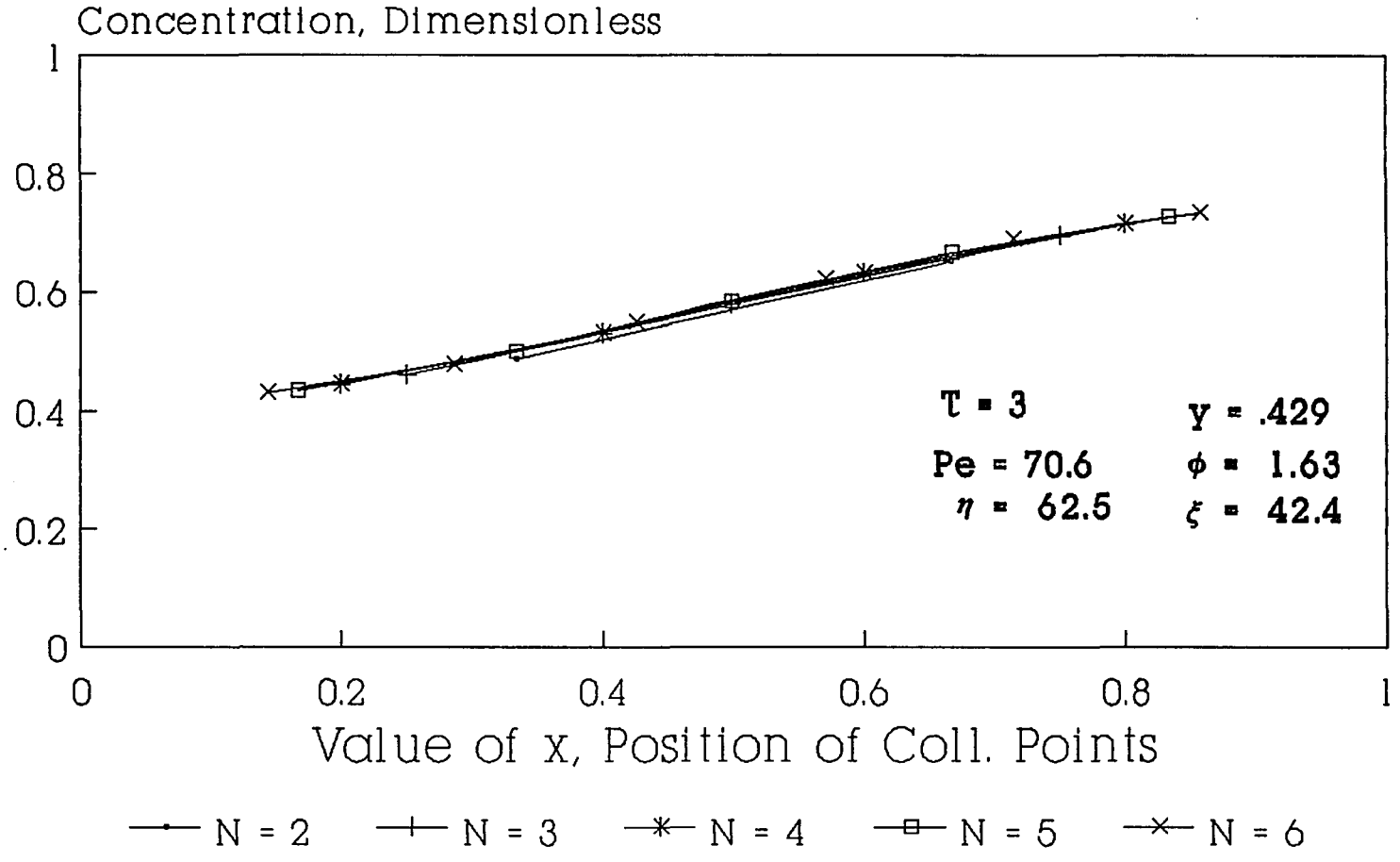

Figure 6-2. (continued)

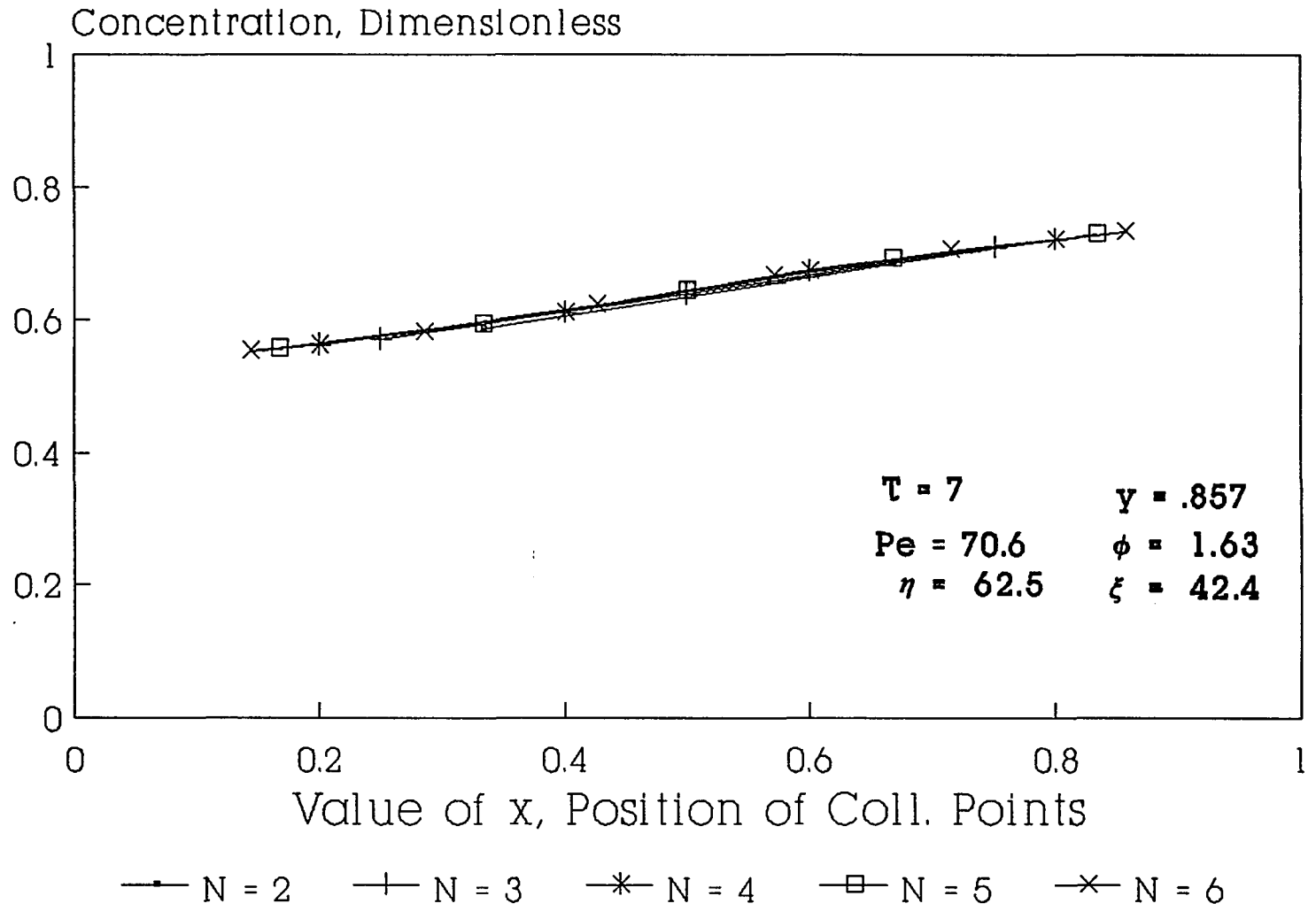

determination of concentration profiles in the contamination/ desorption of soil column system has been performed. Detailed results of numerical solutions are shown in Appendix 9.

These results can now provide us with insights on adsorption and desorption processes. From the results for the concentrations inside particles, we can observe how the concentration profile changes according to time and from the data of fluid phase, we can also observe the concentration distribution along the column. Moreover, from the results describing the end of the column, we can obtain concentration variation at the column outlet and it becomes possible to compare the results from numerical solutions with those from analytical solutions.

Some examples of these analyses are shown in Figures 6-3 and 6-4. Figure 6-3 shows the concentration distribution along the column axis while Figure 6-4 depicts the example of concentration profile change inside particles. The concentration changes at the outlet of the column will be shown in the following chapter when the comparison of results between analytical and numerical solutions is discussed.

Figure 6-3. Example of Concentration Distribution in the Axial Direction in the Adsorption of Soil Column

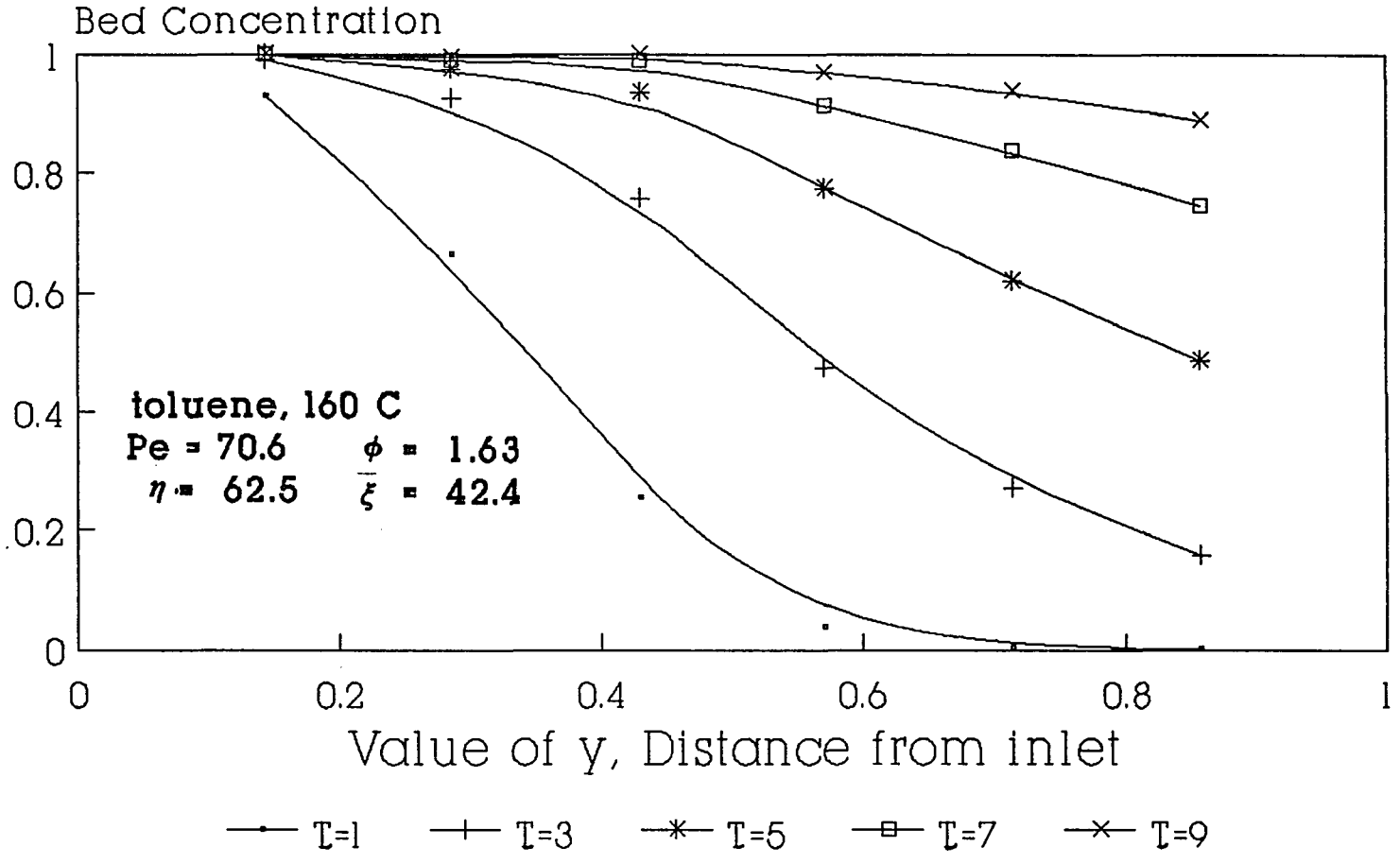

Figure 6-4. Example of Concentration Profile in the Radial Direction of Soil Particles in the Adsoption of the Column

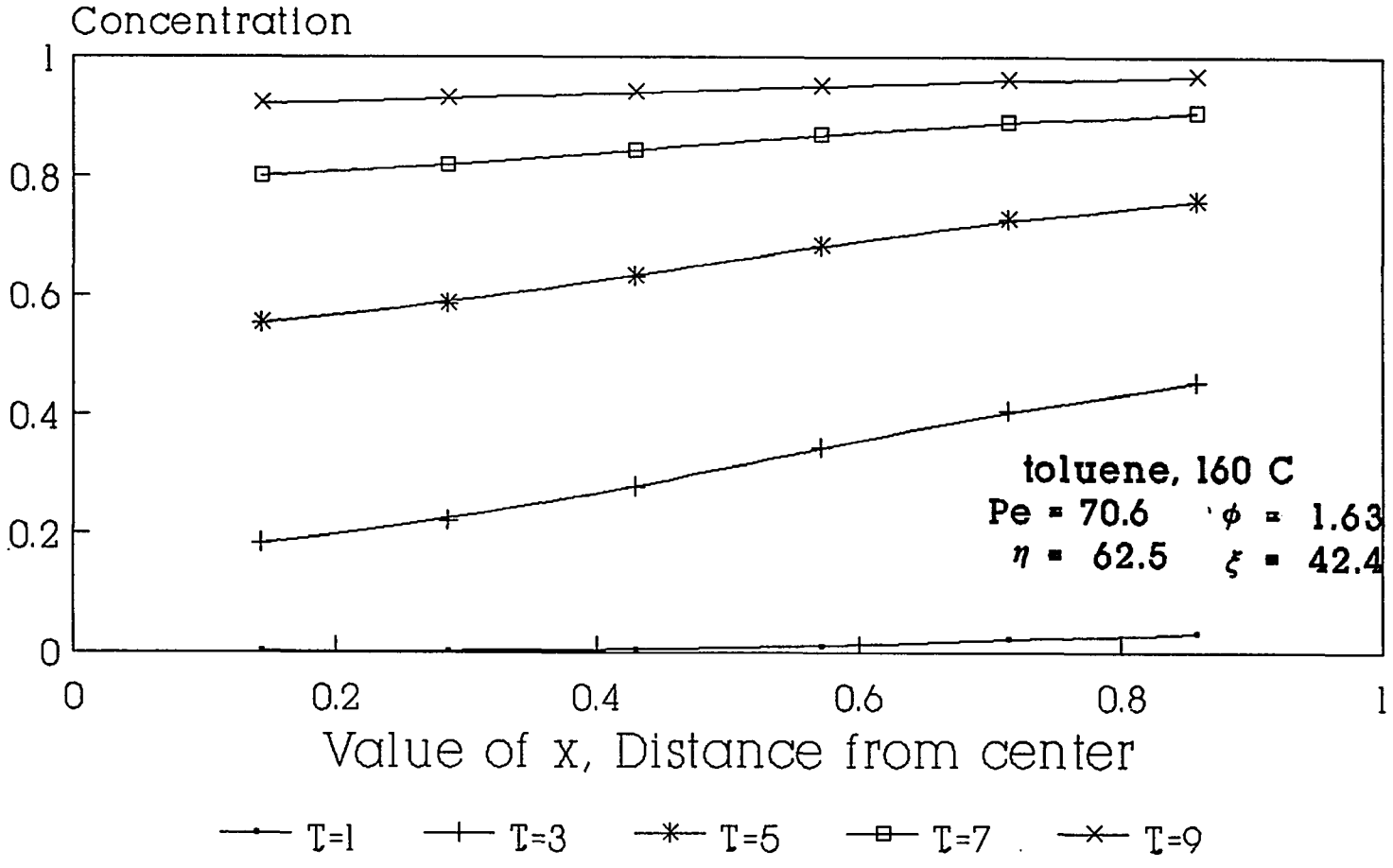

Chapter 7. DISCUSSION OF RESULTS

A. Chromatographic Response Analysis

Chromatographic response analysis for plug flow experiments in a soil column was performed to estimate mass transfer parameters including equilibrium constants and the results were further analyzed to obtain heats of adsorption as described in Chapter 5. The values of $-\Delta H/R$, or heats of adsorption could be obtained from the plots of the van't Hoff equation, as shown in Table 5-7.

Since the difference of the degree of freedom of adsorbed molecules between gas phase and adsorbed phase on the surface of solid, the entropy change on adsorption is necessarily negative (73).

In order for adsorption to occur, the free energy change on adsorption (ΔG) must be negative and from the fundamental thermodynamic relationship that $\Delta G = \Delta H - T\,\Delta S$, ΔH should be negative or adsorption is exothermic as is the case here and as is expected. This must be true to override the opposite effect of entropy.

The absolute values of heats of adsorption of these target compounds on soils are considered to be relatively low, which can be generally categorized as physical adsorption. A general guideline to distinguish physical adsorption from chemisorption is to compare heats of adsorption with latent heats of vaporization.

In Table 7-1, heats of vaporization of target organic compounds at boiling points are estimated using Chen's equation (104). When the resulting values of latent heat of vaporization are compared with

Table 7-1. Caculation of Latent Heats of Vaporization

Chen's equation (104)

$$L_{vb} = \frac{T_b\ (\ 7.9\ T_{br} - 7.82 + 7.11 \log P_c\ )}{1.07 - T_{br}}$$

where L_{vb} = latent heat of vaporization, cal/g mole

T_b = boiling point, °K

T_{br} = T_b/T_c

P_c, T_c = critical pressure and temperature, atm, °K ****

Compound	T_b(K)	T_c(K)	P_c(atm)	T_{br}	$L_{vb}(\frac{cal}{mole})$	$-\Delta H$	$-\Delta H/L_{vb}$
methylene chloride	313.0	510.	60.0	.614	6640	10.53	1.59
chloroform	334.3	536.4	54.0	.623	7044	9.64	1.37
carbon tetrachloride	349.7	556.4	45.0	.629	7060	8.15	1.15
1,1,1-tri-chloroethane*	386.9	602.	41.0	.643	7907	7.91	1.00
benzene	353.3	562.1	48.3	.629	7308	9.40	1.29
toluene	383.8	591.7	40.6	.649	7971	10.14	1.27
chloro-benzene	404.9	632.4	44.6	.640	8440	9.72	1.15
o-dichloro-benzene**	453.6	697.3	40.5	.651	9475		
p-dichloro-benzene**	447.3	685.	39.	.653	9280		
1,2,4-tri-chlorobenzene	486.				10320***	11.80	1.14

* estimated from the data of 1,1,2-trichloroethane
** for comparison purpose
*** estimated from the comparison of mono- and dichlorobenzene data
**** from reference (102)

the estimated heats of adsorption, their ratios ($-\Delta H/L_{vb}$) range from 1.0 to 1.59 . The generally accepted concept is that if heats of adsorption are less than two or three times of latent heats of vaporization, weak physical adsorption is occurring. Here the ratios are ca. 1 or heats of adsorption are close to latent heats of vaporization so this case involving organic compounds on soil matrices can be considered as weak physical adsorption (73).

The forces involved in physical adsorption are considered to include van der Waals forces (dispersion - repulsion) and electrostatic interactions comprising dipole, quadrupole interactions and polarization. For the adsorption of polar molecules like H_2O and NH_3 on zeolite adsorbent, the electrostatic contribution may be very large, causing unusual high heats of adsorption of 25 - 30 kcal/ mole (73). By contrast, the heats of adsorption of n-butane, 1-butene and benzene in silicalite are almost constant over a wide range of concentration and are relatively low, approximately 11.5 kcal/ mole. These hydrocarbon molecules - silicalite may be considered as similar cases to the organic pollutants - soil matrices.

Let us consider the degree of the non-specific contributions (dispersion, repulsion and polarization) on heats of adsorption which are typically 10 kcal/ mole or less (73). The heats of adsorption of target organic compounds in soil matrices may therefore be largely attributed to the non-specific contributions rather than the specific contribution (dipole and quadrupole).

The second central moment data could be also obtained from chromatographic analysis in plug flow experiments. In addition to

the intraparticle diffusion and mass transfer film resistance, longitudinal diffusion effect on the dynamic behavior of adsorption column was first considered by Glueckauf et. al (109) and Lapidus et. al (110), in order to explain the broadening of the response curve. Later, van Deemter et. al (111) introduced the concepts of height equivalent to a theoretical plate into studying partition chromatography in consecutive mixing stages. This has been further investigated by developing chromatographic response theory as proposed initially by Kubin and Kucera (52,54), expanded mainly by Smith et. al (58,64), enabling separation of the effects of each mass transfer step involved.

There have been many considerations for axial dispersion effects on mass transfer in adsorption columns, however, as discussed by Langer et. al (112), there are only two main mechanisms responsible for this phenomenon: molecular diffusion and turbulent mixing arising from the splitting and recombination of gas flows while traveling through the column. These effects may be additive and the dispersion coefficient may be represented for the non-porous materials like glass balls by the following equation (73):

$$D_L = \gamma_1 D_m + \gamma_2 (2R_p v) \qquad (44)$$

where γ_1, γ_2 = constants

If expressed in terms of the Peclet number, it will be

$$\frac{1}{Pe} = \frac{D_L}{2vR_p} = \gamma_1 \frac{D_m}{2vR_p} + \gamma_2 = \frac{\gamma_1 \varepsilon}{Re\ Sc} + \gamma_2 \qquad (45)$$

where ε = void fraction

Following the same equation as the above equation (45) in the case of porous material and strong adsorption leads to a value of γ_1 which is much larger. Following Wakao's suggestion (113,114), $\gamma_1 = 20/\varepsilon$ for porous particles while it is $0.45 + 0.55\ \varepsilon$ in the case of non-porous material (73). As seen in equation (44), for relatively large particles and high gas velocity, the second term in the right-hand side of this equation tends to be dominant and play a more important role rather than molecular diffusion.

At intermediate Reynolds number region, however, this equation may be expressed in a different way (115):

$$\frac{1}{Pe'} = \frac{\gamma_1\ \varepsilon}{Re\ Sc} + \frac{1}{Pe'_\infty\ (\ 1+\frac{\beta\gamma_1\varepsilon}{Re\ Sc}\ )} \qquad (46)$$

Here, β and Pe'_∞ are constants and Pe'_∞ means a limiting Peclet number. The literature data for larger particles ($R_p > 0.15$ cm) appear generally consistent and show a limiting Peclet number close to the theoretically expected value of 2.0, however, data for the smaller particles show smaller limiting Peclet numbers (73).

For particles with diameters less than 0.3 cm, the limiting Peclet number is given approximately by (112):

$$Pe'_\infty = 3.35\ R_p \qquad (47)$$

When these approximations are utilized to estimate the case of chloroform at the middle value of our experimental flow conditions (2.505 cm/sec.) and at 140°C, the dispersion coefficient will be 0.221 cm^2/sec for the non-porous case, and 5.842 cm^2/sec for the porous and strong adsorption case. When these numbers are compared with the experimentally observed value of 1.30 cm^2/sec, it can be said that axial dispersion in soil matrix column is due to interparticle gas flow plus relatively weak adsorption behavior onto the soil particle surfaces.

On the other hand, the values of intraparticle diffusion coefficients are relatively small when compared with those of Knudsen diffusion coefficients in highly porous catalyst particles (57). This is partly because soil matrices considered here are much less porous and diffusion terms are for total area. For more accurate analysis, further structural studies including pore size distribution measurements, tortuosity and effects of experimental variables should be included.

In order to estimate contributions of each mass transfer step to overall variance of our observed chromatograms, the form of equation (11) as below can be utilized:

$$\frac{\mu_2'}{2(L/v)} = \delta_t = \delta_d + \delta_p + \delta_f \qquad (48)$$

where

$$\delta_d = \frac{D_L}{v^2} \left[1 + \frac{1-\theta_b}{\theta_b} \theta_p (1+K_a) \right]^2 \qquad (49)$$

$$\delta_p = \frac{R_p}{15 D_p} \frac{1-\theta_b}{\theta_b} \theta_p^2 (1+K_a)^2 \qquad (50)$$

$$\delta_f = \frac{R_p}{3k_f} \frac{1-\theta_b}{\theta_b} \theta_p^2 (1+K_a)^2 \qquad (51)$$

δ_t = sum of all contributions

This calculation is applied for some of the target compounds and the results are expressed in Table 7-2. As can be seen in this table, major factors in the total variance are intraparticle diffusion and dispersion along the column, which is in good agreement with the mass transfer studies in catalytic beds (57,60). As linear gas velocity increases, the contributions of axial dispersion on δ_t tend to be weaker. The effect of mass trnsfer film resistance is almost negligible in the operating conditions as expected. This results, however, would change with system variables like particle diameter, the ratio of column diameter to particle diameter and operating variables including temperature.

While these results make it possible to have a general idea on the mass transfer behavior of organic substances in soil matrix column; more studies to discern the effect of additional variables such as particle diameter are suggested in order to have a better insight into the mechanism.

B. Prediction of Organic Compound Concentrations in Soil Matrix Columns

Prediction of concentration distributions of organic compounds in the adsorption/desorption process have been made using both analytical

Table 7-2. Estimated Results of Contribution of Each Mass Transfer Step to δ_t in Percent

Compound	Temperature °C	Linear gas vel. cm/s	Contribution to total variance, % δ_d	δ_p	δ_f
chloroform	140	1.16	44.4	55.6	0.040
		1.47	33.2	66.8	0.047
		2.08	19.9	80.1	0.057
		2.72	12.7	87.3	0.062
1,1,1-tri-	120	1.10	47.4	52.6	0.074
chloroethane		1.40	35.7	64.2	0.090
		2.59	14.0	85.9	0.121
		3.07	10.4	89.5	0.126
benzene	140	1.16	31.7	68.3	0.037
		2.08	12.6	87.4	0.048
		2.72	7.7	92.2	0.050
		3.23	5.6	94.3	0.052
toluene	160	1.21	39.8	60.1	0.060
		1.54	29.0	70.9	0.071
		2.18	17.0	82.9	0.083
		2.85	10.7	89.2	0.089

solutions and numerical modeling. As shown in Chapter 6, different numbers of collocation points were utilized to obtain satisfactory concentration distribution in the numerical method. For the purpose of comparison with the analytical solutions, six collocation points along with the radial direction inside particles and the axial direction of the column were selected in the numerical solution. Both results from analytical and numerical solutions were compared in the same figures to show the breakthrough curves in the column. The results for specific case of toluene and chloroform appear in Figure 7-1.

The curves from both approaches as shown in the figure, show essentially identical results and the numerical approach here can be assumed to be valid and utilized for further analysis.

Based on the numerical approach, previously obtained data of mass transfer parameters were utilized to simulate the outlet concentration in the process of contamination/desorption of the soil matrix column. The results are compared with the experimental results of soil column contamination and desorption as shown in Figure 7-2. The experimental and numerically simulated results are reasonably well coincident each other. Experimental results tend to show a little steeper breakthrough curves near the reflection points as opposed to the curves from numerical results, especially in the adsorption cases. In the desorption or decay curves, the two curves from experiments and numerical simulation tend to show closer agreement.

From the desorption/decay curves, it can be observed that there exist two major stages of depleting organic compounds from the soil matrix column: steady effluent concentration stage in the initial

Figure 7-1. Comparison of Analytical and Numerical Solution Results for Soil Column Adsorption Processes

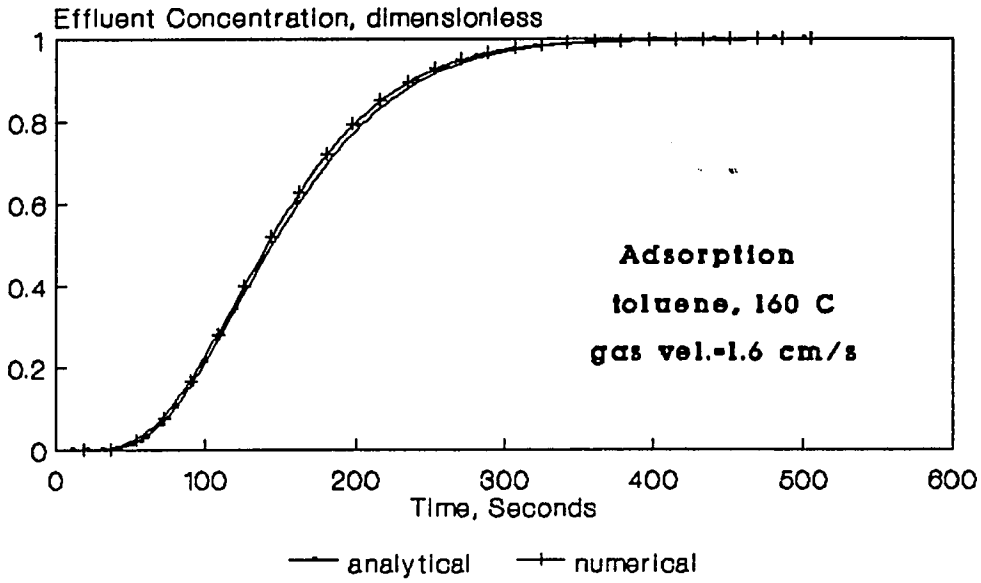

Figure 7-1. (continued)

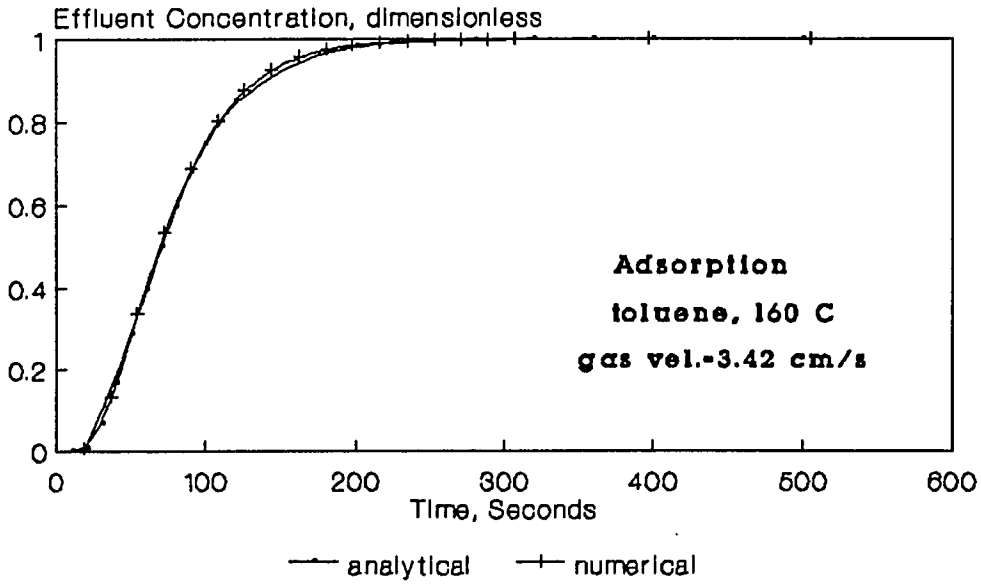

Figure 7-1. (continued)

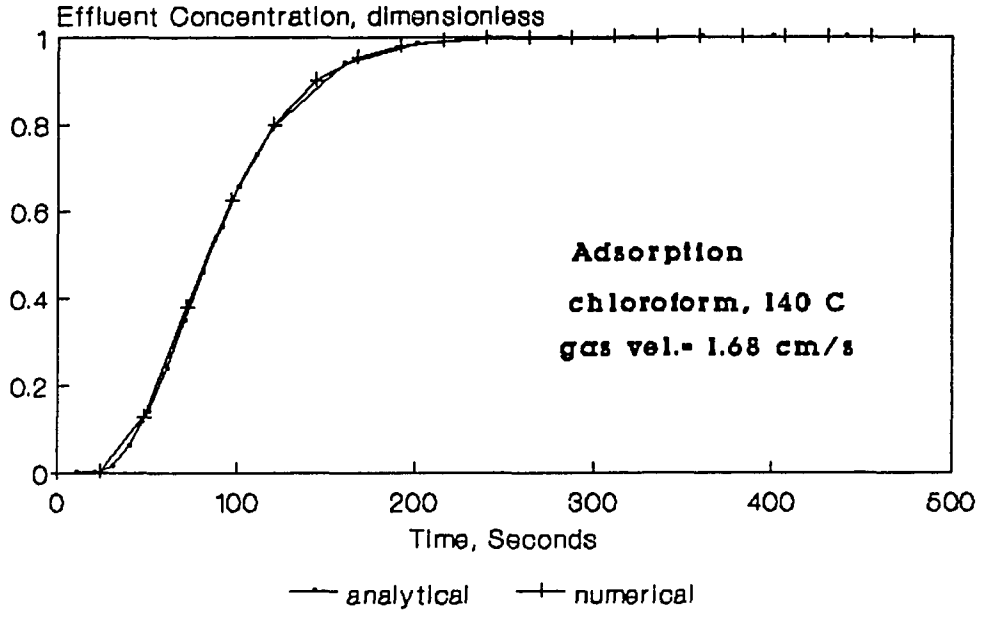

Figure 7-1. (continued)

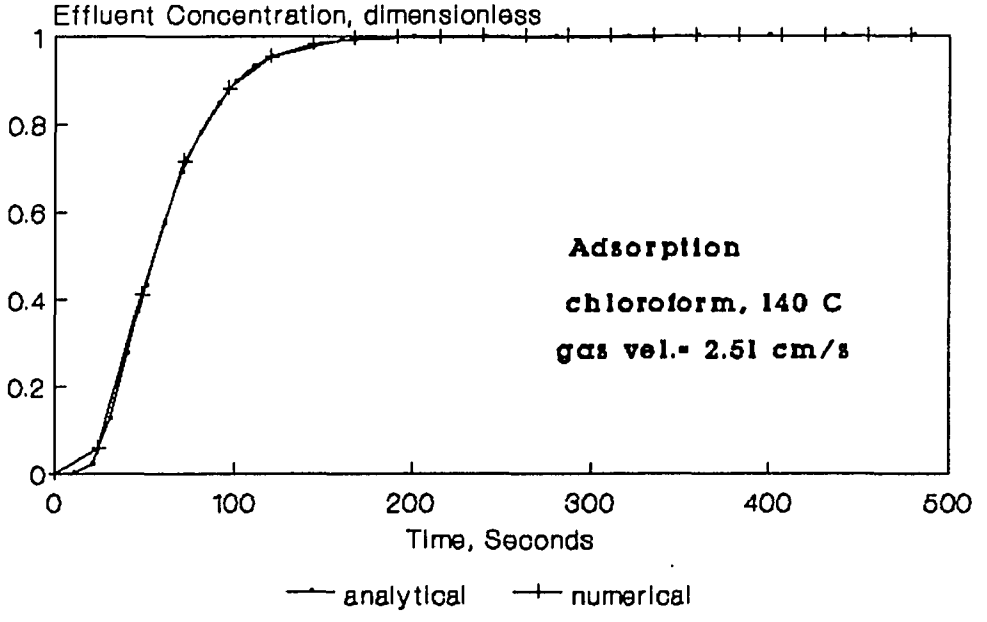

Figure 7-2. Effluent Conc. Profile from Experiments and Numerical Solutions

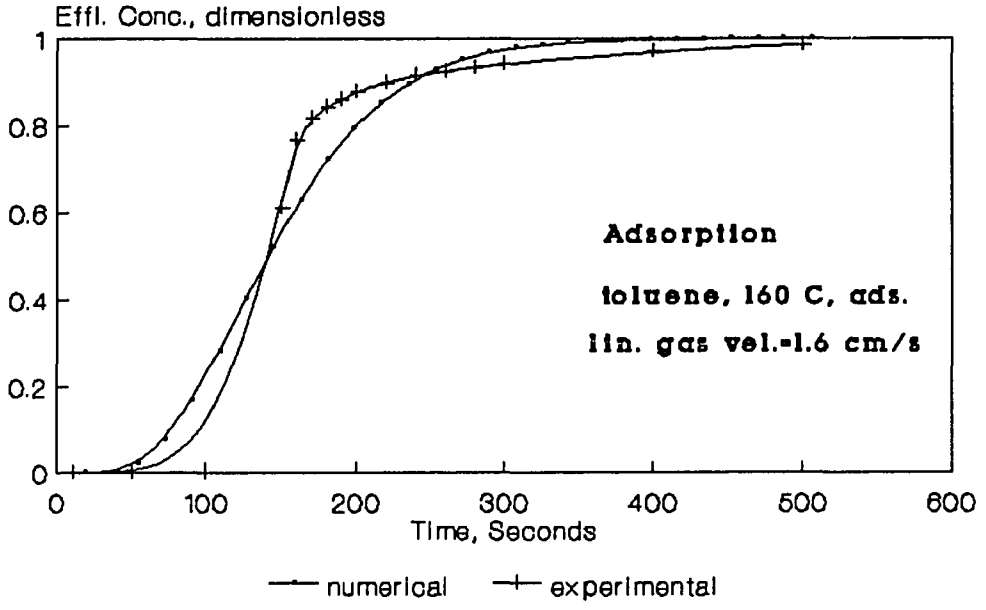

Figure 7-2. (continued)

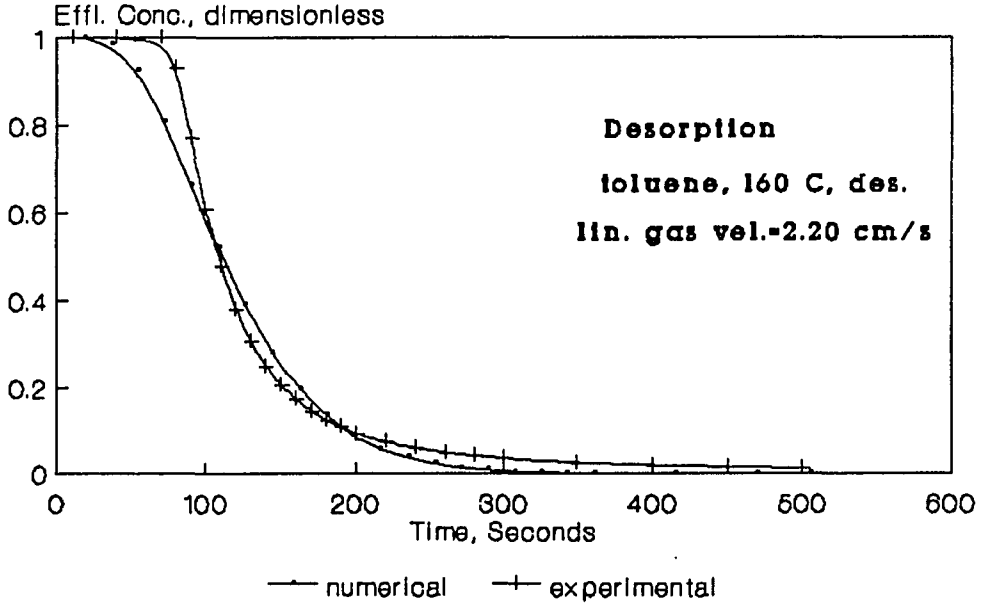

Figure 7-2 (continued)

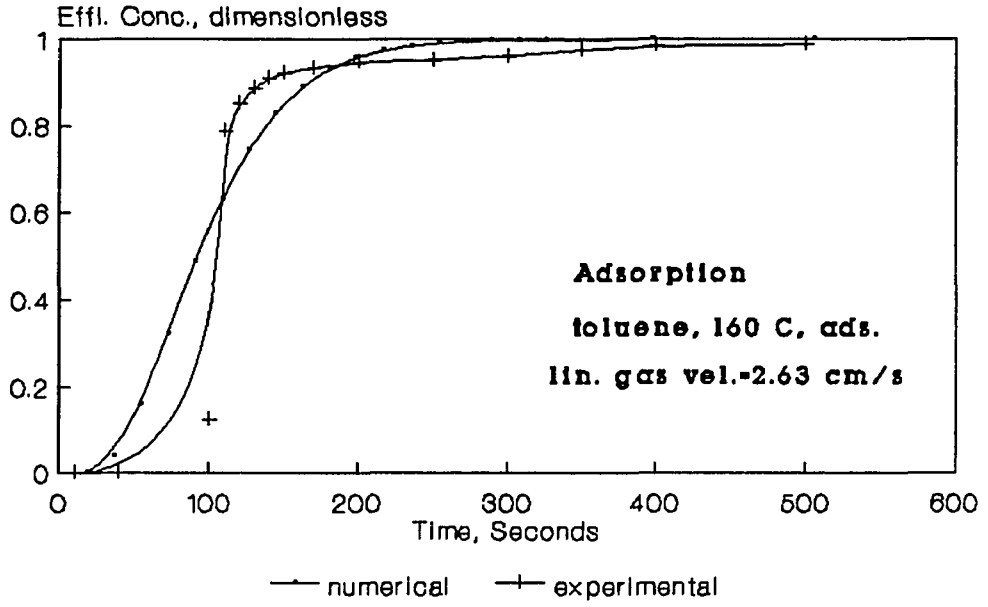

Figure 7-2 (continued)

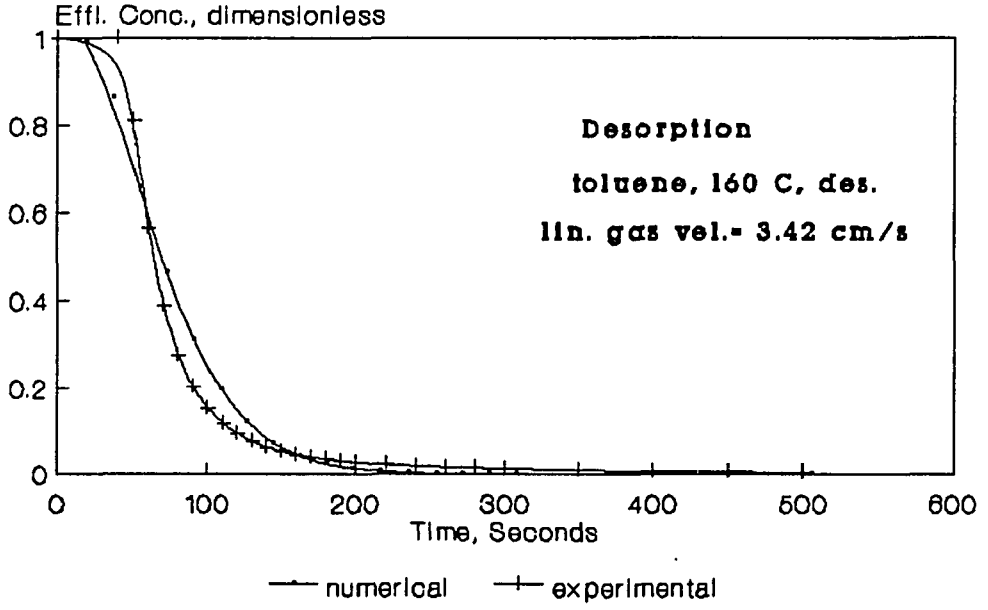

desorption period which is more clearly shown in the lower linear gas velocity case of 2.20 cm/sec and downstream concentration decaying stage. The time period of steady effluent concentration in the experiments tends to be relatively longer than the numerical simulation results. This may be partly attributable to time needed for developing flow in the column when the six-way valve is turned to the desorption mode plus the effect of less sharp breakthrough curves from numerical simulation results.

The effect of temperature on the effluent concentration profile has been also investigated for the toluene adsorption in the soil column and for two temperatures utilizing the estimated mass transfer parameters and numerical simulation. The equilibrium constant for the higher temperature (180°C) is from the chromatographic analysis result and other mass transfer parameters are from the data of 160°C and calibrating them following the equations presented. Results are shown in Figure 7-3. As shown here, the temperature increase of 20°C greatly changes the response of effluent concentration. This is considered largely due to the changes of equilibrium constant and diffusion rates inside and outside particles.

Analysis on sensitivity of specific parameters to these effects is now possible through an analysis of the system with variation of single mass transfer parameter as following.

Figure 7-3 Effluent Conc. Profile for Different Temperatures

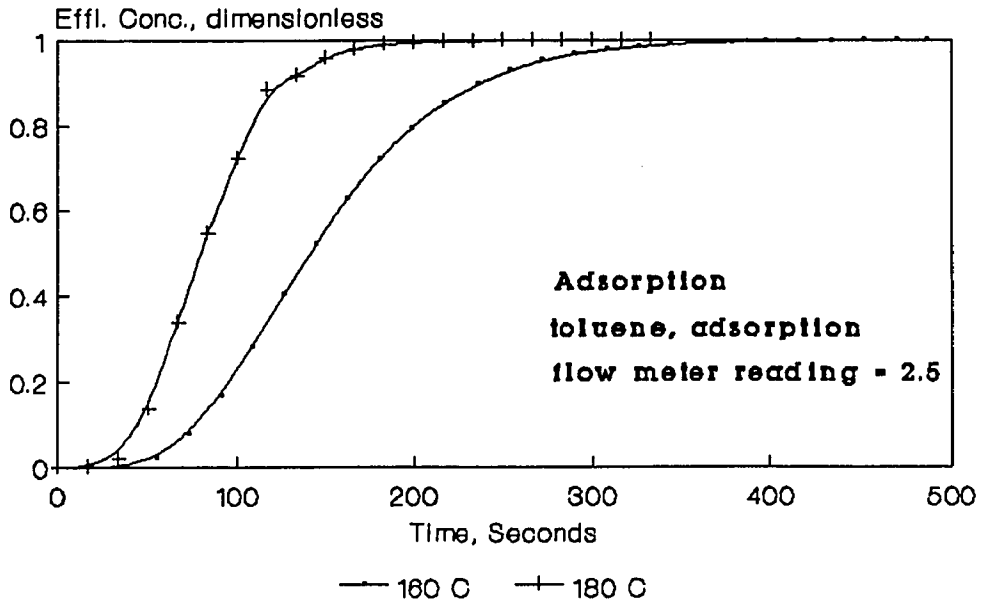

Figure 7-3 (continued)

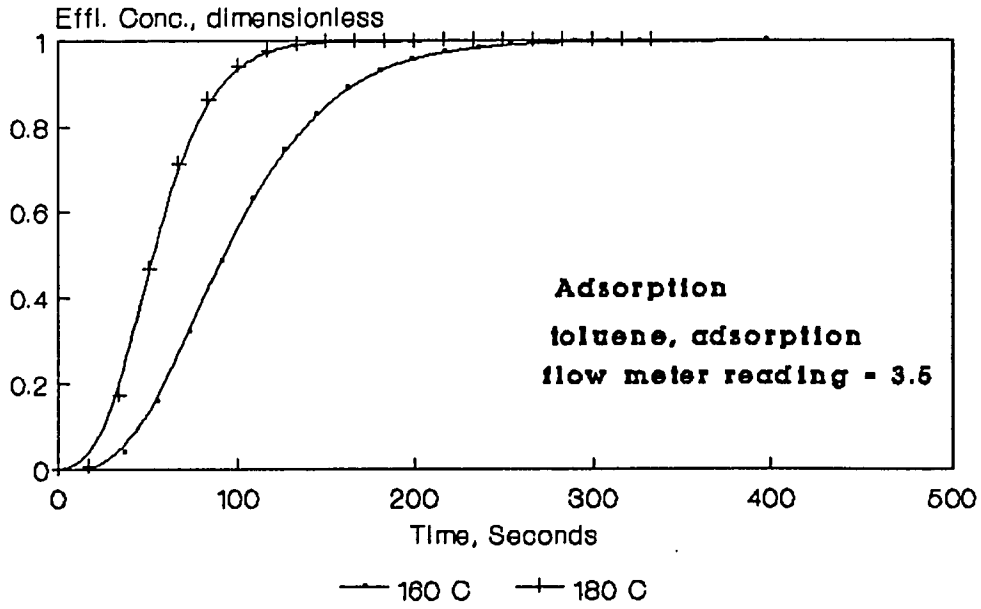

C. Sensitivity Analysis of Mass Transfer Parameters

In order to analyze the effect of mass transfer parameters on the behavior of the adsorption profile and to decide relative importance of each mass transfer step, sensitivity analysis has been performed.

A set of basic data for mass transfer parameters has been utilized in pursuing this analysis. Data used for this and varied parameters are summarized in Table 7-3.

The analysis results appear in Figure 7-4 for axial dispersion coefficient or Pe, Figure 7-5 for intraparticle diffusion coefficient or ϕ and Figure 7-6 for equilibrium constant or η with effluent concentration profiles and axial and/or intraparticle concentrations.

The effect of the variation of Peclet number on the adsorption of soil - organics system is shown in Figure 7-4. Two extreme values of Peclet number (400 and 40) were applied to the simulation and effluent concentration with time and concentration distribution along the axial direction at dimensionless time of 3 are also displayed here. The effect of changing axial dispersion can be seen as the change in shape of the breakthrough curves. As the Peclet number decreases or the axial dispersion coefficient increases, the dispersion along the axial direction is accelerated as expected. The same results can be drawn from the second plot of Figure 7-3 indicating that concentration propagation becomes more broadened or more dispersed as the Peclet number decreases.

Figure 7-5 shows the sensitivity of the intraparticle diffusion coefficient. As shown in these plots, higher intraparticle diffusion rate (lower ϕ) enhances the uptake of adsorbate, resulting in lower

Table 7-3. Basic Data Set of Mass Transfer Parameters and Variation of Dimensionless Groups in Sensitivity Analysis

Data of system and operational variables

Column length = 29.0 cm

Particle radius = 0.023 cm

Linear gas velocity = 2.626 cm/sec

Equilibrium constant = 72.23 (η = 62.5)

Axial dispersion coefficient = 1.079 cm^2/sec (Pe = 70.6)

Mass transfer film coefficient = 6.374 cm/sec (ξ = 42.4)

Intraparticle diffusion coefficient = 2.93 E-05 cm^2/sec (ϕ = 1.64)

Variation of dimensionless groups

Pe	D_L(cm^2/s)	File I.D.
400	0.2	SENS101
70.6	1.08	SENS102
40	7.62	SENS103

ϕ	D_PxE05(cm^2/s)	File I.D.
2.0	2.4	SENS104
1.64	2.93	SENS105
1.0	4.79	SENS106

η	K_a	File I.D.
90	103.97	SENS107
62.5	72.23	SENS108
30	34.65	SENS109

ξ	k_f	File I.D.
289	40	SENS110
42.4	6.37	SENS111
7.2	1.0	SENS112

Figure 7-4. Results of Sensitivity Analysis with Varied Values of Mass Transfer Parameters (Axial Disp. Coeff.)

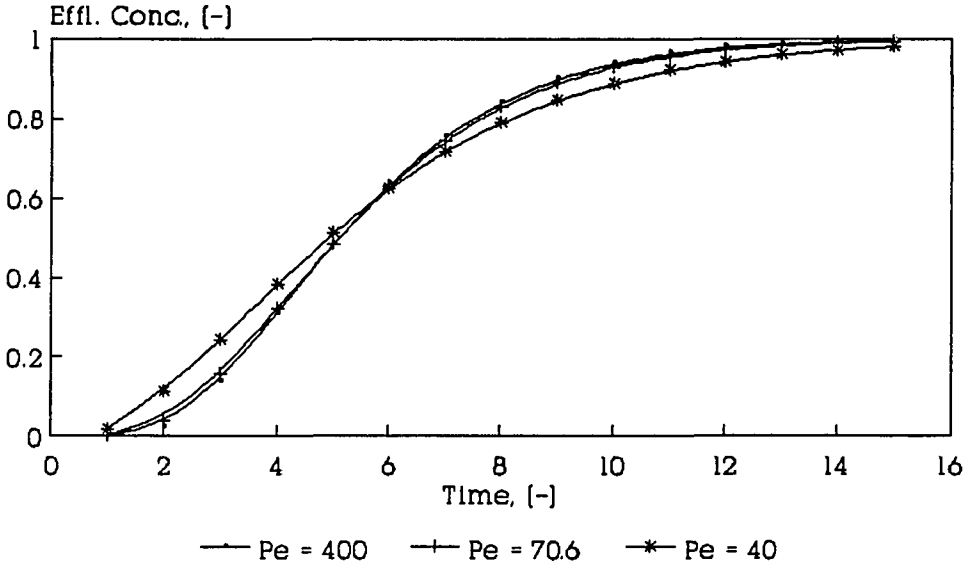

Figure 7-4. (continued)

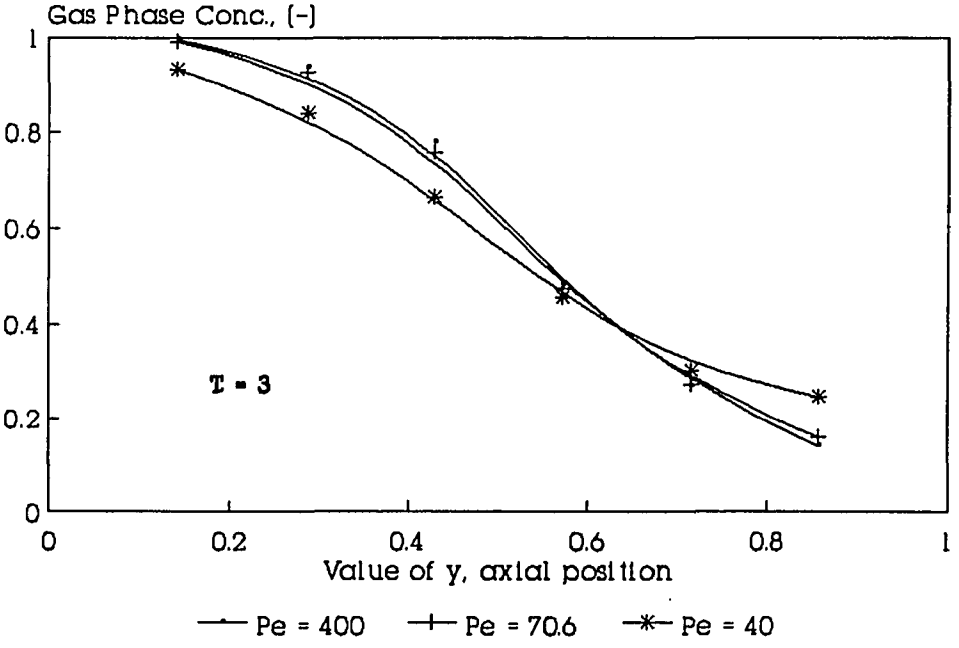

Figure 7-5. Results of Sensitivity Analysis with Varied Values of Mass Transfer Parameters (Intrapart. Diff.)

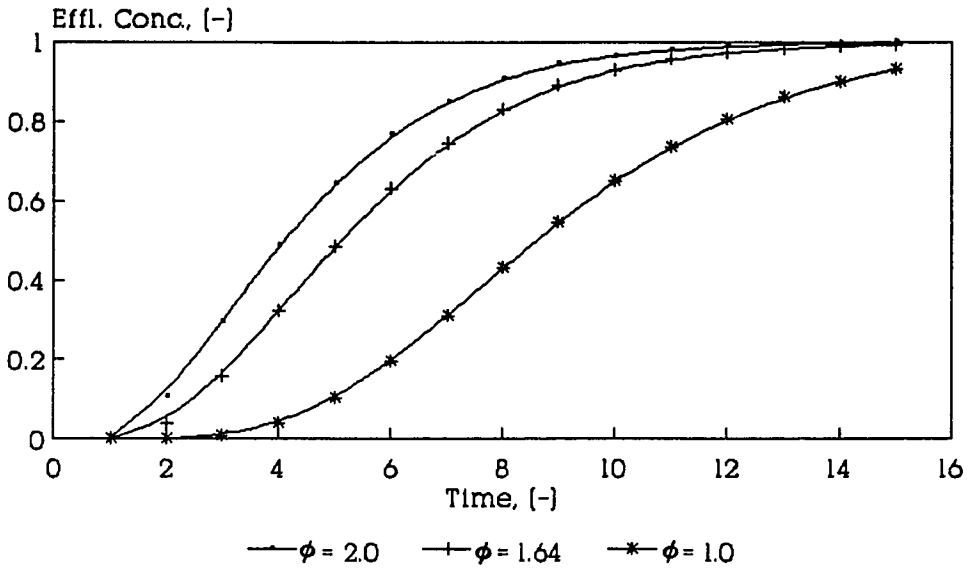

Figure 7-5. (continued)

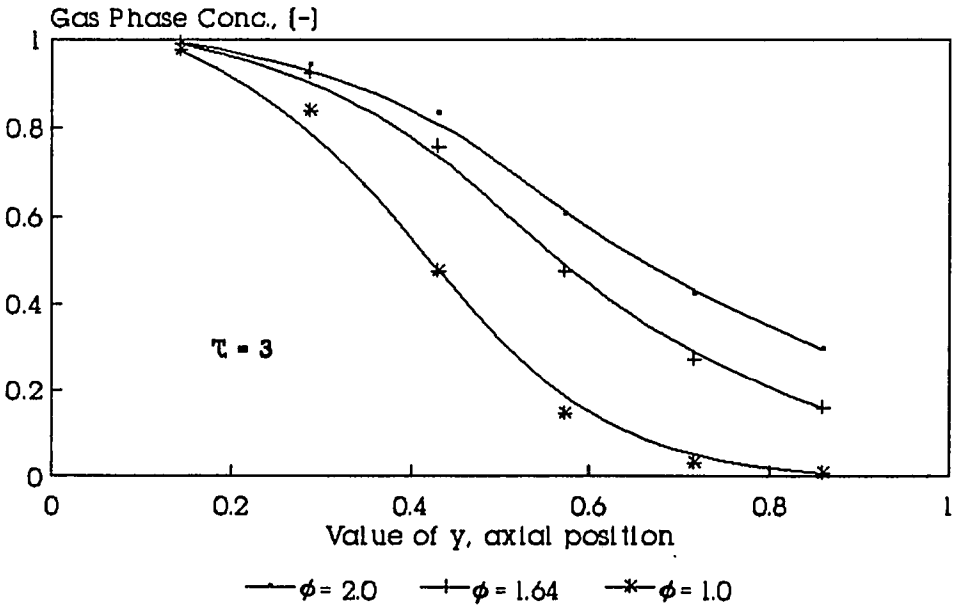

Figure 7-5. (continued)

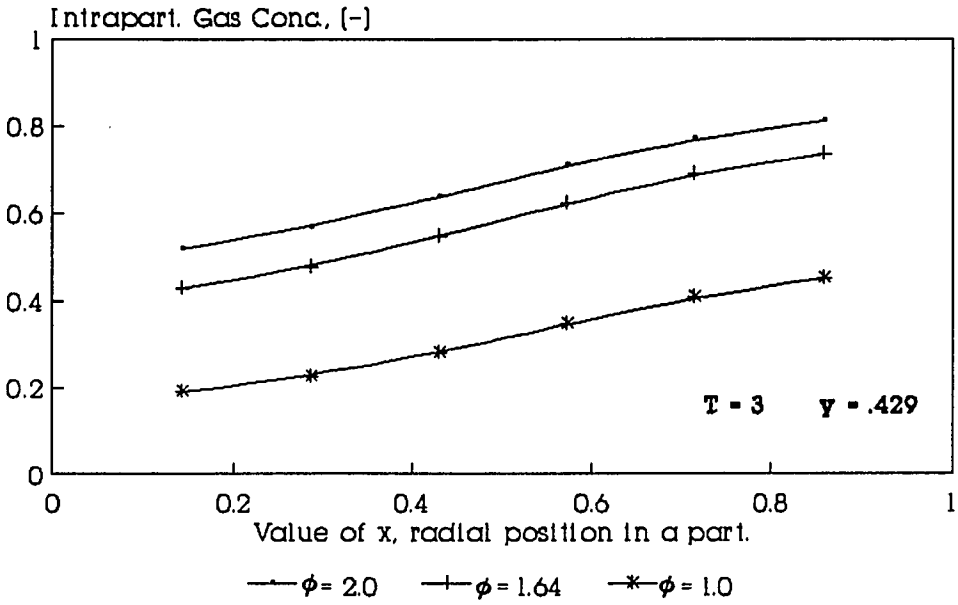

Figure 7-5. (continued)

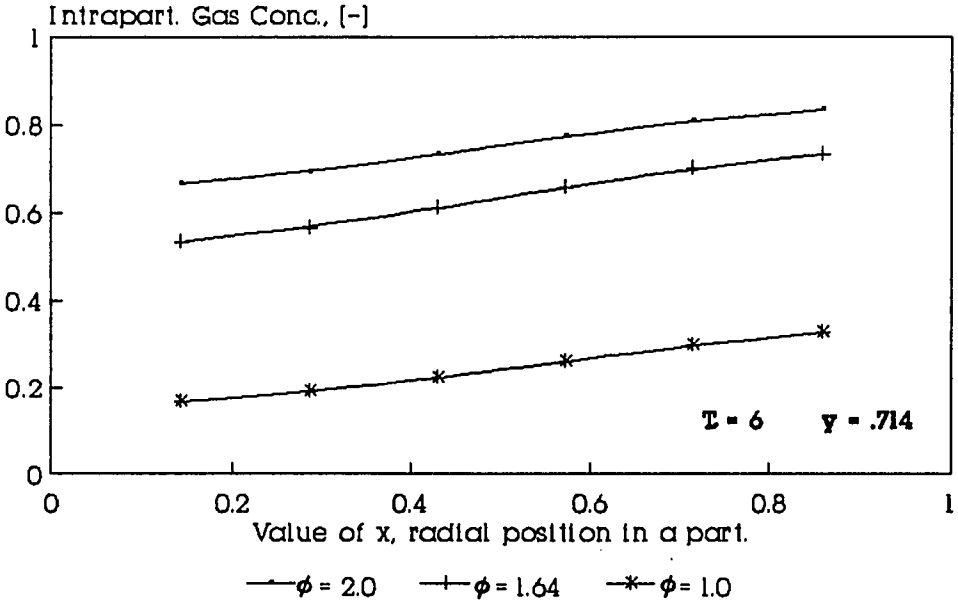

gas phase concentration and delaying the arrival of main concentration wave at the exit.

The effects of equilibrium constants are shown in Figure 7-6. Higher equilibrium constants (higher η) also appear to have the effect of delaying the concentration wave propagation because of higher capacity for the organics on adsorbent surface. In the third and fourth plots of Figure 7-6, concentration distributions along the radial direction inside particles are shown. While absolute values tend to follow those of the external fluid phase, the slopes of the profile tend to be affected by the equilibrium constants, resulting in higher slopes in the cases of higher values of the equilibrium constants (or higher values of η).

The values of mass transfer film coefficients have also been varied to observe their effects on mass transfer behavior in the adsorption column. Although their values were changed even to the extreme cases, their effects were minor, resulting in the concentration changes less than 0.1 %.

When all of these parameters are analyzed in a view of their significance to the behavior of the adsorption system, the major factors must be considered as:

- equilibrium between phases
- intraparticle diffusion
- axial dispersion

These 3 parameters can possibly account for the difference between experimental results and simulated results.

Further studies such as the microscopic structural analysis and varied systems with different operational conditions will be certainly

Figure 7-6. Results of Sensitivity Analysis with Varied Values of Mass Transfer Parameters (Equil. Constant)

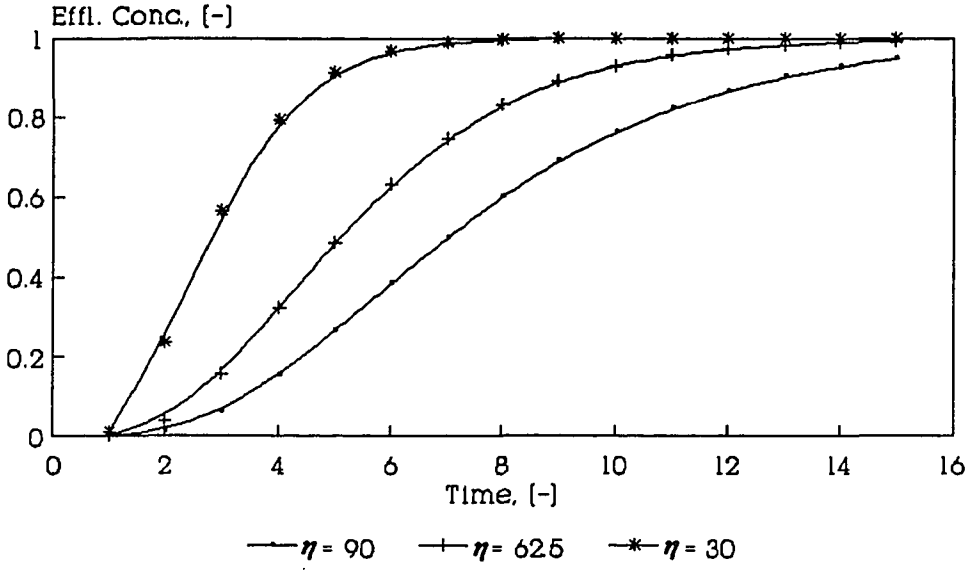

Figure 7-6. (continued)

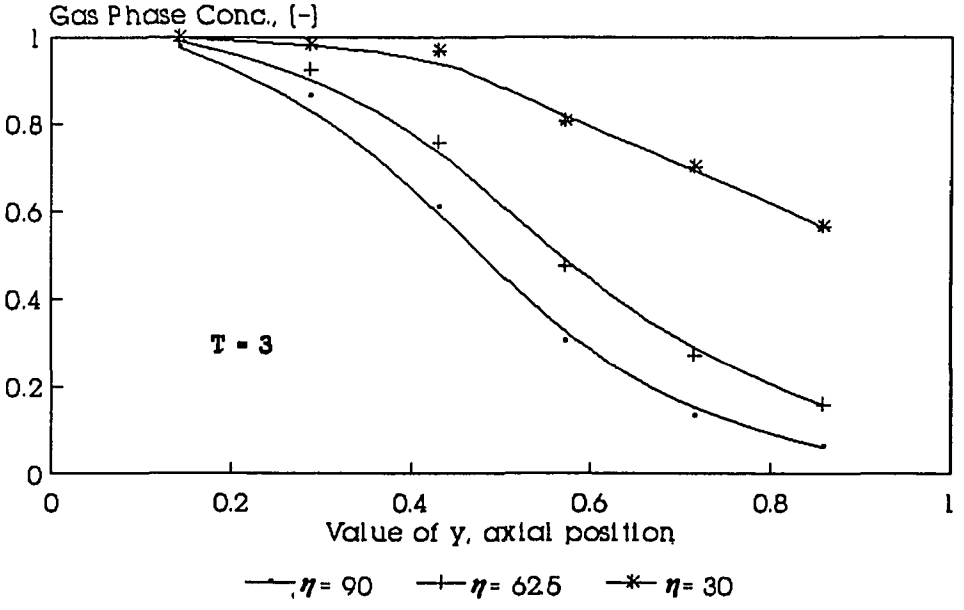

Figure 7-6. (continued)

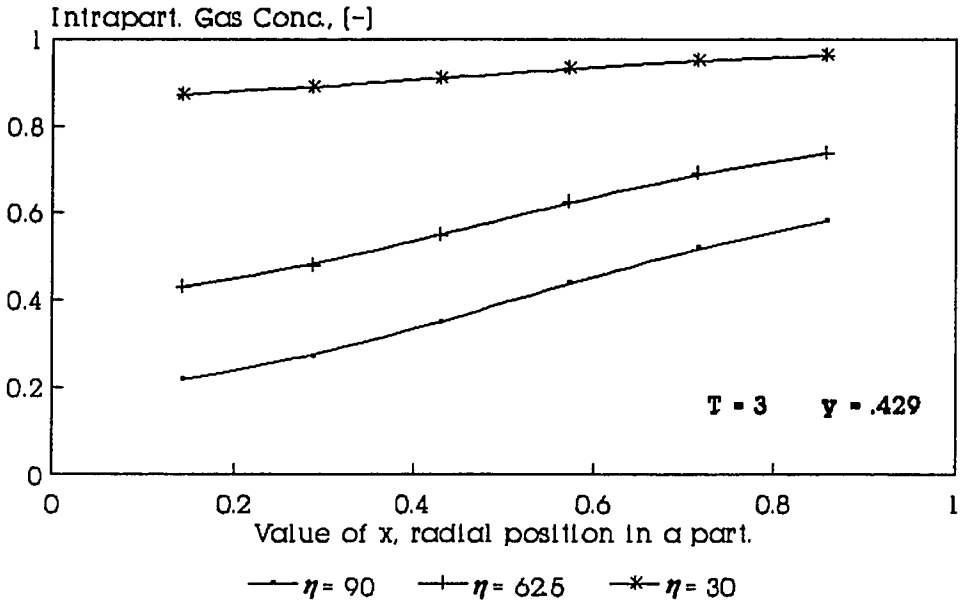

Figure 7-6. (continued)

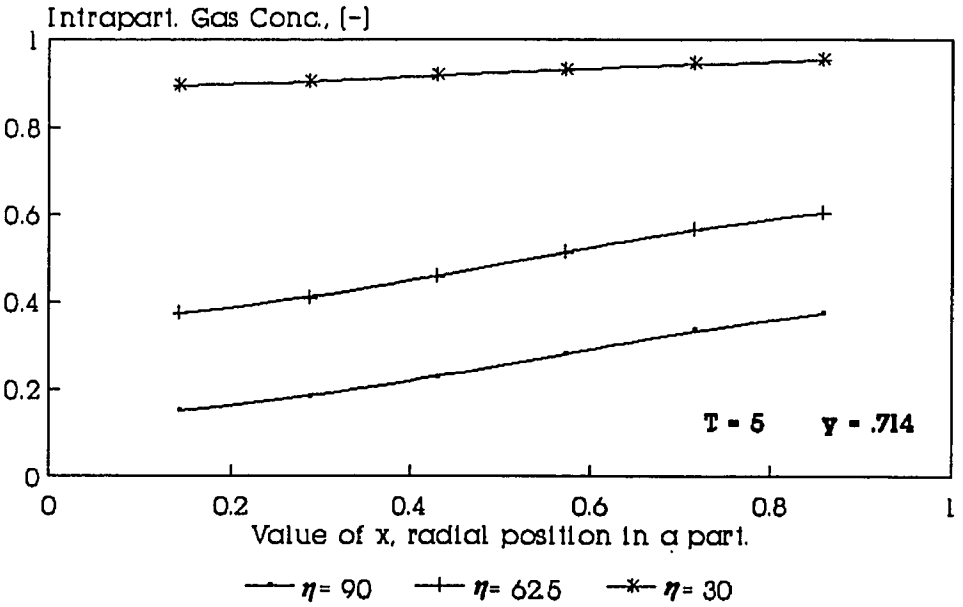

helpful in understanding the mass transfer of organic compounds in soil matrix columns and predicting its behavior in a more thorough way.

Chapter 8. CONCLUSIONS AND RECOMMENDATIONS

A. Summary of Conclusions

Chromatographic response analysis connected with plug deposition experiments has been utilized to study the mass transfer mechanism of organic contaminants in soil matrices. Equilibrium constants, heats of adsorption and mass transfer parameters in a soil matrix column system were successfully determined.

Equilibrium constants were strongly dependent on temperature and showed good linearity with van't Hoff plots for temperatures above the minimum allowable temperatures (MAT's) which indicate the minimum temperature at which 95 % of the input plug of organic material is removed from the soil column after one hour operation at continuous flow. As a result of analysis of heats of adsorption, this system of organics - dry soils is considered to be one of moderately weak physical adsorption.

The analysis of relative contribution of each mass transfer step showed that axial dispersion and intraparticle diffusion in addition to equilibrium between the gas and the particle surface are the main factors affecting the behavior of organics in the system.

A devised equilibrium test system has been utilized to observe the adsorption/desorption behavior of organics in soil matrices. Adsorption isotherms showed good linearity at the lower concentrations and the slopes of this linearity tend to decrease with increasing

temperature (less adsorption). Desorption experiments tend to show hysteresis phenomena at lower temperatures while the hysteresis becomes weaker, more ideally reversible, or closer to ideal adsorption isotherms at higher temperatures.

In order to predict the transient mass transfer in a soil column, both an analytical solution and a numerical approach using orthogonal collocation method have been developed. The results from two modeling approaches showed satisfactory coincidence. Based on the numerical method connected with estimated mass transfer parameters, predicted results were compared with those of soil column contamination/ desorption experiments. Those two results were shown to be reasonably well coincident each other, indicating that our numerical method predicts the mass transfer in soil adsorption columns in a correct way.

Sensitivity analysis involving the variation of mass transfer parameters has been performed to analyze their effects on the adsorption behavior. This analysis with varied dimensionless groups showed that mass transfer parameters including axial dispersion coefficients, intraparticle diffusion coefficients and equilibrium constants have significant effects on the concentration profiles in the system.

In order to utilize these results more efficiently and to improve the prediction of mass transfer behavior in the soil adsorption column, further studies involving different, extended system conditions are considered to be worthy.

B. Recommendations for Future Study

- Mass transfer behavior in soil matrix system may be predicted from a more detailed study involving microscopic investigation of soil particles. Resulting data including the microscopic structure, intraparticle porosity and pore size distributions will be helpful to better understand the mass transfer phenomenon and improve the prediction capability through a numerical simulation.

- Effect of impurities in soil matrices including water and humus substances may be investigated to bring this study closer to the reality.

- Experiments and simulations involving different particle sizes could be utilized in confirming the approaches and improving its applicability.

- Different types of soil matrices including sand, silt, mixtures with clay and standard soils could be tried for experiments such as the equilibrium test and their results can be compared to determine the relative affinities of each for organic compounds and to obtain information concerning applicable temperature limits.

- Effects of heat transfer at the outer surface and inside the soil column could be added to the mass transfer study to analyze its significance toward behavior of organics in the soil adsorption

column. Temperature effects on mass transfer parameters and changes of the contribution of each mass transfer steps involved with varied temperature could be studied with more experimental work.

Appendices

1. Program Lists for Chromatogram Data Analysis

2. Derivation for Chromatographic Response of a Packed Soil Column

3. Derivation for Chromatographic Response of a Non-Porous Soil Matrix Column

4. Program List for the Integration of Analytical Solution

5. Derivation of a Numerical Solution for Contamination/ Desorption of Organics in a Soil Matrix Column

6. Matrix Development Program for Orthogonal Collocation Method

7. Program List of the Numerical Solution Using Orthogonal Collocation Method

8. Matrix Calculation Results for Orthogonal Collocation Method

9. Examples of Numerical Simulation Results of Soil Column Contamination/Desorption Process

Appendix

Appendix 1. Program Lists for Chromatogram Data Analysis

- CHRM.BAS

[BASIC program list to obtain the first absolute and second central moment from chromatogram data]

```
10    OPEN #11: NAME "M:SIGNAL.BNC"
20    INIT_ACCESS #11
25    SUM=0
26    VSUM=0
30    TAREA=0
40    NN=1
45    NX=1
50    PRINT "FILELENGTH (MIN.) "
60    INPUT T
65    PRINT "XBASE ?":INPUT XBASE
70    NT=T*300
80    XAREA=SLICE_AREA+XBASE
82    IF XAREA<0 THEN XAREA=0
90    TAREA=TAREA+XAREA
92    SUM=SUM+SLICE_NUM/300*XAREA
95    INC_SLICE_NUM (1)
100   NN=NN+1
110   IF NN>NT THEN GOTO 130
120   GOTO 80
130   PRINT "TOTAL AREA=",TAREA
135   AVGT=SUM/TAREA
137   PRINT "AVG. RETENTION TIME =",AVGT,"MIN."
140   CLOSE #11
150   OPEN #11: NAME "M:SIGNAL.BNC"
155   INIT_ACCESS #11
157   XAREA=SLICE_AREA+XBASE
158   IF XAREA<0 THEN XAREA=0
160   VSUM=VSUM+(SLICE_NUM/300-AVGT)^2*XAREA
170   INC_SLICE_NUM (1)
180   NX=NX+1
190   IF NX>NT THEN GOTO 210
200   GOTO 157
210   VAR=VSUM/TAREA
220   PRINT "VARIANCE                =",VAR,"MIN."
230   CLOSE #11
240   END
```

- **DSPLY.BAS**

[BASIC program list to display generated bunched data files]

```
 10   OPEN #11: NAME "M:SIGNAL.BNC"
 20   INIT_ACCESS #11
 30   N=1
 40   PRINT N,SLICE_AREA
 50   N=N+5
 60   INC_SLICE_NUM (5)
 70   IF N>50 THEN GOTO 90
 80   GOTO 40
 85
 90   N=N+50
100   INC_SLICE_NUM (50)
110   PRINT N,SLICE_AREA
120   GOTO 90
```

Note]

1. SIGNAL.BNC = bunched data file which is generated from raw data file

2. Input/Output

   - CHRM.BAS

     Input data file = SIGNAL.BNC
     length of data file, min.
     value for baseline

     Output generated = total area
     average retention time, min.
     variance, $min.^2$

   - DSPLY.BAS

     Input data file = SIGNAL.BNC

     Output generated = display of data as a function of time

Appendix 2. Derivation for the Chromatographic Response of a Packed Soil Column

The derivation of equations here largely follow the procedure of Suzuki and Smith (58) and the main purpose of this derivation is to verify the equations in a different system.

From the mass balance for a small shell of a particle,

$$4\pi r^2 \Delta r \theta_p \frac{\partial C_i}{\partial t} + 4\pi r^2 \Delta r (1-\theta_p) \frac{\partial C_p}{\partial t} = N_r \, 4\pi r^2 \Big|_{r=r} - N_r \, 4\pi r^2 \Big|_{r=r+\Delta r} \qquad \text{(A-1)}$$

$$\text{where} \quad N_r = - D_p \frac{\partial C_i}{\partial r} \qquad \text{(A-2)}$$

Manipulating this equation with the definition of an equilibrium constant $(1-\theta_p)C_p = \theta_p K_a C_i$ gives

$$D_p \left(\frac{\partial^2 C_i}{\partial r^2} + \frac{2}{r} \frac{\partial C_i}{\partial r} \right) = \theta_p (1+K_a) \frac{\partial C_i}{\partial t} \qquad \text{(A-3)}$$

From mass balance for a small cross-section of the column,

$$A\Delta z \theta_b \frac{\partial C}{\partial t} = A\theta_b N_z \Big|_{z=z} - A\theta_b N_z \Big|_{z=z+\Delta z} + A\theta_b v C \Big|_{z=z} - A\theta_b v C_z \Big|_{z=z+\Delta z}$$

$$- A\Delta z (1-\theta_b) \frac{4\pi R_p^2}{\frac{4}{3}\pi R_p^3} N_{Rp} \qquad \text{(A-4)}$$

$$\text{where } N_{Rp} = D_p \left.\frac{\partial C_i}{\partial r}\right|_{r=Rp} = k_f \left(C - C_i|_{Rp} \right) \qquad \text{(A-5)}$$

$$\& \quad N_z = - D_L \frac{\partial C}{\partial z} \qquad \text{(A-6)}$$

Manipulating this equation gives

$$D_L \frac{\partial^2 C}{\partial z^2} - v \frac{\partial C}{\partial z} - \frac{3(1-\theta_b)}{R_p \theta_b} N_{Rp} = \frac{\partial C}{\partial t} \qquad \text{(A-7)}$$

with boundary and initial conditions

$$\left.\frac{\partial C_i}{\partial r}\right|_{r=0} = 0 \qquad \text{(A-8)}$$

$$C_i |_{t=0} = 0 \qquad \text{(A-9)}$$

$$C\ (0, 0 \le t \le \tau) = C_o \quad (=0, \text{ otherwise}) \qquad \text{(A-10)}$$

$$C\ (\infty, t) = 0 \qquad \text{(A-11)}$$

$$C\ (z, 0) = 0 \qquad \text{(A-12)}$$

Taking Laplace transform of equations (A-3), (A-5) and (A-7) with respect to time, and solving them,

$$\left(\frac{\partial^2 \overline{C_i}}{\partial r^2} + \frac{2}{r}\frac{\partial \overline{C_i}}{\partial r}\right) = \frac{\theta_p(1+K_a)}{D_p} p\overline{C_i} \qquad \text{(A-13)}$$

$$D_L\frac{\partial^2 \overline{C}}{\partial r^2} - v\frac{\partial \overline{C}}{\partial z} - \frac{3(1-\theta_b)}{R_p\theta_b}\overline{N_{Rp}} = p\,\overline{C} \qquad \text{(A-14)}$$

$$\overline{N_{Rp}} = D_p\frac{\partial \overline{C_i}}{\partial r}\bigg|_{r=Rp} = k_f\left(\overline{C} - \overline{C_i}|_{Rp}\right) \qquad \text{(A-15)}$$

$$\frac{\partial \overline{C_i}}{\partial r}\bigg|_{r=0} = 0 \qquad \text{(A-16)}$$

$$\overline{C}(0) = \frac{C_o}{p}(1-\exp^{-p\tau}) \qquad \text{(A-17)}$$

$$\overline{C}(\infty) = 0 \qquad \text{(A-18)}$$

Solving equation (A-13),

$$\overline{C_i} = \frac{1}{r}\left[B'\exp(\alpha r) + B''\exp(-\alpha r)\right] \qquad \text{(A-19)}$$

$$\text{where} \quad \alpha = \left[\frac{\theta_p(1+K_a)}{D_p}p\right]^{1/2} \qquad \text{(A-20)}$$

Applying the boundary condition (A-16) into this equation,

$$\overline{C_i} = \frac{B(z)}{r}\sinh(\alpha r) \qquad \text{(A-21)}$$

Substituting this equation into equation (A-15) and rearranging,

$$\overline{C} = \frac{B(z)}{RB_i} [\ \phi \cosh \phi - (1-B_i) \sinh \phi\ ] \qquad \text{(A-22)}$$

where $B_i = k_f R/D_p$, $\quad \phi = R\alpha$

Substituting the expression for $\overline{N_{Rp}}$ into equation (A-14) using equation (A-22),

$$D_L \frac{\partial^2}{\partial z^2} B(z) - v \frac{\partial}{\partial z} B(z) - G(p)B(z) = 0 \qquad \text{(A-23)}$$

$$\text{where} \quad G(p) = p + \frac{3(1-\theta_b)}{\theta_b} \frac{B_i}{R_p^{\,2}/D_p} [\ 1 - \frac{B_i}{A_o(p)+B_i}\ ] \qquad \text{(A-24)}$$

$$A_o(p) = \phi \coth \phi - 1 \qquad \text{(A-25)}$$

Solving equation (A-23) by using the boundary condition (A-18),

$$B(z) = H \exp [\ \frac{v}{2D_L} (1-\sqrt{1+\frac{4D_L}{v^2}G(p)}\ )\ z\ ] \qquad \text{(A-26)}$$

Combining this result with equation (A-22) and rearranging it after applying the boundary condition (A-17),

$$\overline{C} = \frac{C_o}{p} (1 - \exp(-p\tau))\ \exp(-\lambda z) \qquad \text{(A-27)}$$

$$\text{where} \quad \lambda = \frac{v}{2D_L} \left[\sqrt{1+\frac{4D_L}{v^2}G(p)} - 1\right] \qquad \text{(A-28)}$$

At the column outlet, z=L and

$$\overline{C_L} = \frac{C_o}{p} \left[1-\exp(-p\tau)\right] \exp(-\lambda L) \qquad \text{(A-29)}$$

Using the Van der Laan's theorem, n-th order of mement is defined as follows :

$$M_n = (-1)^n \lim_{p\to 0} \left[\frac{d^n}{dp^n} \overline{C} \right] \qquad \text{(A-30)}$$

$$\text{where} \quad M_n = \int_0^\infty C\, t^n\, dt \qquad \text{(A-31)}$$

Hence, the first absolute moment is given by

$$\mu_1 = \frac{M_1}{M_0} = \frac{-\lim_{p\to 0} \left(\frac{d\overline{C}}{dp} \right)}{\lim_{p\to 0} \overline{C}} \qquad \text{(A-32)}$$

By L'Hospital's rule,

$$M_0 = \lim_{p\to 0} \overline{C_L} = C_o\tau \qquad \text{(A-33)}$$

$$M_1 = - \lim_{p\to 0} \left(\frac{d\overline{C_L}}{dp} \right) \qquad \text{(A-34)}$$

Applying L'Hospital's rule and rearranging,

$$M_1 = C_o\tau \left(\frac{\tau}{2} + L \lim_{p\to 0} \frac{d\lambda}{dp} \right) \qquad \text{(A-35)}$$

From equation (A-28),

$$\lim_{p\to 0} \frac{d\lambda}{dp} = \frac{1}{v} \lim_{p\to 0} \frac{dG}{dp} \tag{A-36}$$

$$\lim_{p\to 0} \frac{dG}{dp} = 1 + \frac{3(1-\theta_b)}{\theta_b} \frac{Bi^2}{Rp^2/Dp} \frac{1}{(Ao(0)+Bi)^2} \lim_{p\to 0} \frac{dA_o(p)}{dp} \tag{A-37}$$

Using the relation $\frac{d\phi}{dp} = R \frac{d\alpha}{dp} = \frac{R^2}{2} \frac{\theta_p(1+K_a)}{D_p} \frac{1}{\phi}$ (A-38)

$$\lim_{p\to 0} \frac{dA_o(p)}{dp} = \frac{R^2}{2} \frac{\theta_p(1+K_a)}{D_p} \lim_{p\to 0} \frac{\coth\phi - \phi \operatorname{cosech}^2\phi}{\phi} \tag{A-39}$$

Using L'Hospital's rule,

$$\lim_{p\to 0} \frac{\coth\phi - \phi \operatorname{cosech}^2\phi}{\phi} = \frac{2}{3} \tag{A-40}$$

Substituting all the estimated equations backwards,

$$\lim_{p\to 0} \frac{d\lambda}{dp} = \frac{1}{v} \left[1 + \frac{1-\theta_b}{\theta_b} \theta_p (1+K_a) \right] \tag{A-41}$$

Therefore,

$$M_1 = C_o\tau \left[\frac{\tau}{2} + \frac{L}{v} \left[1 + \frac{1-\theta_b}{\theta_b} \theta_p (1+K_a) \right] \right] \tag{A-42}$$

$$\mu_1 = \frac{M_1}{M_0} = \frac{\tau}{2} + \frac{L}{v} \left[1 + \frac{1-\theta_b}{\theta_b} \theta_p (1+K_a) \right] \tag{A-43}$$

On the other hand, the second central moment can be given by

$$\mu_2' = \frac{\int_0^\infty (t-\mu)^2 C_L dt}{\int_0^\infty C_L \, dt}$$

$$= \frac{M_2}{M_0} - \mu_1^2 \qquad \text{(A-44)}$$

$$M_2 = (-1)^2 \lim_{p\to 0} \frac{d^2\overline{C_L}}{dp^2} \qquad \text{(A-45)}$$

Manipulating this equation after substituting the expression for $\overline{C_L}$,

$$M_2 = C_0 \lim_{p\to 0} \left[\left(\frac{-\tau^2 p^2 e^{-p\tau} - 2(p\tau e^{-p\tau} - 1 + e^{-p\tau})}{p^3} - 2L\frac{p\tau e^{-p\tau} - 1 + e^{-p\tau}}{p^2}\frac{d\lambda}{dp} \right.\right.$$

$$\left.\left. + L^2\frac{1-e^{-p\tau}}{p}\left(\frac{d\lambda}{dp}\right)^2 - L\frac{1-e^{-p\tau}}{p}\frac{d^2\lambda}{dp^2} \right) \exp(-\lambda L) \right] \qquad \text{(A-46)}$$

Here,

$$\lim_{p\to 0} \frac{-\tau^2 p^2 e^{-p\tau} - 2(p\tau e^{-p\tau} - 1 + e^{-p\tau})}{p^3} = \frac{\tau^3}{3} \qquad \text{(A-47)}$$

$$\lim_{p\to 0} \frac{p\tau e^{-p\tau} - 1 + e^{-p\tau}}{p^2} = -\frac{\tau^2}{2} \qquad \text{(A-48)}$$

$$\lim_{p\to 0} \frac{1-e^{-p\tau}}{p} = \tau \qquad \text{(A-49)}$$

Substituting these results into equation (A-46),

$$M_2 = C_0 \left[\frac{\tau^3}{3} + L\tau^2 \lim_{p\to 0}\frac{d\lambda}{dp} + L^2\tau \lim_{p\to 0}\left(\frac{d\lambda}{dp}\right)^2 - L\tau \lim_{p\to 0}\frac{d^2\lambda}{dp^2} \right] \qquad \text{(A-50)}$$

In solving this equation, we need expressions for the derivative form of λ.

$$\frac{d^2\lambda}{dp^2} = -\frac{2D_L}{v^3}\left(1+\frac{4D_L}{v^2}G(p)\right)^{-3/2}\left(\frac{dG}{dp}\right)^2 \qquad \text{(A-51)}$$

$$\frac{d^2G}{dp^2} = -\frac{6(1-\theta_b)}{\theta_b}\frac{Bi^2}{Rp^2/Dp}\frac{1}{(A(p)+Bi)^3}\left(\frac{dA_o(p)}{dp}\right)^2$$

$$+\frac{3(1-\theta_b)}{\theta_b}\frac{Bi^2}{Rp^2/Dp}\frac{1}{(A(p)+Bi)^2}\frac{d^2A_o(p)}{dp^2} \qquad \text{(A-52)}$$

$$\frac{d^2A_o(p)}{dp^2} = \left(\frac{R^2}{2}\frac{\theta_p(1+K_a)^2}{D_p}\right)\frac{-\phi\sinh\phi+2\phi^2\cosh\phi-\sinh^2\phi\cosh\phi}{\phi^3\sinh^3\phi} \qquad \text{(A-53)}$$

After manipulating the equations by limiting the value of p to zero in the above equation, the following expression could be obtained :

$$\lim_{p\to 0}\frac{d^2A_o(p)}{dp^2} = -\frac{8}{45}\left(\frac{R^2}{2}\frac{\theta_p(1+K_a)}{D_p}\right)^2 \qquad \text{(A-54)}$$

Substituting this result backwards,

$$\lim_{p\to 0}\frac{d^2G}{dp^2} = -\left(\frac{2}{3}\frac{R_p}{k_f}+\frac{2}{15}\frac{R_p^2}{D_p}\right)\frac{1-\theta_b}{\theta_b}\left[\theta_p(1+K_a)\right]^2 \qquad \text{(A-55)}$$

$$\lim_{p\to 0} \frac{d^2\lambda}{dp^2} = -2 \frac{D_L}{v^3} \left[1 + \frac{1-\theta_b}{\theta_b} \theta_p (1+K_a) \right]^2$$

$$- \frac{1}{v} \left(\frac{2}{3} \frac{R_p}{k_f} + \frac{2}{15} \frac{R_p^2}{D_p}\right) \frac{1-\theta_b}{\theta_b} \left[\theta_p(1+K_a)\right]^2 \qquad \text{(A-56)}$$

$$M_2 = C_o \left[\frac{\tau^3}{3} + L\tau^2 \frac{1}{v} \left(1+\frac{1-\theta_b}{\theta_b}\theta_p(1+K_a)\right) + L\tau^2 \frac{1}{v^2} \left(1+\frac{1-\theta_b}{\theta_b}\theta_p(1+K_a)\right)^2 \right.$$

$$+ L\tau \frac{2D_L}{v^3} \left(1+\frac{1-\theta_b}{\theta_b}\theta_p(1+K_a)\right)^2 + L\tau \frac{1}{v} \left(\frac{2}{3} \frac{R_p}{k_f} + \frac{2}{15} \frac{R_p^2}{D_p}\right)$$

$$\left. \frac{1-\theta_b}{\theta_b} \left(\theta_p(1+K_a)\right)^2 \right] \qquad \text{(A-57)}$$

Substituting this and equation (A-43) into equation (A-44),

$$\mu_2' = \frac{\tau^2}{12} + \frac{2LD_L}{v^3} \left[1 + \frac{1-\theta_b}{\theta_b} \theta_p (1+K_a)\right]^2 + \frac{2}{3} \frac{L}{v} \frac{R_p}{k_f} \frac{1-\theta_b}{\theta_b} \theta_p^2 (1+K_a)^2$$

$$+ \frac{2}{15} \frac{L}{v} \frac{R_p^2}{D_p} \frac{1-\theta_b}{\theta_b} \theta_p^2 (1+K_a)^2 \qquad \text{(A-58)}$$

Appendix 3. Derivation for the Chromatographic Response of a Non-Porous Soil Matrix Column

The main purpose of developing equations here is to obtain the chromatographic response of a column packed with non-porous soil matrices like sand.

From the mass balance for the cross-section of non-porous soil bed,

$$A\Delta z\theta_b \frac{\partial C}{\partial t} = A\theta_b N_z\big|_z - A\theta_b N_z\big|_{z+\Delta z} + A\theta_b vC\big|_z - A\theta_b vC\big|_{z+\Delta z}$$

$$+ A\Delta z(1-\theta_b) \frac{4\pi R_p^2}{\frac{4}{3}\pi R_p^3} N_{Rp} \qquad \text{(B-1)}$$

$$\text{where} \quad N_{Rp} = k_f \left(\frac{C_a}{K_b} - C \right) = - \frac{\partial C_a}{\partial t} \qquad \text{(B-2)}$$

$$N_z = - D_z \frac{\partial C}{\partial z} \qquad \text{(B-3)}$$

K_b = equilibrium constant, defined by

$$C_a = K_b C'$$

Manipulating this equation and rearranging it,

$$\frac{\partial C}{\partial t} = D_L \frac{\partial^2 C}{\partial z^2} - v \frac{\partial C}{\partial z} + \frac{1-\theta_b}{\theta_b} \frac{3}{R} N_{Rp} \qquad \text{(B-4)}$$

with boundary and initial conditions :

$$C\ (0,\ 0 \le t \le \tau) = C_o \qquad (= 0,\ \text{otherwise})$$

$$C\ (\infty,\ t) = 0$$

$$C\ (z,\ 0) = 0$$

Taking Laplace transform in equations (B-4), (B-2) and boundary conditions with respect to time,

$$p\,\bar{C} = D_L \frac{\partial^2 C}{\partial z^2} - v \frac{\partial \bar{C}}{\partial z} + \frac{1-\theta_b}{\theta_b} \frac{3}{R_p} \overline{N_{Rp}} \qquad \text{(B-5)}$$

$$\overline{N_{Rp}} = k_f \left[\frac{\overline{C_a}}{K_b} - \bar{C} \right] = - p\,\overline{C_a} \qquad \text{(B-6)}$$

$$\bar{C}\ (\infty) = 0 \qquad \text{(B-7)}$$

$$\bar{C}\ (0) = \frac{C_o}{p} \left(1 - e^{-p\tau} \right) \qquad \text{(B-8)}$$

Manipulating equations (B-5) and (B-6),

$$\frac{D_L}{v} \frac{\partial^2 \bar{C}}{\partial z^2} - \frac{\partial \bar{C}}{\partial z} - G(p)\,\bar{C} = 0 \qquad \text{(B-9)}$$

$$\text{where} \quad G(p) = \frac{p}{v} + \frac{1-\theta_b}{\theta_b} \frac{3}{vR_p} \frac{p\ k_f}{p + k_f/K_b} \qquad \text{(B-10)}$$

Solving this equation and substituting boundary conditions,

$$\bar{C} = \frac{C_o}{p} \left(1 - e^{-p\tau} \right) \exp(-\lambda z) \qquad \text{(B-11)}$$

$$\text{where} \quad \lambda = \frac{v}{2D_L} \left(\sqrt{1 + \frac{4D_L G}{v}} - 1 \right) \tag{B-12}$$

At the end of the packed column, z = L and

$$\overline{C_L} = \frac{C_o}{p} \left(1 - e^{-p\tau} \right) \exp(-\lambda L) \tag{B-13}$$

Applying van der Laan's theorem,

$$\mu_1 = \frac{M_1}{M_0} \tag{B-14}$$

$$M_0 = \lim_{p \to 0} \overline{C_L} = C_o \tau \tag{B-15}$$

$$M_1 = (-1) \lim_{p \to 0} \frac{d\overline{C_L}}{dp}$$

$$= C_o \left(\frac{\tau^2}{2} + L\tau \lim_{p \to 0} \frac{d\lambda}{dp} \right) \tag{B-16}$$

From equation (B-12),

$$\lim_{p \to 0} \frac{d\lambda}{dp} = \lim_{p \to 0} \frac{dG}{dp} \tag{B-17}$$

From equation (B-10),

$$\lim_{p \to 0} \frac{dG}{dp} = \frac{1}{v} \left(1 + \frac{1 - \theta_b}{\theta_b} \frac{3}{R_p} K_b \right) \tag{B-18}$$

Substituting these equations backwards to obtain an expression for M_1,

$$M_1 = C_o \left[\frac{\tau^2}{2} + L\tau \left(\frac{1}{v} + \frac{1-\theta_b}{\theta_b} \frac{3\ K_b}{vR} \right) \right] \tag{B-19}$$

Hence,

$$\mu_1 = \frac{\tau}{2} + \frac{L}{v} \left(1 + \frac{1-\theta_b}{\theta_b} \frac{3}{R_p} K_b \right) \tag{B-20}$$

The second central moment can be obtained in the similar way,

$$M_2 = (-1)^2 \lim_{p \to 0} \frac{d^2 \overline{C_L}}{dp^2} \tag{B-21}$$

$$= \lim_{p \to 0} C_o e^{-\lambda L} \left[\frac{2(1-e^{-p\tau}) - 2\tau p e^{-p\tau} - \tau^2 p^2 e^{-p\tau}}{p^3} + 2L \frac{1-e^{-p\tau} - \tau p e^{-p\tau}}{p^2} \frac{d\lambda}{dp} \right.$$

$$\left. - L^2 \frac{1-e^{-p\tau}}{p} \left(\frac{d\lambda}{dp} \right)^2 - L \frac{1-e^{-p\tau}}{p} \frac{d^2\lambda}{dp^2} \right] \tag{B-22}$$

Here,

$$\lim_{p \to 0} \frac{2(1-e^{-p\tau}) - 2\tau p e^{-p\tau} - \tau^2 p^2 e^{-p\tau}}{p^3} = \frac{\tau^3}{3} \tag{B-23}$$

$$\lim_{p \to 0} \frac{1 - e^{-p\tau} - \tau p e^{-p\tau}}{p^2} = \frac{\tau^2}{2} \tag{B-24}$$

$$\lim_{p \to 0} \frac{1 - e^{-p\tau}}{p} = \tau \tag{B-25}$$

Substituting these equations and limiting values of λ into equation (B-22),

$$M_2 = C_o \left[\frac{\tau^3}{3} + L\tau^2 \lim_{p\to 0} \frac{d\lambda}{dp} + L^2\tau \lim_{p\to 0} \left(\frac{d\lambda}{dp}\right)^2 - L\tau \lim_{p\to 0} \frac{d^2\lambda}{dp^2} \right] \quad \text{(B-26)}$$

From the expression for λ,

$$\lim_{p\to 0} \frac{d\lambda}{dp} = \frac{1}{v} \left(1 + \frac{1-\theta_b}{\theta_b} \frac{3}{R_p} K_b \right) \quad \text{(B-27)}$$

$$\lim_{p\to 0} \frac{d^2\lambda}{dp^2} = - \frac{2D_L}{v} \lim_{p\to 0} \left(\frac{dG}{dp}\right)^2 + \lim_{p\to 0} \frac{d^2G}{dp^2} \quad \text{(B-28)}$$

From the expression for G,

$$\lim_{p\to 0} \left(\frac{dG}{dp}\right)^2 = \frac{1}{v^2} \left[1 + \frac{1-\theta_b}{\theta_b} \frac{3}{R_p} K_b \right]^2 \quad \text{(B-29)}$$

$$\lim_{p\to 0} \frac{d^2G}{dp^2} = - \frac{1}{v} \frac{1-\theta_b}{\theta_b} \frac{6}{R_p} \frac{K_b^2}{k_f} \quad \text{(B-30)}$$

Substituting these equations backwards,

$$M_2 = C_o \left[\frac{\tau^3}{3} + L\tau^2 \frac{1}{v} \left(1 + \frac{1-\theta_b}{\theta_b} \frac{3}{R_p} K_b \right) + L^2\tau \frac{1}{v^2} \left(1 + \frac{1-\theta_b}{\theta_b} \frac{3}{R_p} K_b \right)^2 \right.$$

$$\left. + L\tau \left[\frac{2D_L}{v^3} \left(1+\frac{1-\theta_b}{\theta_b} \frac{3}{R_p} K_b\right)^2 + \frac{1}{v} \frac{1-\theta_b}{\theta_b} \frac{6}{R_p} \frac{K_b^2}{k_f} \right) \right] \quad \text{(B-31)}$$

Hence,

$$\mu_2' = \frac{M_2}{M_0} - \mu_1^2$$

$$= \frac{\tau^2}{12} + \frac{2LD_L}{v^3}\left(1 + \frac{1-\theta_b}{\theta_b}\frac{3}{R_p}K_b\right)^2 + \frac{L}{v}\frac{1-\theta_b}{\theta_b}\frac{6}{R_p}\frac{K_b}{k_f} \qquad \text{(B-32)}$$

Appendix 4. Program List for the Integration of Analytical Solution

```
C     This program has been written for achieving effluent concentration  C
C     profile of adsoption process in a soil matrix column using          C
C     analytical solutions combined with a numerical integration method   C
C     which is avalilable in IMSL package installed in NJIT VAX system.   C
C                                                                         C
C     Input data set necessary to run this program is                     C
C                                                                         C
C         Dp = intraparticle diffusion coefficient in cm2/sec             C
C         ep = particle porosity                                          C
C         xb = particle radius in cm                                      C
C         xe = column porosity                                            C
C         dl = axial dispersion coefficient in cm2/sec                    C
C        xkf = mass transfer film coefficient in cm/sec                   C
C        xka = equilibrium constant                                       C
C         xv = linear gas velocity in cm/sec                              C
C          z = column length in cm                                        C
C       temp = operation temperature in C                                 C
C                                                                         C
C     Output is given as concentration change as a function of time (sec) C
C                                                                         C


      dimension uval(1000)

      common  t, yka, xv, z, xdp, ep, xb, xe, dl, xkf

      integer interv, nout, mm, nn
      real  bound, errabs, errest, errrel, f, result,
     &      uval, temp

      external f, qdagi, umach

      open (6,file='fint.out',status='new')

      call umach(2,nout)

      data  dp, ep, xb, xe, dl, xkf/
     &      2.93E-05, 0.13, 2.30E-02, 0.536,
     &      1.079, 6.374/

      data  xka, xv, z, temp, tlag/
     &      72.23, 3.423, 29.0, 160., 0./

      yka = xka * ep
      xdp = dp / ep
      nn  = 36
      bound  = 0.0
      interv = 1
      errabs = 0.0001
      errrel = 0.001

      do 100 i = 1, nn

         tintvl = 10.0
         t = tintvl * float(i) - tlag

       if(i.gt.12) then
         tintvl = 40.0
         t = 120. + tintvl * float(i-12) - tlag
       else
       end if
```

```
        if(i.gt.24) then
          tintvl = 80.0
          t = 600. + tintvl * float(i-24) - tlag
        else
        end if

        if(t.le.0.) then
          result = 0.
          go to 50
        else
        end if

       call qdagi (f,bound,interv,errabs,errrel,result,errest)

       result = .5 + 2./3.14159 * result

50     uval(i)=result

100    continue

       write (6,205) temp, xv, xka, dp
       write (6,200)

       mm = nn/3

       do 110 i = 1, mm

          if(i.le.4) then
            write (6,210) ( ( 10.0*(float(i-1)*3.+float(j)),
     &                    uval(3*(i-1)+j) ), j = 1, 3 )
            go to 110
          end if

          if(i.gt.8) then
            go to 120
          end if

            write (6,210) ( ( (120.+40.*(float(i-5)*3.+float(j))),
     &                    uval(3*(i-1)+j) ), j = 1, 3 )
            go to 110

120         write (6,210) ( ( (600.+80.*(float(i-9)*3.+float(j))),
     &                    uval(3*(i-1)+j) ), j = 1, 3 )

110    continue

200    format(1x,'time(s)  u value   time(s)  u value',
     &        '   time(s)  u value ')

205    format(1H1,//'  [ Concentration Profile Calculation ]',
     &       ///'                Chemical =  Toluene',
     &         /'             Temperature =  ', f4.0,' deg. C',
     &         /'       Linear Velocity = ', f5.2,' cm/sec',
     &         /'                    Ka = ', f6.2,
     &         /'                    Dp = ', E9.2,' cm2/sec'////)

210    format( 3 (f7.1, 3x, f7.5, 2x) )

       end
c
c
c
       real function f (x)

       common t, xka, xv, z, dp, ep, xb, xe, dl, xkf
```

```
      double precision x, hd1, hd2, h1, h2, z2x, z2y, pex, psin

      xm   = xe / (1.-xe)
      xk   = xka + ep
      r1   = xk / xm
      xgama=3. * dp * ep / xb**2
      rf   = xb / (3.*xkf)
      xnu = xgama * rf

      delcof = xgama / ( xm * xv )
      peccof = xv / dl
      ycof   = 2. * dp * ep / ( xk * xb**2 )

      del = delcof * z
      pe  = peccof * z

      if(x.le.50.) then

         vsin = sin(2.*x) / cosh(2.*x)
         vcos = cos(2.*x) / cosh(2.*x)

      else

         vsin=0.
         vcos=0.

      end if

      hd1 = x * ( tanh(2.*x) + vsin ) / ( 1. - vcos ) - 1.
      hd2 = x * ( tanh(2.*x) - vsin ) / ( 1. - vcos )

      h1  = ( hd1 + xnu * (hd1**2+hd2**2) )/
     &        ( (1.+xnu*hd1)**2 + (xnu*hd2)**2 )
      h2  = hd2 / ( (1.+xnu*hd1)**2 + (xnu*hd2)**2 )

      z2x = pe * ( .25 * pe + del * h1 )
      z2y = del * pe * ( 2. * x**2 / ( 3. * r1 ) + h2 )

      y   = ycof * t
      pex = pe / 2. - sqrt ( ( sqrt(z2x**2 + z2y**2)
     &                + z2x ) / 2. )
      psin= y * x**2 - sqrt ( (sqrt(z2x**2 + z2y**2)
     &                - z2x ) / 2. )

      if (x.gt.0.0) then

          f = exp(pex) * sin(psin) / x

      else

          f = 0.0

      end if

      return
      end
```

Appendix 5. Derivation of a Numerical Solution for Contamination/ Desorption of Organics in a Soil Matrix Column

The main purpose of this numerical solution is to predict the behavior of organics in a soil matrix column and the procedure followed mainly the method of Finlayson et al. (89,90,94).

From the mass balance equation for a contaminant in the external fluid of a soil matrix column,

$$\frac{\partial c}{\partial t} = D_L \frac{\partial^2 c}{\partial z^2} - v\frac{\partial c}{\partial z} - \frac{1-\theta_b}{\theta_b}\frac{3k_f}{R_p}\left(c - c_i|_{r=R_p}\right) \qquad \text{(C-1)}$$

with boundary and initial conditions,

$$D_L \frac{\partial c}{\partial z}\Big|_{z=0} = - v \left(c|_{z=0} - c|_{z=0+} \right) \qquad \text{(C-2)}$$

$$\frac{\partial c}{\partial z}\Big|_{z=L} = 0 \qquad \text{(C-3)}$$

$$c\ (z,0) = c_o \qquad \text{(C-4)}$$

From mass balance equations for the contaminants inside the particles :

$$\theta_p \frac{\partial c_i}{\partial t} + (1-\theta_p)\frac{\partial c_p}{\partial t} = D_p\left(\frac{\partial^2 c_i}{\partial r^2} + \frac{2}{r}\frac{\partial c_i}{\partial r} \right) \qquad \text{(C-5)}$$

with boundary and initial conditions,

$$\left.\frac{\partial c_i}{\partial r}\right|_{r=0} = 0 \qquad \text{(C-6)}$$

$$D_p \left.\frac{\partial c_i}{\partial r}\right|_{r=Rp} = k_f \left(c - c_i|_{r=Rp} \right) \qquad \text{(C-7)}$$

$$c_i\,(r,0) = c_o \qquad \text{(C-8)}$$

Above equations can be reduced in dimensionless form as following :

The dimensionless parameters are defined by

$$C = \frac{c}{q_o} \qquad Pe = \frac{vL}{D_L}$$

$$Q = \frac{c_i}{q_o} \qquad \phi = \frac{vR_p^2}{LD_p}$$

$$\tau = \frac{tD_p}{R_p^2} \qquad \eta = K\,\frac{1-\theta_b}{\theta_b}$$

$$x = \frac{z}{L} \qquad \xi = \frac{Lk_f}{vRK_a}$$

$$y = \frac{r}{R_p} \qquad \gamma = \frac{\theta_p}{\theta_p\,(1+K_a)}$$

where q_o = concentration equivalent to the initial concentration of a column bed or input depending on the phase of adsorption or desorption

Equations (C-1) - (C-8) can be expressed as follows :

$$\frac{\partial^2 C}{\partial \tau} = \frac{1}{Pe}\,\phi\,\frac{\partial^2 C}{\partial x^2} - \phi\,\frac{\partial C}{\partial x} - 3\,(\eta\phi\xi)\,(C - Q|_{y=1}) \qquad \text{(C-9)}$$

$$\left.\frac{\partial C}{\partial x}\right|_{x=0} = -\,Pe\,(C|_{x=0-} - C|_{x=0+}) \qquad \text{(C-10)}$$

$$\left.\frac{\partial C}{\partial x}\right|_{x=1} = 0 \qquad \text{(C-11)}$$

$$C|_{\tau=0} = C_o/q_o \qquad \text{(C-12)}$$

$$\frac{\partial Q}{\partial \tau} = \gamma\,\nabla^2 Q \qquad \text{(C-13)}$$

$$\left.\frac{\partial Q}{\partial y}\right|_{y=0} = 0 \qquad \text{(C-14)}$$

$$\left.\frac{\partial Q}{\partial y}\right|_{y=1} = K\phi\xi\,(C - Q|_{y=1}) \qquad \text{(C-15)}$$

$$Q|_{\tau=0} = c_o/q_o \qquad \text{(C-16)}$$

Above partial differential equations can be reduced to a series of ordinary differential equations by orthogonal collocation method. The concentration profile inside particles is symmetrical with respect to the distance from the center, hence, it can be estimated by the following trial function when boundary conditions are considered.

$$Q(\eta,\tau) = Q(1,\tau) + (1-\eta^2)\sum_{i=1}^{N} a_i(\tau)\,P_{i-1}(\eta^2) \qquad \text{(C-17)}$$

where $P_i(\eta^2)$ are orthogonal polynomials defined by

$$\int_0^\infty w(\eta^2)\, P_j(\eta^2)\, P_i(\eta^2)\, \eta^{a-1}\, d\eta = C_i\, \delta_{ij} \qquad \text{(C-18)}$$

where $w(\eta^2)$ = weighting function ($= 1-\eta^2$)

a = 1,2,3 for planar, cylindrical or spherical coordinates each other

$$C_i = \frac{[\Gamma(\frac{a}{2})]^2\ \Gamma(i+1)\ \Gamma(i+2)}{(4i+a+2)\,\Gamma(i+\frac{a}{2})\,\Gamma(i+\frac{a}{2}+1)} \quad \text{as defined by ref.89}$$

$\delta_{ij} = 1$ if $i = j$

$= 0$ if $i \neq j$

$j = 1,2,\ldots\ldots,i-1$

Following the expressions by Finlayson, equations (C-13) to (C-15) may be written as follows :

$$\frac{dQ_k}{d\tau} = \gamma \sum_{i=1}^{N+1} B_{k,i}\, Q_i \qquad k = 1,2,\ldots N \qquad \text{(C-19)}$$

$$\sum_{i=1}^{N+1} A_{1,i}\, Q_i(j) = 0 \qquad \text{(C-20)}$$

$$\sum_{i=1}^{N+1} A_{N+1,i}\, Q_i(j) = K\phi\xi\ (\ C(j) - Q_{N+1}(j)\ ) \qquad \text{(C-21)}$$

where j denotes the collocation points of longitudinal coordinate.

Q_{N+1} in equation (C-21) can be substituted into equation (C-19) to reduce the degree of polynomials. From equation (C-21),

$$Q_{N+1}(j) = \frac{K\phi\xi}{K\phi\xi + A_{N+1,N+1}} C(j) - \sum_{i=1}^{N} \frac{A_{N+1,N+1}}{K\phi\xi + A_{N+1,N+1}} Q(j) \qquad \text{(C-22)}$$

Substituting this equation into equation (C-19), and rearranging it,

$$\frac{dQ_k^{(j)}}{d\tau} = \gamma \sum_{i=1}^{N} [\, B_{k,i} - \psi\, B_{k,N+1} A_{N+1,i}] \, Q_i(j) + Po\, B_{k,N+1} C(j) \qquad \text{(C-23)}$$

$$j = 2,3,.....,M+1$$

$$k = 1,2,.....,N$$

where M = the number of collocation points in the longitudinal direction

N = the number of collocation points in the radial direction inside particles

$\psi = 1 / (K\phi\xi + A_{N+1,N+1})$

$Po = \gamma K \psi \phi \xi$

The concentration profile along the longitudinal direction is nonsymmetrical and it can be expressed as the following trial function:

$$C(x,\tau) = x\ C(1,\tau) + (1-x)\ C(0,\tau) + x(1-x) \sum_{i=1}^{M} a_i(\tau)\ P_{i-1}(x) \qquad \text{(C-24)}$$

where $P_i(x)$ are orthogonal polynomials defined by

$$\int_0^\infty w(x)\ P_j(x)\ P_i(x)\ dx = 0 \qquad \text{(C-25)}$$

with $w(x) = 1$

$j = 1,2,\ldots\ldots,i-1$

Similarly to the above case, equations (C-9) to (C-11) can be expressed as following :

$$\frac{dC(j)}{d\tau} = \frac{1}{Pe}\,\phi \sum_{i=1}^{M+2} B'_{j,i}\ C(i) - \phi \sum_{i=1}^{M+2} A'_{j,i}\ C(i) - 3\ (\eta\phi\xi)\ (\ C(j) - Q_{N+1}(j)\ ) \qquad \text{(C-26)}$$

$j = 2,3,\ldots\ldots,M+1$

$$\sum_{i=1}^{M+2} A'_{1,i} C(i) = -Pe\ (C|_{x=0-} - C(1)) \qquad \text{(C-27)}$$

$$\sum_{i=1}^{M+2} A'_{M+2,i} C(i) = 0 \qquad \text{(C-28)}$$

C(1) and C(M+2) can be calculated from equation (C-27) and (C-28) :

$$C(1) = \frac{1}{\alpha}\ [\ -Pe\ A'_{M+2,M+2}\ C|_{x=-0} - A'_{M+2,M+2} \sum_{i=2}^{M+1} A'_{1,i}\ C(i)$$

$$+ A'_{1,M+2} \sum_{i=2}^{M+1} A'_{M+2,i}\, C(i) \,] \qquad \text{(C-29)}$$

$$C(M+2) = \frac{Pe}{\alpha} A'_{M+2,1}\, C|_{x=-0} + \frac{1}{\alpha} A'_{M+2,1} \sum_{i=2}^{M+1} A'_{1,i}\, C(i)$$

$$- \frac{(A'_{1,1} - Pe)}{\alpha} \sum_{i=2}^{M+1} A'_{M+1,i}\, C(i) \qquad \text{(C-30)}$$

$$\text{where} \quad \alpha = A'_{M+2,M+2} (A'_{1,1} - Pe) - A'_{1,M+2}\, A'_{M+2,i} \qquad \text{(C-31)}$$

Substituting equations (C-22), (C-29) and (C-30) into equation (C-26) and rearranging it,

$$\frac{dC(j)}{d\tau} = \sum_{i=2}^{M+1} \phi \, [\, (\frac{1}{Pe} B'_{j,i} - A'_{j,i}) + (\frac{1}{Pe} B'_{j,1} - A'_{j,1})$$

$$x \, (\frac{A'_{1,M+2}}{\alpha} A'_{M+2,i} - \frac{A'_{M+2,M+2}}{\alpha} A'_{1,i}) + (\frac{B'_{j,M+2}}{Pe} - A'_{j,M+2})$$

$$x \, (\frac{A'_{M+2,1}}{\alpha} A'_{1,i} - \frac{A'_{1,1} - Pe}{\alpha} A'_{M+2,i}) \,] \; C(i)$$

$$- Pe\, C|_{x=0-} \, \phi \, [\, \frac{A'_{M+2,M+2}}{\alpha} (\frac{1}{Pe} B'_{j,1} - A'_{j,1})$$

$$- \frac{A'_{M+2,1}}{\alpha} (\frac{1}{Pe} B'_{j,M+2} - A'_{j,M+2}) \,]$$

$$- \frac{3(\eta\phi\xi) \sum_{i=1}^{N} A_{N+1,i} Q_i(j)}{K\phi\xi + A_{N+1,N+1}} - 3(\eta\phi\xi) \frac{A_{N+1,N+1}}{K\phi\xi + A_{N+1,N+1}} C(J)$$

$$j = 2,..M+1 \qquad \text{(C-32)}$$

This equation can be expressed more simply with defined parameters,

$$\frac{dC(j)}{d\tau} = \sum_{i=2}^{M+1} \phi \left[\left(\frac{1}{Pe}B'_{j,i} - A'_{j,i}\right) + \left(\frac{1}{Pe}B'_{j,1} - A'_{j,1}\right)\left(P_1 A'_{M+2,i} - P_2 A'_{1,i}\right) \right.$$

$$\left. + \left(\frac{1}{Pe}B'_{j,M+2} - A'_{j,M+2}\right)\left(P_3 A'_{1,i} - P_4 A'_{M+2,i}\right) \right] C(i)$$

$$- Pe\, C|_{x=0-} \phi \left[P_2\left(\frac{1}{Pe}B'_{j,1} - A'_{j,1}\right) - P_3\left(\frac{1}{Pe}B'_{j,M+2} - A'_{j,M+2}\right) \right]$$

$$- P_5 \sum_{i=1}^{N} A_{N+1,i}\, Q_i(j) - P_6\, C(j) \qquad \text{(C-33)}$$

$$j = 2,3,.....,M+1$$

with parameters defined by

$$P_1 = \frac{A'_{1,M+2}}{\alpha} \qquad P_2 = \frac{A'_{M+2,M+2}}{\alpha}$$

$$P_3 = \frac{A'_{M+2,1}}{\alpha} \qquad P_4 = \frac{A'_{1,1} - Pe}{\alpha}$$

$$P_5 = \frac{3(\eta\phi\xi)}{K\phi\xi + A_{N+1,N+1}} \qquad P_6 = A_{N+1,N+1}\, P_5$$

Equations (C-23) and (C-33) can be expressed in a more simplified and combined form as follows:

$$\frac{dQ_1^{(J)}}{d\tau} = a_{11}^{(J)} Q_1^{(J)} + \ldots\ldots + a_{1N}^{(J)} Q_N^{(J)} + b_1^{(J)} C(J)$$

$$\vdots \qquad\qquad\qquad\qquad \vdots$$

$$\frac{dQ_N^{(J)}}{d\tau} = a_{N1}^{(J)} Q_1^{(J)} + \ldots\ldots + a_{NN}^{(J)} Q_N^{(J)} + b_N^{(J)} C(J)$$

$$\frac{dC(J)}{d\tau} = g_2^{(J)} C(2) + g_3^{(J)} C(3) + \ldots + g_{M+1}^{(J)} C(M+1)$$

$$+ h^{(J)} \sum_{i=1}^{N} A_{N+1,i} Q_i(J) + m^{(J)} C(J) \qquad \text{(C-34)}$$

where $J = 2,3,\ldots\ldots M+1$

Hence, (N+1)xM ordinary differential equations should be solved simultaneously to obtain the solution.

Appendix 6. Matrix Development Program for Orthogonal Collocation Method

```
C                                                                       C
C     This program has been written to develop matrices which are to    C
C     to be utilized to run mass transfer simulation program using      C
C     orthogonal collocation method.                                    C
C                                                                       C
C     This part is for matrices in the radial direction.                C
C                                                                       C
C     Input data are a set of values of collocation points.             C
C                                                                       C

      DIMENSION AA(30,30), BB(30,30), CC(30,30), DD(30,30),
     &          Q(30,30), QINV(30,30), XX(30)

      REAL AA, BB, CC, DD, Q, QINV, XX, DUM, DUMMY

      INTRINSIC FLOAT

      OPEN(6,FILE='MTRX.OUT',STATUS='NEW')

C
C     READING INPUT DATA AND GENERATING INPUT MATRIX
C

      N=7

      DATA XX(1),XX(2),XX(3),XX(4),XX(5),XX(6),XX(7)
     &    /0.2153539554, 0.4206380547, 0.6062532055,
     &     0.7635196900, 0.8850820442, 0.9652459265, 1.0/

      DO 110 J=1,N
         DO 120 I=1,N
            Q(J,I)=XX(J)**(2*I-2)
120   CONTINUE
110   CONTINUE

      DO 130 J=1,N
         DO 140 I=1,N
            IF(I.EQ.J) THEN
              Q(J,I+N)=1.0
            ELSE
              Q(J,I+N)=0.0
            END IF
140   CONTINUE
130   CONTINUE

      DO 150 J=1,N
         DO 160 I=1,2*N
            QINV(J,I)=Q(J,I)
160   CONTINUE
150   CONTINUE

      DO 170 J=1,N
           DUM=QINV(J,J)
         DO 180 I=1,2*N
           QINV(J,I)=QINV(J,I)/DUM
180   CONTINUE

      DO 190 K=1,N
         IF(K.EQ.J) THEN
           GO TO 190
```

```
         ELSE
         END IF
           DUMMY=QINV(K,J)
       DO 200 I=1,2*N
           QINV(K,I)=QINV(K,I)-QINV(J,I)*DUMMY
200    CONTINUE
190    CONTINUE

170    CONTINUE

       DO 210 J=1,N
          DO 220 I=1,N
            QINV(J,I)=QINV(J,I+N)
220    CONTINUE
210    CONTINUE

C
C      GENERATION OF Cji AND Dji MATRICES
C

       DO 230 J=1,N

          DO 240 I=1,N
              KC=2*I-3
              KD=2*I-4

            IF(I.EQ.1) THEN
              CC(J,I)=0.0
            ELSE
              CC(J,I)=(FLOAT(2*I-2))*XX(J)**KC
            END IF

            IF(I.EQ.1) THEN
              DD(J,I)=0.0
            ELSE
              DD(J,I)=(FLOAT((2*I-2)*(2*I-1)))*XX(J)**KD
            END IF
240    CONTINUE

230    CONTINUE

C
C      GENERATION OF Aji AND Bji MATRICES
C

       DO 250 J=1,N

          DO 260 I=1,N
             AA(J,I)=0.0
             BB(J,I)=0.0

          DO 270 K=1,N
             AA(J,I)=AA(J,I)+CC(J,K)*QINV(K,I)
             BB(J,I)=BB(J,I)+DD(J,K)*QINV(K,I)

270    CONTINUE
260    CONTINUE
250    CONTINUE

C
C
       WRITE(6,710) N-1,(XX(I),I=1,N)
       WRITE(6,720)

       DO 310 J=1,N
          WRITE(6,730)  (Q(J,I),I=1,N)
```

```
310   CONTINUE

      WRITE(6,740)

      DO 320 J=1,N
         WRITE(6,730)  (QINV(J,I),I=1,N)
320   CONTINUE

      WRITE(6,750)

      DO 330 J=1,N
         WRITE(6,999)  (AA(J,I),I=1,N)
330   CONTINUE

      WRITE(6,760)

      DO 340 J=1,N
         WRITE(6,999)  (BB(J,I),I=1,N)
340   CONTINUE

710   FORMAT(///
     &'  CALCULATION RESULTS OF MATRICES GENERATED FOR'/
     &'  ORTHOGONAL COLLOCATION SIMULATION'/
     &' _____'///
     &'  NUMBER OF COLLOCATION POINTS = ',I3//
     &'  ROOTS OF POLYNOMIALS',//(2X,F13.10))
720   FORMAT(//2X,'Qji'/)
730   FORMAT(6F10.4)
740   FORMAT(//2X,'QINVji'/)
750   FORMAT(//2X,'Aji'/)
760   FORMAT(//2X,'Bji'/)
999   FORMAT(6F10.4)

      STOP
      END
```

```
C                                                                       C
C     This part is for the matrices in the axial direction.             C
C                                                                       C


      DIMENSION AA(30,30),BB(30,30),CC(30,30),DD(30,30),
     &Q(30,30),QINV(30,30),XX(30)

      REAL AA,BB,CC,DD,Q,QINV,XX,DUM,DUMMY

      OPEN(6,FILE='MTRXL.OUT',STATUS='NEW')

C
C     READING INPUT DATA AND GENERATING INPUT MATRIX
C

      N=8

      DATA XX(1),XX(2),XX(3),XX(4),XX(5),XX(6),XX(7),XX(8)
     &    /0., 0.0337652429, 0.1693953068, 0.3806904070,
     &         0.6193095931, 0.8306046933, 0.9662347571, 1.0/
```

```
      DO 110 J=1,N
         Q(J,1)=1.
110   CONTINUE

      DO 112 I=2,N
         Q(1,I)=0.
112   CONTINUE

      DO 114 J=2,N
         DO 120 I=2,N
            Q(J,I)=XX(J)**(I-1)
120      CONTINUE
114   CONTINUE

      DO 130 J=1,N

         DO 140 I=1,N
            IF(I.EQ.J) THEN
              Q(J,I+N)=1.
         ELSE
            Q(J,I+N)=0.
         END IF
140      CONTINUE

130   CONTINUE

      DO 150 J=1,N
         DO 160 I=1,2*N
            QINV(J,I)=Q(J,I)
160      CONTINUE
150   CONTINUE

      DO 170 J=1,N

         DUM=QINV(J,J)
         DO 180 I=1,2*N
            QINV(J,I)=QINV(J,I)/DUM
180      CONTINUE

      DO 190 K=1,N
         IF(K.EQ.J) THEN
            GO TO 190
         ELSE
         END IF

         DUMMY=QINV(K,J)

      DO 200 I=1,2*N
         QINV(K,I)=QINV(K,I)-QINV(J,I)*DUMMY
200   CONTINUE
190   CONTINUE

170   CONTINUE

      DO 210 J=1,N
         DO 220 I=1,N
            QINV(J,I)=QINV(J,I+N)
220      CONTINUE
210   CONTINUE

C
C     GENERATION OF Cji AND Dji MATRICES
C

      DO 230 J=1,N
```

```
         CC(J,1)=0.

         DO 235 I=1,2
            DD(J,I)=0.
235   CONTINUE

      DO 240 I=2,N
         KC=I-2
         KD=I-3

      IF(I.EQ.2) THEN
         CC(J,I)=FLOAT(I-1)
      ELSE
         CC(J,I)=(FLOAT(I-1))*XX(J)**KC
      END IF

      IF(I.EQ.2) THEN
        GO TO 240
      ELSE
      END IF

      IF(I.EQ.3) THEN
        DD(J,I)=FLOAT((I-1)*(I-2))
      ELSE
        DD(J,I)=(FLOAT((I-1)*(I-2)))*XX(J)**KD
      END IF
240   CONTINUE

230   CONTINUE

C
C     GENERATION OF Aji AND Bji MATRICES
C

      DO 250 J=1,N

         DO 260 I=1,N
            AA(J,I)=0.
            BB(J,I)=0.

         DO 270 K=1,N
            AA(J,I)=AA(J,I)+CC(J,K)*QINV(K,I)
            BB(J,I)=BB(J,I)+DD(J,K)*QINV(K,I)
270      CONTINUE
260      CONTINUE

250   CONTINUE


      WRITE(6,710) N-2,(XX(I),I=1,N)

      WRITE(6,720)

      DO 310 J=1,N
         WRITE(6,730) (Q(J,I),I=1,N)
310   CONTINUE

      WRITE(6,740)

      DO 320 J=1,N
         WRITE(6,730) (QINV(J,I),I=1,N)
320   CONTINUE

      WRITE(6,750)
```

```
      DO 330 J=1,N
         WRITE(6,999) (AA(J,I),I=1,N)
330   CONTINUE

      WRITE(6,760)

      DO 340 J=1,N
         WRITE(6,999) (BB(J,I),I=1,N)
340   CONTINUE

710   FORMAT(///
     &'  CALCULATION RESULTS OF MATRICES GENERATED FOR'/
     &'  ORTHOGONAL COLLOCATION SIMULATION'/
     &' ____________________________________________'///
     &'  NUMBER OF COLLOCATION POINTS = ',I3//
     &'  ROOTS OF POLYNOMIALS',//(2X,F13.10))
720   FORMAT(//2X,'Qji'/)
730   FORMAT(8F8.2)
740   FORMAT(//2X,'QINVji'/)
750   FORMAT(//2X,'Aji'/)
760   FORMAT(//2X,'Bji'/)
999   FORMAT(8F8.2)
      STOP
      END
```

Appendix 7. Program List of the Numerical Solution Using Orthogonal Collocation Method

```
C                                                                       C
C     This program has been written to estimate concentration distri-   C
C     bution profiles in the adsorption and desorption process in soil  C
C     columns.  Orthogonal collocation method was utilized to simulate  C
C     the mass transfer and IMSL package was used to solve simultaneous C
C     differential equations.                                           C
C                                                                       C
C     Basic input data are mass transfer parameter values and two       C
C     matrices in the radial direction of particles and axial direction C
C     of the column.                                                    C
C                                                                       C


      PARAMETER ( NEQ = 42, NPARAM=50)

      COMMON AA(30,30), BB(30,30), AAP(30,30), BBP(30,30),
     &       M, N, GAMA, PE, PSI, P0, P1, P2, P3, P4, P5, P6,
     &       P7, P8, PI

      EXTERNAL FCN, DIVPAG, SSET, UMACH

      INTEGER IDO,IEND,IMETH,INORM,NOUT,M,N

      DOUBLE PRECISION A(1,1), FCN, FCNJ, HINIT, PARAM(NPARAM), X,
     &     XEND, Y(NEQ), YPRIME(NEQ), MXSTEP, XV, XR, XL, DP, XK,
     &     XE, XKF, DL, EP, CO, P0, P1, P2, P3, P4, P5, P6, P7,
     &     P8, PI, ETA, XI, PE, GAMA, ALPA, PSI, AA, BB, AAP, BBP, TOL

C                              INITIALIZE

      DATA XV, XR, XL, DP, XK, XE, XKF, DL, EP, CO/
     &     2.626, .03, 29.0, 2.93D-05, 72.23,
     &     0.536, 6.374, 1.0788, 0.13, .0/

      INTRINSIC  DFLOAT

      OPEN (5,FILE='MTRX6_6.DAT',STATUS='OLD')
      OPEN (6,FILE='SENS1T7.OUT',STATUS='NEW')

      HINIT=1.0D-7
      MXSTEP=100000.

      INORM=2
      IMETH=1

      CALL SSET(NPARAM,0.0,PARAM,1)

      PARAM(1)=HINIT
      PARAM(4)=MXSTEP
      PARAM(10)=INORM
      PARAM(12)=IMETH

      N = 7
      M = 8

      DO 110 J = 1, M
         DO 110 I = 1, M
            READ(5,*) AAP(J,I)
110   CONTINUE

      DO 120 J=1, M
```

```
         DO 120 I=1, M
            READ(5,*) BBP(J,I)
120   CONTINUE

      DO 130 J=1, N
         DO 130 I=1, N
            READ(5,*) AA(J,I)
130   CONTINUE

      DO 140 J=1, N
         DO 140 I=1, N
            READ(5,*) BB(J,I)
140   CONTINUE

C                        PARAMETER CALCULATION

      PI   = XV * XR**2 /XL /DP
      ETA  = XK *(1.-XE) /XE
      XI   = XL * XKF / (XV*XR*XK)
      PE   = XV * XL / DL
      GAMA = 1. / (EP * (1.+XK))
      ALPA = AAP(M,M) * (AAP(1,1) - PE) - AAP(1,M) * AAP(M,1)
      PSI  = 1. / ( XK*PI*XI + AA(N,N) )
      P0   = GAMA * XK * PSI * PI * XI
      P1   = AAP(1,M) / ALPA
      P2   = AAP(M,M) / ALPA
      P3   = AAP(M,1) / ALPA
      P4   = (AAP(1,1)-PE) / ALPA
      P5   = AAP(M,M) / ALPA
      P6   = 3. *ETA *PI *XI / ( XK*PI*XI + AA(N,N) )
      P7   = AA(N,N) * P6
      P8   = PE * CO * PI

      IDO=1
      X=0.0D00
      TOL=1.0D-3

      IF( CO .EQ. 0.0D00 ) THEN

       DO 205 J=1,M-2
         DO 210 K=1,N-1
           Y((J-1)*N+K)=1.0D00
210      CONTINUE
205    CONTINUE

       DO 215 J=1,M-2
        Y(J*N)=1.0D00
215    CONTINUE

      ENDIF

      IF( CO .EQ. 1.0D00 ) THEN

       DO 405 J=1,M-2
         DO 410 K=1,N-1
          Y((J-1)*N+K) = 0.0D00
410      CONTINUE
405    CONTINUE

       DO 415 J=1,M-2
        Y(J*N)=0.0D00
415    CONTINUE

      ENDIF

C                        WRITE TITLE
```

```
      CALL UMACH(2,NOUT)
      WRITE(NOUT,1110)

C                             INTEGRATE ODE

      DO 220 IEND = 1, 20

        XEND = 0.0D00 + 1.0D00 * DFLOAT(IEND)
        CALL DIVPAG (IDO,NEQ,FCN,FCNJ,A,X,XEND,TOL,PARAM,Y)
        WRITE(NOUT,1120) X, ( Y(I), I = 1, NEQ )

220   CONTINUE

C                             FINISH UP
      IDO = 3
      CALL DIVPAG (IDO,NEQ,FCN,FCNJ,A,X,XEND,TOL,PARAM,Y)
C
610   FORMAT(7F9.3)
620   FORMAT(8F9.3)
1110  FORMAT('   T       Q(1)    Q(2)','    Q(3)    Q(4)    Q(5)    Q(6)',
     &'    C(T)'/)
C     &         '____________________________________________________',
C     &                '_________________________')
1120  FORMAT(/F6.1, 1X, 6F7.3, F8.3/ (7X, 6F7.3, F8.3))

      STOP
      END
C
```

```
      SUBROUTINE FCN (NEQ,X,Y,YPRIME)

      COMMON AA(30,30), BB(30,30), AAP(30,30), BBP(30,30),
     &       M,N, GAMA,PE,PSI, P0,P1,P2,P3,P4,P5,P6,P7,P8, PI

      DOUBLE PRECISION AA, BB, AAP, BBP, GAMA, PE, PSI,
     &   P0, P1, P2, P3, P4, P5, P6, P7, P8, P11, PI,
     &   X, Y(NEQ), YPRIME(NEQ), FIRST_CONST, SECOND_CONST,
     &   THIRD_CONST, FOURTH_CONST

      INTEGER M, N
C
      DO 310 J=1,M-2

         DO 320 I=1,N-1

            YPRIME((J-1)*N+I) = 0.0D00
            FIRST_CONST       = 0.0D00

           DO 330 K = 1, N - 1

            FIRST_CONST = GAMA * (BB(I,K)-PSI*BB(I,N)*AA(N,K))
            YPRIME((J-1)*N+I) = YPRIME((J-1)*N+I) + FIRST_CONST
     &                          * Y((J-1)*N+K)
330   CONTINUE

         SECOND_CONST = P0 * BB(I, N)
         YPRIME((J-1)*N+I) = YPRIME((J-1)*N+I) + SECOND_CONST * Y(J*N)

320   CONTINUE
310   CONTINUE

      DO 340 J=2,M-1

         YPRIME((J-1)*N) = 0.0D00
         P11             = P8 * ( P5 * (BBP(J,1)/PE-AAP(J,1))
     &                      - P3 * ( BBP(J,M)/PE-AAP(J,M) ) )

      DO 350 K=2,M-1

         THIRD_CONST = PI * ( BBP(J,K)/PE - AAP(J,K)
     &      + (BBP(J,1)/PE-AAP(J,1)) * (P1*AAP(M,K)-P2*AAP(1,K))
     &      + (BBP(J,M)/PE-AAP(J,M)) * (P3*AAP(1,K)-P4*AAP(M,K)) )

         YPRIME((J-1)*N) = YPRIME((J-1)*N) + THIRD_CONST * Y((K-1)*N)

350   CONTINUE

      DO 360 I=1,N-1
         FOURTH_CONST    = P6 * AA( N, I )
         YPRIME((J-1)*N) = YPRIME((J-1)*N) - FOURTH_CONST*Y((J-2)*N+I)
360   CONTINUE

         YPRIME((J-1)*N) = YPRIME((J-1)*N) - P11 - P7 * Y((J-1)*N)

340   CONTINUE

      RETURN
      END
C
      SUBROUTINE FCNJ (NEQ,X,Y,DYPDY)
      INTEGER NEQ
      REAL X,Y(NEQ),DYPDY(*)
      RETURN
      END
```

Appendix 8. Matrix Calculation Results for Orthogonal Collocation Method

CALCULATION RESULTS OF MATRICES GENERATED FOR ORTHOGONAL COLLOCATION SIMULATION (Radial)

NUMBER OF COLLOCATION POINTS = 3

ROOTS OF POLYNOMIALS

0.3631174564
0.6771862507
0.8997579813
1.0000000000

Qji

1.0000	0.1319	0.0174	0.0023
1.0000	0.4586	0.2103	0.0964
1.0000	0.8096	0.6554	0.5306
1.0000	1.0000	1.0000	1.0000

QINVji

1.9313	-1.7193	1.3348	-0.5469
-8.5283	16.8820	-14.3693	6.0156
11.7991	-31.2690	35.1105	-15.6406
-5.2021	16.1063	-22.0760	11.1719

Aji

-4.1309	6.8819	-4.5475	1.7965
-1.3389	-2.2150	5.2890	-1.7351
0.6257	-3.7406	-1.6671	4.7820
-1.0727	5.3256	-20.7528	16.5000

Bji

-23.8531	30.5936	-9.7463	3.0057
11.0999	-43.2376	40.8187	-8.6810
-3.3228	38.3568	-125.4092	90.3752
-33.6755	152.3749	-311.1994	192.4999

CALCULATION RESULTS OF MATRICES GENERATED FOR ORTHOGONAL COLLOCATION SIMULATION (Radial)

NUMBER OF COLLOCATION POINTS = 4

ROOTS OF POLYNOMIALS

0.2957581282
0.5652353168
0.7844834924
0.9340014458
1.0000000000

Qji

1.0000	0.0875	0.0077	0.0007	0.0001
1.0000	0.3195	0.1021	0.0326	0.0104
1.0000	0.6154	0.3787	0.2331	0.1434
1.0000	0.8724	0.7610	0.6639	0.5791
1.0000	1.0000	1.0000	1.0000	1.0000

QINVji

1.9551	-1.8179	1.5792	-1.2085	0.4922
-13.4924	27.6389	-26.3857	20.7705	-8.5313
32.1372	-86.8021	107.6744	-91.4005	38.3910
-31.9983	99.6933	-147.6429	142.1047	-62.1569
11.3985	-38.7123	64.7750	-70.2661	32.8050

Aji

-5.0717	8.6586	-6.3672	4.6459	-1.8656
-1.4346	-2.6538	6.3921	-3.7114	1.4077
0.5229	-3.1686	-1.9121	6.6240	-2.0661
-0.3860	1.8614	-6.7019	-1.6061	6.8325
0.7616	-3.4684	10.2688	-33.5621	26.0002

Bji

-34.4654	44.1493	-14.2678	7.0025	-2.4186
13.9799	-52.3164	48.8372	-15.1778	4.6771
-3.1084	33.6005	-94.5288	80.8953	-16.8583
1.8384	-12.5807	97.4502	-286.6931	199.9860
38.5481	-170.3696	457.9712	-794.1523	468.0035

CALCULATION RESULTS OF MATRICES GENERATED FOR ORTHOGONAL COLLOCATION SIMULATION (Radial)

NUMBER OF COLLOCATION POINTS = 5

ROOTS OF POLYNOMIALS

0.2492869347
0.4829098284
0.6861884594
0.8463475704
0.9533098340
1.0000000000

Qji

1.0000	0.0621	0.0039	0.0002	0.0000	0.0000
1.0000	0.2332	0.0544	0.0127	0.0030	0.0007
1.0000	0.4709	0.2217	0.1044	0.0492	0.0231
1.0000	0.7163	0.5131	0.3675	0.2633	0.1886

```
  1.0000    0.9088    0.8259    0.7506    0.6821    0.6199
  1.0000    1.0000    1.0000    1.0000    1.0000    1.0000


QINVji

  1.9683   -1.8722    1.7076   -1.4639    1.1114   -0.4512
-19.5029   40.6495  -40.7705   36.0189  -27.6742   11.2792
 69.9910 -190.7735  246.3896 -235.1856  186.2772  -76.6988
-116.5945 364.1147 -554.9321  596.0466 -496.8170  208.1823
 91.6751 -310.4077  528.6072 -631.4850  564.4897 -242.8794
-27.5370   98.2893 -181.0018  236.0690 -227.3871  101.5678


Aji

 -6.0172   10.4035   -8.0183    6.5339   -4.8627    1.9608
 -1.5818   -3.1062    7.4840   -4.8017    3.3072   -1.3016
  0.5108   -3.1358   -2.1860    7.2924   -3.9368    1.4553
 -0.3018    1.4590   -5.2876   -1.7722    8.4699   -2.5671
  0.2727   -1.2196    3.4652  -10.2825   -1.5737    9.3382
 -0.5782    2.5245   -6.7356   16.3857  -49.0959   37.4999


Bji

-47.3998   60.6450  -19.5628    9.9598   -5.7271    2.0848
 17.8626  -65.6704   60.8297  -19.1990    9.4559   -3.2788
 -3.4308   36.2177  -97.2104   81.5476  -24.6736    7.5493
  1.5620  -10.2217   72.9287 -182.5938  148.9590  -30.6326
 -1.2278    6.8853  -30.1719  203.6992 -569.6211  390.4390
-42.6313  183.7080 -474.4570 1047.0371-1676.1445  962.4961


CALCULATION RESULTS OF MATRICES GENERATED FOR
ORTHOGONAL COLLOCATION SIMULATION  (Radial)

NUMBER OF COLLOCATION POINTS =  6

ROOTS OF POLYNOMIALS

  0.215354
  0.420638
  0.606253
  0.763520
  0.885082
  0.965246
  1.000000


Qji

    1.000    0.046    0.002    0.000    0.000    0.000    0.000
    1.000    0.177    0.031    0.006    0.001    0.000    0.000
    1.000    0.368    0.135    0.050    0.018    0.007    0.002
    1.000    0.583    0.340    0.198    0.115    0.067    0.039
    1.000    0.783    0.614    0.481    0.377    0.295    0.231
    1.000    0.932    0.868    0.809    0.754    0.702    0.654
    1.000    1.000    1.000    1.000    1.000    1.000    1.000


QINVji

   1.976   -1.905    1.785   -1.609    1.369   -1.034    0.419
 -26.560   55.919  -57.603   53.563  -46.161   35.086  -14.245
 132.925 -364.177  480.349 -482.617  429.736 -331.540  135.324
-325.924 1018.957-1575.085 1771.050-1662.041 1314.337 -541.295
 420.635-1421.281 2439.257-3026.140 3036.447-2486.401 1037.481
-274.490  975.211-1799.825 2416.809-2594.942 2220.399 -943.163
 71.436 -262.725  511.122 -731.055  835.591 -750.847  326.479


Aji

  -6.965   12.133   -9.596    8.215   -6.836    5.114   -2.064
  -1.752   -3.566    8.587   -5.766    4.412   -3.186    1.270
   0.528   -3.270   -2.474    8.051   -4.767    3.157   -1.225
  -0.278    1.351   -4.956   -1.965    8.709   -4.498    1.635
   0.205   -0.918    2.604   -7.727   -1.695   10.724   -3.193
  -0.208    0.895   -2.330    5.391  -14.485   -1.553   12.290
   0.459   -1.956    4.951  -10.739   23.630  -67.345   51.000


Bji

 -62.623   80.052  -25.737   13.188   -7.990    4.976   -1.865
  22.579  -82.223   75.799  -23.893   12.242   -7.102    2.597
  -3.984   41.600 -109.319   90.628  -27.801   13.572   -4.696
   1.583  -10.168   70.266 -166.995  132.725  -39.387   11.976
  -0.989    5.365  -22.180  136.529 -322.507  255.965  -52.183
   0.909   -4.590   15.957  -59.687  377.023-1024.361  694.749
  46.274 -195.859  488.575-1024.626 2044.828-3127.217 1768.025


CALCULATION RESULTS OF MATRICES GENERATED FOR
ORTHOGONAL COLLOCATION SIMULATION (Longitudinal)

NUMBER OF COLLOCATION POINTS =  3

ROOTS OF POLYNOMIALS

 0.0000000000
 0.1127016619
 0.5000000000
 0.8872983456
 1.0000000000


Qji

  1.0000    0.0000    0.0000    0.0000    0.0000
  1.0000    0.1127    0.0127    0.0014    0.0002
  1.0000    0.5000    0.2500    0.1250    0.0625
  1.0000    0.8873    0.7873    0.6986    0.6198
  1.0000    1.0000    1.0000    1.0000    1.0000


QINVji

  1.0000    0.0000    0.0000    0.0000    0.0000
-13.0000   14.7883   -2.6667    1.8784   -1.0000
 42.0000  -61.0316   29.3334  -22.3018   12.0000
-50.0000   79.5767  -53.3334   53.7568  -30.0000
 20.0000  -33.3334   26.6667  -33.3334   20.0000
```

Aji

-13.0000	14.7883	-2.6667	1.8784	-1.0000
-5.3238	3.8730	2.0656	-1.2910	0.6762
1.5000	-3.2275	0.0000	3.2275	-1.5000
-0.6762	1.2910	-2.0656	-3.8730	5.3238
1.0000	-1.8784	2.6667	-14.7883	13.0000

Bji

84.0000	-122.0632	58.6667	-44.6035	24.0000
53.2379	-73.3334	26.6667	-13.3333	6.7621
-6.0000	16.6667	-21.3334	16.6667	-6.0000
6.7621	-13.3334	26.6667	-73.3334	53.2379
24.0001	-44.6036	58.6668	-122.0633	84.0001

CALCULATION RESULTS OF MATRICES GENERATED FOR
ORTHOGONAL COLLOCATION SIMULATION (Longitudinal)

NUMBER OF COLLOCATION POINTS = 4

ROOTS OF POLYNOMIALS

0.0000000000
0.0694318414
0.3300094903
0.6699905396
0.9305681586
1.0000000000

Qji

1.0000	0.0000	0.0000	0.0000	0.0000	0.0000
1.0000	0.0694	0.0048	0.0003	0.0000	0.0000
1.0000	0.3300	0.1089	0.0359	0.0119	0.0039
1.0000	0.6700	0.4489	0.3008	0.2015	0.1350
1.0000	0.9306	0.8660	0.8058	0.7499	0.6978
1.0000	1.0000	1.0000	1.0000	1.0000	1.0000

QINVji

1.0000	0.0000	0.0000	0.0000	0.0000	0.0000
-21.0000	23.6304	-3.6799	1.8125	-1.7631	1.0000
109.9998	-155.8988	66.1264	-35.3582	35.1308	-19.9999
-229.9989	353.9916	-204.4076	146.6060	-156.1908	89.9997
209.9984	-336.5714	226.9679	-198.0675	237.6720	-139.9995
-69.9992	114.8481	-85.0068	85.0071	-114.8489	69.9997

Aji

-21.0000	23.6304	-3.6799	1.8125	-1.7631	1.0000
-8.7783	6.6640	2.8405	-1.2325	1.1613	-0.6550
2.4953	-5.1848	0.7688	2.9413	-2.2496	1.2290
-1.2291	2.2497	-2.9413	-0.7688	5.1848	-2.4953
0.6550	-1.1614	1.2326	-2.8406	-6.6639	8.7783
-0.9997	1.7628	-1.8123	3.6796	-23.6302	20.9999

Bji

219.9996	-311.7976	132.2527	-70.7163	70.2616	-39.9999
135.8637	-183.0295	59.6593	-20.5306	18.1742	-10.1371
-11.2854	31.8223	-36.9703	21.8257	-10.9511	5.5587
5.5586	-10.9509	21.8257	-36.9704	31.8224	-11.2855
-10.1354	18.1715	-20.5289	59.6580	-183.0283	135.8630
-39.9974	70.2578	-70.7140	132.2512	-311.7964	219.9989

CALCULATION RESULTS OF MATRICES GENERATED FOR
ORTHOGONAL COLLOCATION SIMULATION (Longitudinal)

NUMBER OF COLLOCATION POINTS = 5

ROOTS OF POLYNOMIALS

0.0000000000
0.0469100773
0.2307653427
0.5000000000
0.7692346573
0.9530899525
1.0000000000

Qji

1.000	0.000	0.000	0.000	0.000	0.000	0.000
1.000	0.047	0.002	0.000	0.000	0.000	0.000
1.000	0.231	0.053	0.012	0.003	0.001	0.000
1.000	0.500	0.250	0.125	0.063	0.031	0.016
1.000	0.769	0.592	0.455	0.350	0.269	0.207
1.000	0.953	0.908	0.866	0.825	0.786	0.750
1.000	1.000	1.000	1.000	1.000	1.000	1.000

QINVji

1.000	0.000	0.000	0.000	0.000	0.000	0.000
-31.000	34.700	-5.032	2.133	-1.509	1.708	-1.000
240.000	-335.985	134.174	-61.867	44.830	-51.153	30.000
-770.000	1165.633	-626.140	388.270	-303.986	356.227	-210.003
1189.998	-1870.603	1160.975	-866.141	767.088	-941.327	560.007
-881.997	1416.454	-956.578	806.408	-799.023	1044.748	-630.008
251.999	-410.200	292.601	-268.803	292.600	-410.202	252.003

Aji

-31.000	34.700	-5.032	2.133	-1.509	1.708	-1.000
-13.096	10.134	3.880	-1.446	0.988	-1.104	0.645
3.732	-7.625	1.517	3.412	-1.857	1.941	-1.120
-1.875	3.368	-4.043	0.000	4.043	-3.368	1.875
1.120	-1.941	1.857	-3.412	-1.517	7.625	-3.732
-0.644	1.103	-0.987	1.446	-3.879	-10.134	13.096
1.000	-1.709	1.511	-2.134	5.032	-34.700	31.000

Bji

480.000	-671.969	268.348	-123.734	89.661	-102.306	60.001
292.915	-390.421	120.839	-35.698	22.750	-24.803	14.417
-21.025	59.817	-66.913	35.698	-12.531	11.261	-6.307
7.500	-14.868	30.034	-45.334	30.034	-14.868	7.500
-6.306	11.259	-12.531	35.698	-66.912	59.818	-21.025
14.418	-24.808	22.756	-35.701	120.844	-390.426	292.919
60.000	-102.314	89.669	-123.739	268.353	-671.978	480.005

CALCULATION RESULTS OF MATRICES GENERATED FOR ORTHOGONAL COLLOCATION SIMULATION (Longitudinal)

NUMBER OF COLLOCATION POINTS = 6

ROOTS OF POLYNOMIALS

0.0000000000
0.0337652415
0.1693953127
0.3806903958
0.6193096042
0.8306046724
0.9662347436
1.0000000000

Qji

1.00	0.00	0.00	0.00	0.00	0.00	0.00	0.00
1.00	0.03	0.00	0.00	0.00	0.00	0.00	0.00
1.00	0.17	0.03	0.00	0.00	0.00	0.00	0.00
1.00	0.38	0.14	0.06	0.02	0.01	0.00	0.00
1.00	0.62	0.38	0.24	0.15	0.09	0.06	0.03
1.00	0.83	0.69	0.57	0.48	0.40	0.33	0.27
1.00	0.97	0.93	0.90	0.87	0.84	0.81	0.79
1.00	1.00	1.00	1.00	1.00	1.00	1.00	1.00

QINVji

1.00	0.00	0.00	0.00	0.00	0.00	0.00	0.00
-43.00	47.99	-6.68	2.62	-1.61	1.36	-1.68	1.00
-8590026	-6889356	-2624980	-1951669	-685580	-561996	-702487	-420014
[illegible]	[illegible]	[illegible]	[illegible]	[illegible]	[illegible]	[illegible]	[illegible]
3697.14	-5940.44	4009.11	-3332.61	3112.86	-3316.99	4543.78	-2772.92
-924.39	1497.93	-1046.71	920.86	-920.82	1046.59	-1497.74	924.31

Aji

-43.00	47.99	-6.68	2.62	-1.61	1.36	-1.68	1.00
-18.28	14.29	5.15	-1.77	1.05	-0.88	1.07	-0.64
5.21	-10.55	2.35	4.16	-1.96	1.51	-1.80	1.06
-2.64	4.69	-5.38	0.51	4.19	-2.53	2.78	-1.62
1.62	-2.78	2.53	-4.19	-0.51	5.38	-4.69	2.64
-1.06	1.79	-1.51	1.95	-4.16	-2.35	10.56	-5.22
0.63	-1.05	0.86	-1.04	1.77	-5.14	-14.30	18.28
-1.02	1.72	-1.39	1.63	-2.63	6.70	-48.01	43.01

Bji

924.03	-1284.62	495.96	-211.33	133.17	-113.99	140.80	-84.03
560.23	-742.30	223.23	-60.87	33.60	-27.27	32.96	-19.58
-37.06	106.01	-116.34	58.98	-17.89	11.69	-12.95	7.56
11.19	-22.29	45.48	-65.38	39.37	-13.79	12.30	-6.88
-6.87	12.30	-13.78	39.37	-65.38	45.48	-22.29	11.19
7.56	-12.96	11.70	-17.90	59.00	-116.35	106.03	-37.07
-19.87	33.46	-27.59	33.85	-61.09	223.46	-742.58	560.41

Appendix 9. Examples of Numerical Simulation Results of Soil Column Contamination/ Desorption Process

T = dimensionless time
Q(i) = intraparticle gas concentration
C(T) = fluid phase concentration

Filename = TOL301.OUT
Compound = toluene
Temperature = 160 C
Phase = adsorption

T	Q(1)	Q(2)	Q(3)	Q(4)	Q(5)	Q(6)	C(T)
1.0	0.223	0.321	0.464	0.617	0.745	0.830	0.866
	0.049	0.088	0.159	0.255	0.355	0.433	0.469
	0.002	0.004	0.012	0.028	0.051	0.073	0.085
	0.000	0.001	0.001	0.002	0.003	0.004	0.004
	0.000	0.000	-0.001	-0.001	0.000	0.000	0.000
	0.000	0.000	0.000	0.000	0.000	-0.001	-0.001
2.0	0.622	0.682	0.759	0.833	0.891	0.928	0.943
	0.315	0.375	0.461	0.554	0.635	0.693	0.718
	0.068	0.095	0.139	0.195	0.252	0.297	0.318
	0.007	0.011	0.019	0.032	0.047	0.061	0.068
	0.000	0.001	0.002	0.004	0.007	0.010	0.011
	0.000	0.000	0.000	0.001	0.001	0.003	0.001
3.0	0.827	0.855	0.890	0.924	0.951	0.967	0.974
	0.573	0.617	0.678	0.741	0.795	0.831	0.847
	0.234	0.273	0.331	0.398	0.460	0.506	0.527
	0.053	0.069	0.095	0.128	0.162	0.190	0.203
	0.010	0.014	0.022	0.033	0.046	0.056	0.062
	0.003	0.004	0.007	0.011	0.016	0.021	0.023
4.0	0.922	0.934	0.950	0.966	0.978	0.986	0.989
	0.748	0.777	0.815	0.853	0.886	0.907	0.916
	0.425	0.463	0.517	0.577	0.631	0.670	0.688
	0.155	0.180	0.220	0.266	0.311	0.345	0.361
	0.048	0.060	0.079	0.103	0.128	0.149	0.158
	0.018	0.024	0.034	0.047	0.061	0.072	0.078
5.0	0.965	0.971	0.978	0.985	0.991	0.995	0.996
	0.856	0.873	0.895	0.917	0.936	0.948	0.953
	0.595	0.626	0.671	0.718	0.760	0.790	0.803
	0.291	0.321	0.365	0.415	0.462	0.496	0.512
	0.123	0.143	0.173	0.209	0.245	0.272	0.285
	0.060	0.072	0.091	0.115	0.139	0.158	0.167
6.0	0.985	0.988	0.991	0.995	0.997	0.999	1.000
	0.918	0.928	0.940	0.953	0.963	0.969	0.972
	0.729	0.753	0.786	0.821	0.851	0.872	0.881
	0.436	0.465	0.507	0.554	0.597	0.628	0.642
	0.231	0.256	0.293	0.335	0.376	0.406	0.420
	0.133	0.151	0.179	0.212	0.244	0.268	0.280
7.0	0.995	0.996	0.998	0.999	1.001	1.002	1.002
	0.953	0.958	0.965	0.971	0.977	0.980	0.982
	0.827	0.844	0.867	0.891	0.911	0.926	0.932
	0.570	0.596	0.632	0.672	0.708	0.733	0.745
	0.356	0.382	0.421	0.464	0.505	0.535	0.548
	0.231	0.253	0.287	0.325	0.362	0.389	0.402
8.0	0.999	1.000	1.001	1.002	1.003	1.003	1.003
	0.972	0.974	0.978	0.981	0.984	0.986	0.987
	0.895	0.906	0.921	0.937	0.950	0.959	0.963
	0.683	0.704	0.734	0.766	0.794	0.814	0.822
	0.482	0.507	0.544	0.585	0.622	0.648	0.661
	0.344	0.368	0.404	0.444	0.481	0.509	0.521
9.0	1.002	1.002	1.003	1.003	1.003	1.003	1.004
	0.981	0.983	0.985	0.987	0.988	0.989	0.990
	0.939	0.946	0.956	0.966	0.974	0.980	0.982
	0.774	0.790	0.812	0.836	0.858	0.872	0.879
	0.599	0.621	0.653	0.688	0.720	0.742	0.753
	0.460	0.484	0.518	0.557	0.592	0.617	0.629
10.0	1.003	1.003	1.003	1.003	1.004	1.004	1.004
	0.987	0.987	0.989	0.990	0.991	0.991	0.991
	0.967	0.971	0.977	0.983	0.988	0.991	0.993
	0.842	0.854	0.870	0.888	0.904	0.914	0.919
	0.699	0.718	0.744	0.773	0.798	0.816	0.825
	0.571	0.592	0.623	0.657	0.688	0.710	0.721
11.0	1.003	1.003	1.003	1.003	1.003	1.003	1.003
	0.990	0.990	0.991	0.992	0.992	0.993	0.993
	0.984	0.986	0.990	0.993	0.996	0.998	0.999
	0.892	0.900	0.912	0.925	0.936	0.943	0.946
	0.780	0.795	0.816	0.839	0.858	0.872	0.878
	0.668	0.687	0.713	0.742	0.768	0.787	0.794
12.0	1.003	1.003	1.003	1.003	1.003	1.003	1.003
	0.992	0.992	0.993	0.993	0.994	0.994	0.994
	0.993	0.995	0.996	0.998	1.000	1.001	1.001
	0.927	0.933	0.941	0.950	0.958	0.963	0.965
	0.844	0.855	0.871	0.888	0.903	0.913	0.918
	0.751	0.766	0.788	0.811	0.832	0.846	0.853
13.0	1.003	1.003	1.003	1.003	1.003	1.002	1.002
	0.993	0.994	0.994	0.994	0.995	0.995	0.995
	0.998	0.999	1.000	1.001	1.001	1.002	1.002
	0.952	0.956	0.961	0.967	0.972	0.976	0.977
	0.892	0.900	0.911	0.924	0.934	0.942	0.945
	0.817	0.829	0.846	0.864	0.880	0.892	0.896
14.0	1.003	1.003	1.002	1.002	1.002	1.002	1.002
	0.995	0.995	0.995	0.996	0.996	0.996	0.996
	1.001	1.001	1.001	1.002	1.002	1.002	1.002
	0.968	0.971	0.975	0.979	0.982	0.985	0.986
	0.926	0.932	0.940	0.949	0.957	0.962	0.964
	0.869	0.878	0.891	0.904	0.917	0.925	0.929
15.0	1.002	1.002	1.002	1.002	1.002	1.002	1.001
	0.996	0.996	0.996	0.997	0.997	0.997	0.997
	1.002	1.002	1.002	1.002	1.002	1.002	1.002
	0.979	0.981	0.984	0.986	0.989	0.990	0.991
	0.951	0.955	0.961	0.967	0.972	0.975	0.977
	0.908	0.914	0.924	0.934	0.943	0.949	0.952
16.0	1.002	1.002	1.002	1.001	1.001	1.001	1.001
	0.997	0.997	0.997	0.997	0.998	0.998	0.998
	1.002	1.002	1.002	1.002	1.002	1.002	1.001
	0.987	0.988	0.990	0.991	0.993	0.994	0.994
	0.968	0.970	0.974	0.978	0.982	0.984	0.985

	0.936	0.941	0.948	0.955	0.961	0.965	0.968
17.0	1.001	1.001	1.001	1.001	1.001	1.001	1.001
	0.997	0.998	0.998	0.998	0.998	0.998	0.998
	1.002	1.002	1.002	1.001	1.001	1.001	1.001
	0.992	0.992	0.993	0.995	0.995	0.996	0.996
	0.979	0.981	0.983	0.986	0.988	0.990	0.991
	0.957	0.960	0.965	0.970	0.974	0.977	0.979
18.0	1.001	1.001	1.001	1.001	1.001	1.001	1.001
	0.998	0.998	0.998	0.999	0.999	0.999	0.999
	1.001	1.001	1.001	1.001	1.001	1.001	1.001
	0.995	0.995	0.996	0.997	0.997	0.998	0.998
	0.987	0.988	0.990	0.991	0.993	0.994	0.994
	0.971	0.973	0.977	0.980	0.983	0.986	0.985
19.0	1.001	1.001	1.001	1.001	1.001	1.000	1.000
	0.999	0.999	0.999	0.999	0.999	0.999	0.999
	1.001	1.001	1.001	1.001	1.001	1.001	1.001
	0.997	0.997	0.997	0.998	0.998	0.998	0.999
	0.992	0.992	0.993	0.995	0.996	0.996	0.996
	0.981	0.982	0.985	0.987	0.989	0.991	0.991
20.0	1.001	1.001	1.000	1.000	1.000	1.000	1.000
	0.999	0.999	0.999	0.999	0.999	0.999	1.000
	1.001	1.001	1.001	1.001	1.000	1.000	1.000
	0.998	0.998	0.998	0.999	0.999	0.999	0.999
	0.995	0.995	0.996	0.997	0.997	0.998	0.998
	0.987	0.989	0.990	0.992	0.993	0.994	0.995
21.0	1.000	1.000	1.000	1.000	1.000	1.000	1.000
	0.999	0.999	0.999	0.999	1.000	1.000	1.000
	1.001	1.000	1.000	1.000	1.000	1.000	1.000
	0.999	0.999	0.999	0.999	0.999	0.999	0.999
	0.997	0.997	0.997	0.998	0.998	0.999	0.999
	0.992	0.993	0.994	0.995	0.996	0.996	0.996
22.0	1.000	1.000	1.000	1.000	1.000	1.000	1.000
	1.000	1.000	1.000	1.000	1.000	1.000	1.000
	1.000	1.000	1.000	1.000	1.000	1.000	1.000
	0.999	0.999	0.999	0.999	1.000	1.000	1.000
	0.998	0.998	0.998	0.999	0.999	0.999	0.999
	0.995	0.995	0.996	0.997	0.997	0.997	0.999
23.0	1.000	1.000	1.000	1.000	1.000	1.000	1.000
	1.000	1.000	1.000	1.000	1.000	1.000	1.000
	1.000	1.000	1.000	1.000	1.000	1.000	1.000
	0.999	1.000	1.000	1.000	1.000	1.000	1.000
	0.999	0.999	0.999	0.999	0.999	0.999	0.999
	0.997	0.997	0.997	0.998	0.998	0.999	0.999
24.0	1.000	1.000	1.000	1.000	1.000	1.000	1.000
	1.000	1.000	1.000	1.000	1.000	1.000	1.000
	1.000	1.000	1.000	1.000	1.000	1.000	1.000
	1.000	1.000	1.000	1.000	1.000	1.000	1.000
	0.999	0.999	0.999	1.000	1.000	1.000	1.000
	0.998	0.998	0.998	0.999	0.999	0.999	0.999
25.0	1.000	1.000	1.000	1.000	1.000	1.000	1.000
	1.000	1.000	1.000	1.000	1.000	1.000	1.000
	1.000	1.000	1.000	1.000	1.000	1.000	1.000
	1.000	1.000	1.000	1.000	1.000	1.000	1.000
	1.000	1.000	1.000	1.000	1.000	1.000	1.000
	0.999	0.999	0.999	0.999	0.999	0.999	1.000
26.0	1.000	1.000	1.000	1.000	1.000	1.000	1.000
	1.000	1.000	1.000	1.000	1.000	1.000	1.000
	1.000	1.000	1.000	1.000	1.000	1.000	1.000
	1.000	1.000	1.000	1.000	1.000	1.000	1.000
	1.000	1.000	1.000	1.000	1.000	1.000	1.000
	0.999	0.999	0.999	0.999	1.000	1.000	1.000
27.0	1.000	1.000	1.000	1.000	1.000	1.000	1.000
	1.000	1.000	1.000	1.000	1.000	1.000	1.000
	1.000	1.000	1.000	1.000	1.000	1.000	1.000
	1.000	1.000	1.000	1.000	1.000	1.000	1.000
	1.000	1.000	1.000	1.000	1.000	1.000	1.000
	0.999	1.000	1.000	1.000	1.000	1.000	1.000
28.0	1.000	1.000	1.000	1.000	1.000	1.000	1.000
	1.000	1.000	1.000	1.000	1.000	1.000	1.000
	1.000	1.000	1.000	1.000	1.000	1.000	1.000
	1.000	1.000	1.000	1.000	1.000	1.000	1.000
	1.000	1.000	1.000	1.000	1.000	1.000	1.000
	1.000	1.000	1.000	1.000	1.000	1.000	1.000
29.0	1.000	1.000	1.000	1.000	1.000	1.000	1.000
	1.000	1.000	1.000	1.000	1.000	1.000	1.000
	1.000	1.000	1.000	1.000	1.000	1.000	1.000
	1.000	1.000	1.000	1.000	1.000	1.000	1.000
	1.000	1.000	1.000	1.000	1.000	1.000	1.000
	1.000	1.000	1.000	1.000	1.000	1.000	1.000
30.0	1.000	1.000	1.000	1.000	1.000	1.000	1.000
	1.000	1.000	1.000	1.000	1.000	1.000	1.000
	1.000	1.000	1.000	1.000	1.000	1.000	1.000
	1.000	1.000	1.000	1.000	1.000	1.000	1.000
	1.000	1.000	1.000	1.000	1.000	1.000	1.000
	1.000	1.000	1.000	1.000	1.000	1.000	1.000

Filename = TOL302.OUT
Compound = toluene
Temperature = 160 C
Phase = desorption

T	Q(1)	Q(2)	Q(3)	Q(4)	Q(5)	Q(6)	C(T)
1.0	0.750	0.645	0.495	0.338	0.210	0.127	0.092
	0.928	0.875	0.784	0.665	0.547	0.458	0.417
	0.995	0.988	0.970	0.937	0.894	0.854	0.833
	1.000	0.999	0.998	0.996	0.993	0.988	0.986
	1.000	1.000	1.000	1.000	0.999	0.998	0.998
	1.000	1.000	1.000	1.000	1.000	1.000	1.001
2.0	0.341	0.283	0.209	0.139	0.084	0.051	0.037
	0.610	0.545	0.454	0.359	0.278	0.222	0.198
	0.879	0.838	0.775	0.699	0.624	0.568	0.542
	0.981	0.970	0.949	0.920	0.887	0.859	0.845
	0.997	0.995	0.991	0.983	0.974	0.965	0.960
	1.000	0.999	0.998	0.995	0.992	0.989	0.987
3.0	0.146	0.121	0.089	0.059	0.035	0.021	0.015
	0.348	0.306	0.249	0.192	0.145	0.113	0.100
	0.660	0.613	0.545	0.471	0.404	0.356	0.334
	0.886	0.858	0.814	0.761	0.709	0.669	0.650

	0.967	0.955	0.935	0.908	0.879	0.855	0.844
	0.988	0.983	0.973	0.959	0.944	0.931	0.924
4.0	0.062	0.051	0.037	0.024	0.013	0.007	0.004
	0.189	0.165	0.134	0.102	0.077	0.060	0.053
	0.449	0.410	0.356	0.298	0.247	0.211	0.195
	0.730	0.695	0.643	0.584	0.529	0.489	0.471
	0.882	0.858	0.822	0.778	0.735	0.701	0.685
	0.942	0.927	0.904	0.874	0.844	0.820	0.808
5.0	0.025	0.020	0.014	0.008	0.003	0.000	-0.001
	0.102	0.089	0.072	0.056	0.042	0.034	0.030
	0.286	0.258	0.219	0.178	0.143	0.119	0.108
	0.560	0.526	0.478	0.424	0.376	0.341	0.325
	0.751	0.721	0.676	0.625	0.577	0.541	0.524
	0.851	0.828	0.793	0.752	0.711	0.681	0.665
6.0	0.008	0.006	0.003	0.001	-0.001	-0.003	-0.003
	0.056	0.049	0.041	0.032	0.026	0.021	0.019
	0.172	0.153	0.127	0.100	0.078	0.063	0.056
	0.408	0.379	0.339	0.295	0.257	0.230	0.217
	0.602	0.571	0.526	0.476	0.430	0.397	0.381
	0.728	0.700	0.659	0.613	0.569	0.536	0.521
7.0	0.001	0.000	-0.001	-0.003	-0.004	-0.004	-0.004
	0.033	0.029	0.025	0.021	0.017	0.015	0.014
	0.097	0.086	0.070	0.053	0.040	0.030	0.026
	0.285	0.263	0.232	0.199	0.170	0.151	0.142
	0.458	0.430	0.390	0.346	0.307	0.279	0.266
	0.592	0.564	0.523	0.477	0.435	0.404	0.390
8.0	-0.002	-0.003	-0.003	-0.004	-0.004	-0.004	-0.004
	0.021	0.019	0.017	0.014	0.012	0.011	0.011
	0.052	0.045	0.035	0.026	0.018	0.013	0.011
	0.192	0.176	0.154	0.131	0.110	0.096	0.090
	0.334	0.310	0.278	0.243	0.212	0.190	0.180
	0.460	0.434	0.397	0.357	0.320	0.294	0.281
9.0	-0.004	-0.004	-0.004	-0.004	-0.004	-0.004	-0.004
	0.014	0.013	0.012	0.010	0.009	0.009	0.008
	0.025	0.021	0.016	0.011	0.007	0.004	0.003
	0.126	0.115	0.100	0.084	0.070	0.061	0.057
	0.234	0.216	0.191	0.165	0.141	0.125	0.118
	0.344	0.322	0.291	0.257	0.228	0.206	0.197
10.0	-0.004	-0.004	-0.004	-0.004	-0.004	-0.003	-0.003
	0.010	0.010	0.009	0.008	0.007	0.007	0.006
	0.011	0.009	0.006	0.003	0.001	0.000	-0.001
	0.081	0.074	0.064	0.053	0.044	0.038	0.035
	0.159	0.146	0.128	0.109	0.092	0.080	0.075
	0.248	0.231	0.207	0.180	0.157	0.141	0.134
11.0	-0.004	-0.003	-0.003	-0.003	-0.003	-0.003	-0.003
	0.008	0.007	0.007	0.006	0.005	0.005	0.005
	0.003	0.002	0.001	0.000	-0.001	-0.002	-0.002
	0.051	0.046	0.040	0.033	0.027	0.023	0.021
	0.105	0.096	0.083	0.070	0.058	0.051	0.047
	0.174	0.161	0.143	0.123	0.106	0.094	0.089
12.0	-0.003	-0.003	-0.003	-0.002	-0.002	-0.002	-0.002
	0.006	0.006	0.005	0.005	0.004	0.004	0.004
	0.000	0.000	-0.001	-0.001	-0.002	-0.002	-0.002
	0.032	0.029	0.025	0.020	0.016	0.014	0.013
	0.068	0.061	0.053	0.044	0.036	0.031	0.029
	0.119	0.109	0.096	0.082	0.070	0.061	0.057

13.0	-0.002	-0.002	-0.002	-0.002	-0.002	-0.001	-0.002
	0.004	0.004	0.004	0.003	0.003	0.003	0.003
	-0.001	-0.001	-0.002	-0.002	-0.002	-0.002	-0.002
	0.020	0.018	0.015	0.012	0.010	0.008	0.008
	0.043	0.039	0.033	0.027	0.022	0.019	0.018
	0.079	0.073	0.063	0.053	0.045	0.039	0.038
14.0	-0.002	-0.002	-0.002	-0.001	-0.001	-0.001	-0.001
	0.003	0.003	0.003	0.002	0.002	0.002	0.002
	-0.002	-0.002	-0.002	-0.001	-0.001	-0.001	-0.001
	0.012	0.011	0.009	0.007	0.006	0.005	0.005
	0.026	0.024	0.020	0.016	0.013	0.011	0.010
	0.052	0.047	0.041	0.034	0.029	0.024	0.024
15.0	-0.001	-0.001	-0.001	-0.001	-0.001	-0.001	-0.001
	0.002	0.002	0.002	0.002	0.001	0.001	0.001
	-0.001	-0.001	-0.001	-0.001	-0.001	-0.001	-0.001
	0.007	0.006	0.005	0.004	0.004	0.003	0.003
	0.016	0.014	0.012	0.010	0.008	0.007	0.006
	0.033	0.030	0.026	0.022	0.018	0.015	0.014
16.0	-0.001	-0.001	-0.001	-0.001	-0.001	-0.001	-0.001
	0.002	0.001	0.001	0.001	0.001	0.001	0.001
	-0.001	-0.001	-0.001	-0.001	-0.001	-0.001	-0.001
	0.004	0.004	0.003	0.003	0.002	0.002	0.002
	0.010	0.009	0.007	0.006	0.005	0.004	0.004
	0.021	0.019	0.016	0.013	0.011	0.009	0.009
17.0	-0.001	-0.001	-0.001	0.000	0.000	0.000	0.000
	0.001	0.001	0.001	0.001	0.001	0.001	0.001
	-0.001	-0.001	-0.001	-0.001	0.000	0.000	0.000
	0.003	0.002	0.002	0.002	0.001	0.001	0.001
	0.006	0.005	0.004	0.003	0.003	0.002	0.002
	0.013	0.012	0.010	0.008	0.007	0.006	0.005
18.0	0.000	0.000	0.000	0.000	0.000	0.000	-0.001
	0.001	0.001	0.001	0.001	0.000	0.000	0.001
	-0.001	0.000	0.000	0.000	0.000	0.000	-0.001
	0.002	0.001	0.001	0.001	0.001	0.000	0.001
	0.003	0.003	0.002	0.002	0.002	0.001	0.001
	0.008	0.007	0.006	0.005	0.004	0.003	0.005
19.0	0.000	0.000	0.000	0.000	0.000	0.000	0.000
	0.000	0.000	0.000	0.000	0.000	0.000	0.000
	0.000	0.000	0.000	0.000	0.000	0.000	0.000
	0.001	0.001	0.001	0.001	0.000	0.000	0.000
	0.002	0.002	0.001	0.001	0.001	0.001	0.001
	0.005	0.004	0.004	0.003	0.002	0.002	0.002
20.0	0.000	0.000	0.000	0.000	0.000	0.000	0.000
	0.000	0.000	0.000	0.000	0.000	0.000	0.000
	0.000	0.000	0.000	0.000	0.000	0.000	0.000
	0.001	0.000	0.000	0.000	0.000	0.000	0.000
	0.001	0.001	0.001	0.001	0.000	0.001	0.000
	0.003	0.003	0.002	0.002	0.001	0.002	0.000
21.0	0.000	0.000	0.000	0.000	0.000	0.000	0.000
	0.000	0.000	0.000	0.000	0.000	0.000	0.000
	0.000	0.000	0.000	0.000	0.000	0.000	0.000
	0.000	0.000	0.000	0.000	0.000	0.000	0.000
	0.001	0.001	0.000	0.000	0.000	0.000	0.000
	0.002	0.002	0.001	0.001	0.001	0.001	0.000
22.0	0.000	0.000	0.000	0.000	0.000	0.000	0.000
	0.000	0.000	0.000	0.000	0.000	0.000	0.000
	0.000	0.000	0.000	0.000	0.000	0.000	0.000

	0.000	0.000	0.000	0.000	0.000	0.000	0.000
	0.000	0.000	0.000	0.000	0.000	0.000	0.000
	0.001	0.001	0.001	0.001	0.000	0.001	0.000
23.0	0.000	0.000	0.000	0.000	0.000	0.000	0.000
	0.000	0.000	0.000	0.000	0.000	0.000	0.000
	0.000	0.000	0.000	0.000	0.000	0.000	0.000
	0.000	0.000	0.000	0.000	0.000	0.000	0.000
	0.000	0.000	0.000	0.000	0.000	0.000	0.000
	0.001	0.001	0.000	0.000	0.000	0.000	0.000
24.0	0.000	0.000	0.000	0.000	0.000	0.000	0.000
	0.000	0.000	0.000	0.000	0.000	0.000	0.000
	0.000	0.000	0.000	0.000	0.000	0.000	0.000
	0.000	0.000	0.000	0.000	0.000	0.000	0.000
	0.000	0.000	0.000	0.000	0.000	0.000	0.000
	0.000	0.000	0.000	0.000	0.000	0.000	0.000
25.0	0.000	0.000	0.000	0.000	0.000	0.000	0.000
	0.000	0.000	0.000	0.000	0.000	0.000	0.000
	0.000	0.000	0.000	0.000	0.000	0.000	0.000
	0.000	0.000	0.000	0.000	0.000	0.000	0.000
	0.000	0.000	0.000	0.000	0.000	0.000	0.000
	0.000	0.000	0.000	0.000	0.000	0.000	0.000
26.0	0.000	0.000	0.000	0.000	0.000	0.000	0.000
	0.000	0.000	0.000	0.000	0.000	0.000	0.000
	0.000	0.000	0.000	0.000	0.000	0.000	0.000
	0.000	0.000	0.000	0.000	0.000	0.000	0.000
	0.000	0.000	0.000	0.000	0.000	0.000	0.000
	0.000	0.000	0.000	0.000	0.000	0.000	0.000
27.0	0.000	0.000	0.000	0.000	0.000	0.000	0.000
	0.000	0.000	0.000	0.000	0.000	0.000	0.000
	0.000	0.000	0.000	0.000	0.000	0.000	0.000
	0.000	0.000	0.000	0.000	0.000	0.000	0.000
	0.000	0.000	0.000	0.000	0.000	0.000	0.000
	0.000	0.000	0.000	0.000	0.000	0.000	-0.001
28.0	0.000	0.000	0.000	0.000	0.000	0.000	0.000
	0.000	0.000	0.000	0.000	0.000	0.000	0.000
	0.000	0.000	0.000	0.000	0.000	0.000	0.000
	0.000	0.000	0.000	0.000	0.000	0.000	0.000
	0.000	0.000	0.000	0.000	0.000	0.000	0.000
	0.000	0.000	0.000	0.000	0.000	0.000	0.000
29.0	0.000	0.000	0.000	0.000	0.000	0.000	0.000
	0.000	0.000	0.000	0.000	0.000	0.000	0.000
	0.000	0.000	0.000	0.000	0.000	0.000	0.000
	0.000	0.000	0.000	0.000	0.000	0.000	0.000
	0.000	0.000	0.000	0.000	0.000	0.000	0.000
	0.000	0.000	0.000	0.000	0.000	0.000	0.000
30.0	0.000	0.000	0.000	0.000	0.000	0.000	0.000
	0.000	0.000	0.000	0.000	0.000	0.000	0.000
	0.000	0.000	0.000	0.000	0.000	0.000	0.000
	0.000	0.000	0.000	0.000	0.000	0.000	0.000
	0.000	0.000	0.000	0.000	0.000	0.000	0.000
	0.000	0.000	0.000	0.000	0.000	0.000	0.000

REFERENCES

1] Thielen, D.R., P.S. Foreman and A. Davis, *Env. Sci. & Tech.*, **21**, 2, 145-148, 1987

2] Daley, P.S., *Env. Sci. & Tech.*, **23**, 8, 912-916, 1989

3] Webster, D.M., *J. of Air & Waste Management Assoc.*, **36**, 10, 1156 - 1163, 1986

4] Mackay, D.M., P.V. Roberts and J.A. Cherry, *Env. Sci. & Tech.*, **19**, 5, 384-392, 1985

5] Glenn, J., *Biocycle*, Mar., 1990, 48-53

6] Crawford, M., *Science*, **235**, 156-157, 1987

7] Hazaga, D., S. Fields and G.P. Clemons, "Thermal Treatment of Solvent Contaminated Soils", *The 5th Nat'l Conference on Management of Uncontrolled Hazardous Waste Sites*, Nov. 7-9, 1984, Washington, D.C.

8] Singh, U.P., T.C. Emenhiser, J.I. Garcia-Bengochea and J.E. Orban, *J. of Env. Eng.*, **110**, 343-355, 1984

9] *Chem. Eng., Currents*, Nov. 26, 1984, 22-25

10] Stinson, M.K., *J. of Air & Waste Management Assoc.*, **39**, 8, 1054 - 1062, 1989

11] Eiceman, G.A., B. Davani and J. Ingram, *Env. Sci. & Tech.*, **20**, 5, 508-514, 1986

12] Berlincioni, M. and A. di Domenico, *Env. Sci. & Tech.*, **21**, 11, 1063-1069, 1987

13] Porter, J.W., *Chem. Eng. Progr.*, Apr., 1989, 16-25

14] MacKerron, *Chem. Eng.*, Nov.7, 1988, 26-31

15] Hazardous Waste News, *J. of Air & Waste Management Assoc.*, **39**, 7, 908-910, 1989

16] Grumbly, J.P., *Env. Progr.*, **8**, 1, F2-F3, 1989

17] Simes, G.F. and J.S. Harrington, *J. of Air & Waste Management Assoc.*, **39**, 4, 431-436, 1989

18] Bates, E.R., J.G. Herrmann and D.E. Sanning, *J. of Air & Waste Management Assoc.*, **39**, 7, 927-935, 1989

19] Civil Eng./News, *Civil Eng./ASCE*, 16-22 year

20] Koltuniak, D.L., *Chem. Eng.*, Aug. 18, 1986, 30-31

21] Doty, C.B. and C.C. Travis, *J. of Air & Waste Management Assoc.*, **39**, 12, 1535-1543, 1989

22] Marrin, D.L. and H.B. Kerfoot, *Env. Sci. & Tech.*, **22**, 7, 740-745, 1988

23] Kirkham, D. and W.L. Powers, "Advanced Soil Physics", *John Wiley & Sons*, 1972

24] Means, R.E. and J.V. Parcher, "Physical Properties of Soils", *Charles E. Merrill Pub. Co.*, 1963

25] Baver, L.D., W.H. Gardner and W.R. Gardner, "Soil Physics", *John-Wiley & Sons*, 1972

26] Dragun, J., *Haz. Mat'l Control*, Mar./Apr. 1988, 31-78

27] Laszlo, P., *Science*, Mar. 1987, 1473-1477

28] Dragun, J., "The Soil Chemistry of Hazardous Materials", *HMCRI*, 1988

29] Jury, W.A., W.F. Spencer and W.J. Farmer, *J. of Env. Quality*, **12**, 4, 558-564, 1983

30] Jury, W.A., W.J. Farmer and W.F. Spencer, *J. of Env. Quality*, **13**, 4, 567-572, 1984

31] Valverde-Garcia, A., E. Gonzales-Pradas et al., *Soil Sci. Soc. Am. J.*, **52**, 1571-1574, 1988

32] Elabd, H., W.A. Jury and M.M. Cliath, *Env. Sci & Tech.*, **20**, 4, 256-260, 1986

33] Leffe laar, *Soil Sci.*, **143**, 2, 79-91, 1987

34] Dragun, G., *Haz. Mat'l Control*, Sep./Oct., 1988, 24-43

35] Walters, R.W. and A. Guiseppi-Elie, *Env. Sci. & Tech.*, **22**, 7, 819 -825, 1988

36] Chiou, C.T., D.E. Kile and R.M. Malcolm, *Env. Sci. & Tech.*, **22**, 3, 298-303, 1988

37] Rogers, R.D., J.C. McFarlane and A.J. Cross, *Env. Sci. & Tech.*, **14**, 4, 457-460, 1980

38] Dao, T.H. and T.L. Lavy, *Soil Sci.*, **143**, 1, 66-72, 1987

39] Garbarini, D.R. and L.W. Lion, *Env. Sci. & Tech.*, **20**, 12, 1263-1269, 1986

40] Nkedi-Kizza, P., P.S.C. Rao and A.G. Hornsby, *Env. Sci. & Tech.*, **19**, 10, 975-979, 1985

41] Garbarini, D.R. and L.W. Lion, *Env. Sci. & Tech.*, **19**, 11, 1122-1128, 1985

42] Estes T.J., R.V. Shah and V.L. Vilker, *Env. Sci. & Tech.*, **22**, 4, 377-381, 1988

43] von Oepen, B., W. Kordel and W. Klein, *Chemosphere*, **18**, 7-8, 1495-1511, 1989

44] Nkedi-Kizza, P., M.L. Brusseau et al., *Env. Sci. & Tech.*, **23**, 7, 814-820, 1989

45] Sabljic, A., *Env. Sci. & Tech.*, **21**, 4, 358-366, 1987

46] Collin, M. and A. Rasmuson, *Soil Sci. Soc. Am. J.*, **52**, 1559-1565, 1988

47] Lighty, J.S., D.W. Pershing and V.A. Cundy, *Nucl. & Chem. Waste Management*, **8**, 225, 1988

48] Lighty, J.S., G.D. Silcox, D.W. Pershing, V.A. Cundy and D.G. Linz, *Env. Progr.*, **8**, 1, 57-61, 1989

49] Chemburkar, A., "Thermal Desorption of Haz. and Toxic Organic Compounds from Soil Matrices: Dichloromethane, Chloroform, Benzene, Toluene, 1-Chloronaphthalene, 1,2,4-Trichlorobenzene", *Master Thesis*, New Jersey Inst. of Tech., 1988

50] Hornsby, M.L., "Thermal Desorption of Haz. and Toxic Organic Compounds from Soil Matrices", *Master Thesis*, New Jersey Inst. of Tech., 1987

51] Calandra, S., "Thermal Desorption of Haz. and Toxic Organic Compounds from Soil Matrices: 4,4-Dichlorobiphenyl, p-Chlorobiphenyl", *Master Thesis*, New Jersey Inst. of Tech., 1989

52] Kubin, M., *Collection Czechoslov. Chem. Commun.*, **30**, 1105-1118, 1965

53] Kubin, M., *Collection Czechoslov. Chem. Commun.*, **30**, 2901-2907, 1965

54] Kucera, E., *J. of Chromatography*, **19**, 237-248, 1965

55] Kocirik, M., *J. of Chromatography*, **30**, 459-468, 1967

56] van der Laan, E.Th., *Chem. Eng. Sci.*, **7**, 187-191, 1958

57] Schneider, P. and J.M. Smith, *Am Inst. Chem. Engrs. J.*, **14**, 5, 762 -771, 1968

58] Suzuki, M. and J.M. Smith, *Chem. Eng. Sci.*, **26**, 221-235, 1971

59] Suzuki, M. and J.M. Smith, *Chem. Eng. J.*, **3**, 256-264, 1972

60] Chihara, K., J.M. Smith and K. Kawazoe, *Am. Inst. Chem. Engrs. J.*, **24**, 2, 237-246, 1978

61] Andrieu, J. and J.M. Smith, *Am. Inst. Chem. Engrs. J.*, **26**, 6, 944-948, 1980

62] Wang C.T. and J.M. Smith, *Am. Inst. Chem. Engrs. J.*, **29**, 1, 132-136, 1983

63] Park, I.S., J.M. Smith and B.J. McCoy, *Am. Inst. Chem. Engrs. J.*, **33**, 7, 1102-1109, 1987

64] Haynes Jr., H.W. and P.N. Sarma, *Am. Inst. Chem. Engrs. J.*, **19**, 5, 1043-1046, 1973

65] Haynes Jr., H.W., *Chem. Eng. Sci.*, **30**, 955-961, 1975

66] Hsu, L.-K.P. and H.W. Haynes Jr., *Am. Inst. Chem. Engrs. J.*, **27**, 1, 81-91, 1981

67] Fu, C.C., M.S.P. Ramesh and H.W. Haynes Jr., *Am. Inst. Chem. Engrs. J.*, **32**, 11, 1848-1857, 1986

68] Haynes Jr., H.W., *Am. Inst. Chem. Engrs. J.*, **32**, 10, 1750-1753, 1986

69] Ruthven, D.M. and R. Kumar, *Can. J. Chem. Eng.*, **57**, 342-348, 1979

70] Kumar, R., R.C. Duncan and D.M. Ruthven, *Can. J. of Chem. Eng.*, **60**, 493-499, 1982

71] DeVault, D., *J. of Amer. Chem. Soc.*, **65**, 532-540, 1943

72] Walter, J.E., *J. of Chem. Phys.*, **13**, 6, 229-234, 1945

73] Ruthven, D.M., "Priciples of Adsorption and Adsorption Processes", *John-Wiley & Sons*, 1984

74] Rosen, J.B., *J. of Chem Phys.*, **20**, 3, 387-394, 1952

75] Rosen, J.B., *Industrial & Eng. Chemistry*, **46**, 8, 1590-1594, 1954

76] Rasmuson, A. and A. Neretnieks, *Am. Inst. Chem. Engrs. J.*, **26**, 4, 686-690, 1980

77] Rasmuson, A., *Am. Inst. Chem. Engrs. J.*, **27**, 6, 1032-1035, 1981

78] Rasmuson, A., *Chem. Eng. Sci.*, **37**, 3, 411-415, 1982

79] Huang, J.C., D. Rothstein and R. Madey, *Am. Inst. Chem. Engrs. J.*, **30**, 4, 660-662, 1984

80] Kawazoe, K. and Y. Takeuchi, *J. of Chem Eng. of Japan*, **7**, 6, 431-437, 1974

81] Rasmuson, A., *Chem. Eng. Sci.*, **37**, 5, 787-788, 1982

82] Ruthven, D.M. and D.R. Garg, *Chem. Eng. Sci.*, **28**, 791-798, 1973

83] Ruthven, D.M. and D.R. Garg, *Chem. Eng. Sci.*, **29**, 571-581, 1974

84] Ruthven, D.M. and D.R. Garg, *Chem. Eng. Sci.*, **29**, 1961-1967, 1974

85] Ruthven, D.M. and D.R. Garg, *Chem. Eng. Sci.*, **30**, 1192-1194, 1975

86] Schneider, P., *Chem. Eng. Sci.*, **39**, 5, 927-929, 1984

87] Hansen, K.W., *Chem. Eng. Sci.*, **26**, 1555-1569, 1971

88] Karanth, N.G. and R. Hughes, *Chem. Eng. Sci.*, **29**, 197-205, 1974

89] Villadson, J.V. and W.E. Stewart, *Chem. Eng. Sci.*, **22**, 1483-1501, 1967

90] Finlayson, B.A., "The Method of Weighted Residuals and Variational Principles", *Academic Press*, 1972

91] Liapis, A.I. and D.W.T. Rippin, *Chem. Eng. Sci.*, **32**, 619-627, 1977

92] Liapis, A.I. and D.M.T. Rippin, *Chem. Eng. Sci.*, **33**, 593-600, 1978

93] Liapis, A.I. and R.J. Litchfield, *Chem. Eng. Sci.*, **35**, 2366-2369, 1980

94] Raghavan, N.S. and D.M. Ruthven, *Am. Inst. Chem. Engrs. J.*, **29**, 6, 922-925, 1983

95] Raghavan, N.S., M.M. Hassan and D.M. Ruthven, *Am. Inst. Chem. Engrs. J.*, **31**, 3, 385-392, 1985

96] Hsu, J.T., *Extended Abstracts of AIChE 1989 Annual Meeting*, San Francisco, Nov. 5-10, 1989

97] *IMSL User's Manual*, Math/Library v1.0, Apr. 1987

98] Wehner, J.F. and R.H. Wilhelm, *Chem. Eng. Sci.*, **6**, 89-93, 1956

99] Chapra S.C. and R.P. Canale, "Numerical Methods for Engineers", *McGraw-Hill*, 1985

100] Wu, S.C. and P.M. Gschwend, *Env. Sci. & Tech.*, **20**, 717-725, 1986

101] Wu, S.C., *Water Resources Research*, **24**, 8, 1373-1383, 1988

102] Reid, R.C., J.M. Prausnitz and T.K. Sherwood, "The properties of Gases and Liquids", 3rd ed., *McGraw-Hill*, 1966

103] Bird, R.B., W.E. Stewart and E.N. Lightfoot, "Transport Phenomena", *Jhon-Wiley & Sons*, 1960

104] Perry, R.H. and C.H. Chilton, "Chemical Engineers' Handbook", 5th ed., *McGraw-Hill*, 1973

105] Curl, R.L. and G.A. Keoleian, *Env. Sci. Tech.*, **18**, 12, 916-922, 1984

106] Smith, E.H. and W.J. Weber, Jr., *Env. Sci. Tech.*, **23**, 6, 713-722, 1989

107] Di Toro, D.M. and L.M. Horzempa, *Env. Sci. Tech.*, **16**, 594-602, 1982

108] Stroud, A.H. and D. Secrest, "Gaussian Quadrature Formulas", *Prentice-Hall*, 1966

109] Gluekauf, E., *Trans. Faraday Soc.*, **51**, 1540-1551, 1955

110] Lapidus, L. and N.R. Amunson, *J. Phys. Chem.*, **56**, 984-988, 1952

111] van Deemter, J.J., F.J. Zuiderweg and A. Klinkenberg, *Chem. Eng. Sci.*, **5**, 271-289, 1956

112] Langer, G., A. Roethe, K.-P. Roethe and D. Gelbin, *Int. J. Heat and Mass Transfer*, **21**, 751-759, 1978

113] Wakao, N., S. Kaguei and H. Nagai, *Chem. Eng. Sci.*, **33**, 183-187, 1978

114] Wakao, N. and T. Funazkri, *Chem. Eng. Sci.*, **33**, 1375-1384, 1978

115] Edwards, M.F. and J.F. Richardson, *Chem. Eng. Sci.*, **23**, 109-123, 1968